

# 54èmes Journées des Actinides

## Abstract Booklet

With thanks to our sponsors:



Tuesday 18th March		
12:30 - 13:50	Lunch	
13:50 - 14:00	Welcome	
14:00 - 14:20	Frédéric Jutier	Enhancing European Pu-238 Production from Np-237: The Role of NpO <sub>2</sub> Liquid-to-Solid Conversion
14:20 - 14:40	Wenting Lv	Theoretical investigation of the intrinsic oxygen defects in UO <sub>2</sub> (111) and PuO <sub>2</sub> (111) surfaces
14:40 - 15:00	Lewis Blackburn	Application of X-ray absorption spectroscopy in support of Pu disposition strategy
15:00 - 15:20	Thomas Colin	Radiolysis of adsorbed water on PuO <sub>2</sub>
15:20 - 15:40	Guillaume Lasnier	Impact of the alkali of background salt on Pu and Np V hydrolysis
15:40 - 16:10	Break	
16:10 - 16:30	Daniil Shirokiy	Comprehensive structural and chemical analysis of secondary phases forming in Cr-doped (U,Ln)O <sub>2±x</sub>
16:30 - 16:50	Samuel M. Webb	Chemical Imaging and Applications Using High Energy Resolution Fluorescence Detection for the Actinides
16:50 - 17:10	Yu Yang	Effects of interfaces
17:10 - 17:30	Egor Iwaschko	Insights into the structure and redox chemistry of surrogate MIMAS MOX ceramic materials
17:30 - 18:30		
18:30 - 19:30	Poster Session	
19:30 - 20:30	Cocktail Dinner	
Wednesday 19th March		
7:30 - 9:00	Breakfast	
9:00 - 9:20	Romuald Béjaud	Invar effect in Ga/Al alloyed δ-Pu
9:20 - 9:40	Ladislav Havela	Th-H films: Synthesis and PES study
9:40 - 10:00	Juan Cui	Electronic Structures and Physical Properties of α-Uranium Hydride under Shock Compression
10:00 - 10:20	Chris Bell	Low temperature physics and materials science of elemental uranium thin films and alloys
10:20 - 10:40	Oleksandra Koloskova	Uranium hydrides with substitutions: thin films studies
10:40 - 11:10	Break	
11:10 - 11:30	Itzhak Halevy	Innovative Lexan-Aerogel detector for fission track for Nuclear Forensics
11:30 - 11:50	Liubov Kononova	Structural incorporation of U(V) as a dominant U stabilization pathway during Fe(II)-promoted recrystallization of Fe-oxyhydroxysulfates
11:50 - 12:10	Claire Corkhill	New insight to U(V) stability in ancient titanate minerals
12:10 - 12:30	Carla Soto Ruiz	Uranium retention by chukanovite an Fe(II) hydroxycarbonate corrosion product of canisters in deep geological repositories
12:30 - 14:00	Lunch	

14:00 - 14:20	Lottie Harding	Revealing the crystal chemistry and dissolution kinetics of doped uranium dioxide nuclear fuel
14:20 - 14:40	Alejandro Vieyra Huerta	Probing the local disorder in $U_3O_7$ and $U_3O_8$ by neutron total scattering
14:40 - 15:00	Marat Khafizov	Magneto-elastic and multipolar interactions in $U_xTh_{1-x}O_2$
15:00 - 15:20	Gregory Leinders	Examining the uranium valence states from anomalous diffraction
15:20 - 15:40	Elena F. Bazarkina	New insights into the $UO_2$ oxidation process from in situ HERFD at the U $M_4$ edge
15:40 - 16:10	Break	
16:10 - 16:30	Gaël Ung	Luminescence and Circularly Polarized Luminescence of Molecular Complexes of Actinides (Am to Es)
16:30 - 16:50	Qixian Wang	Lanthanide nanoparticles and MOFs heterostructures boosting NIR-II imaging-guided photodynamic therapy
16:50 - 17:10	Fabrice Wilhelm	
17:10 - 17:30	Tamara Shaaban	Experimental Characterization and Theoretical Modelling of X-ray Absorption Spectra of Protactinium(V) Complexes
17:30 - 18:30		
18:30 - 19:30	Paganini talk	
19:30 - 20:30	Dinner	
<b>Thursday 20th March</b>		
7:30 - 9:00	Breakfast	
9:00 - 9:20	Clara Lisa Silva	Probing actinide electronic structure using high-energy resolution X-ray spectroscopy
9:20 - 9:40	Harry Ramanantoanina	Advanced x-ray spectroscopy study of Pu(III-VI) aqua ions
9:40 - 10:00	Lucia Amidani	A journey through the interpretation of uranyl $M_{4,5}$ edges HERFD-XANES
10:00 - 10:20	Jindrich Kolorenc	Evolution of the Eu $L_3$ edge RIXS spectra across the paramagnetic–ferromagnetic transition in EuS
10:20 - 10:40	Andrea Severing	Probing U multiplet excitations with high resolution $M_{4,5}$ -edge RIXS
10:40 - 11:10	Break	
11:10 - 11:30	Eilidh MacCormick	Using experimental actinide chemistry to solve technical challenges in spent fuel and nuclear material management within the NDA Group
11:30 - 11:50	Matthieu Viot	Freezing Pu(IV) Hexanuclear Clusters in the Formation of Plutonium Oxide Nanoparticles
11:50 - 12:10	Kevin D. Stuke	The role of structure and redox in the solid-state chemistry of Ce doped $UO_2$ nanoparticles
12:10 - 12:30	Fanny Gignac	Electrophoretic techniques: Setting up characterization tools for radioactive nanoparticles
12:30 - 14:00	Lunch	
14:00 - 17:30	Excursion	
17:30 - 19:30		
19:30 - 20:30	Dinner	

Friday 21st March		
7:30 - 9:00	Breakfast	
9:00 - 9:20	Myrtille Hunault	MARS beamline: an x-ray toolbox serving actinide science
9:20 - 9:40	Damien Prieur	Fission Product Speciation in $U_{1-y}Pu_yO_{2-x}$ SIMMOx Using Synchrotron Techniques
9:40 - 10:00	Florent Réal	The Coordination Chemistry of $U^{4+}$ in Aqueous Solutions: Challenges and Insights from Spectroscopy and Theory
10:00 - 10:20	Mickael Bernar	Development of a spent PWR MOx fuel using the SIMMOx approach
10:20 - 10:40	Gabriel Murphy	Radiation Stability and Structural Chemistry of $(Zr_{0.95}^{241}Am_{0.05})_{1-x}Nd_xO_{2-x0.5}$ Phases
10:40 - 11:10	Break	
11:10 - 11:30	Maëva Munoz	Synthesis of polynuclear neodymium structures as a model for actinide clusters
11:30 - 11:50	Xuejiao Li	Chemical footprints of thorium, uranium, and lanthanum in molten LiF-BeF <sub>2</sub> explored through molecular dynamic simulation technology
11:50 - 12:10	Melody Maloubier	Complexation of Protactinium(V) with Chlorides in aqueous solution: Thermodynamic and Structural Insights
12:10 - 12:30	Christelle Tamain	Molecular Compounds of Actinide(IV) Oxalate: Structure and Bond Characterization
12:30 - 14:00	Lunch	
14:00 - 14:20	Frederic Gendron	A DFT+DMFT look at the Magnetic Properties of $\delta$ Plutonium
14:20 - 14:40	Evgenia Chitrova Tereshina	Magnetic Structure Changes Under External Stimuli in UO <sub>2</sub> : High-Field and Strain-Induced Transitions
14:40 - 15:00	Eric Colineau	Magnetic properties of mixed actinide oxides
15:00 - 15:20	Daniel Braithwaite	Connecting High Field and High Pressure Superconductivity in UTe <sub>2</sub>
15:20 - 15:40	Alexander Shick	Perpendicular magnetic anisotropy in a single Dy adatom ferrimagnet
15:40 - 16:10	Break	
16:10 - 16:30	Midori Amano Patino	Exploring New Uranium Materials Containing Kagome Networks
16:30 - 16:50	Haiyan Lu	Tracing quasiparticle dynamics and hybridization dynamics in PuCoGa <sub>5</sub>
16:50 - 17:10	Mathieu Pasturel	U <sub>13</sub> Pd <sub>47</sub> Ge <sub>25</sub> : a quasicrystalline Tsai-type approximant with spin-glass behaviour
17:10 - 17:30	Jean-Christophe Griveau	Low Temperature Ground State Properties of 4f and 5f based phosphate compounds [RE or An]PO <sub>4</sub> with RE= Ce, Sm (sc) and An= <sup>239</sup> Pu, <sup>241</sup> Am
17:30 - 19:30		
19:30 - 20:30	Gourmet Dinner & Music	
Saturday 22nd March		
7:30 - 9:30	Breakfast	
10:00 -	Departing bus	

# Enhancing European Pu-238 Production from Np-237: The Role of NpO<sub>2</sub> Liquid-to-Solid Conversion

Frédéric Jutier\*, Beatriz Acevedo, Gregory Leinders and Marc Verwerft

*Belgian Nuclear Research Centre (SCK CEN), Institute of Nuclear Energy Technology, Boeretang 200, B-2400 Mol, Belgium.*

*\*e-mail: frederic.jutier@sckcen.be*

Deep space missions currently rely on Radioisotope Power Systems (RPS) that generate power up to 5 kWe for extended periods. These systems produce electricity using the heat released from the spontaneous decay of radioisotopes such as Plutonium-238 (Pu-238), which is the only isotope that has been used for RPS for flown missions. Currently, there is no production of Pu-238 in Europe, although it is plausible by neutron irradiation of Neptunium-237 (Np-237). Producing this isotope involves several steps, including the fabrication of Np-237 targets, their irradiation, and subsequent processing which include Pu/Np separation and conversion of recovered Pu-238 to solid PuO<sub>2</sub> pellets.

The synthesis of Np targets primarily involves a liquid-to-solid conversion step, where the Np feed solution is converted into a solid precursor, followed by mechanical fabrication into a suitable target material. The Np-237 feedstock, in secular equilibrium with its progeny, is a neptunium nitrate solution containing a mixture of Np(+V) & Np(+VI) ions (respectively NpO<sub>2</sub><sup>+</sup> & NpO<sub>2</sub><sup>2+</sup> ions). The reference conversion route is a neptunium heterogeneous oxalate conversion with a high degree of supersaturation, using hydrazine and ascorbic acid [1, 2]. Precipitating Np using oxalic acid requires the full conversion of Np to the +IV oxidation state since Np(+IV) oxalate has a lower solubility in an aqueous solution while Np(+V) is soluble [1, 2]. Therefore, ascorbic acid is generally used as a reducing agent and hydrazine, a highly toxic and carcinogenic compound, acts as an oxidation inhibitor..

In this work, we have studied the reductive behavior of ascorbic acid in detail to evaluate the possibility to omit hydrazine from the process. Additionally, we examined the oxalate precipitation with both high and low degrees of supersaturation and the subsequent calcination steps.

We acknowledge the European Union who funded this research under the HORIZON-EURATOM action 2021-NRT-01-11, contract 101061251. Views and opinions expressed are however those of the author(s) only and do not necessarily reflect those of the European Union or the European Atomic Energy Community. Neither the European Union nor the European Atomic Energy Community can be held responsible for them.

## References

- [1] Porter, J.A., Production of Neptunium Dioxide. Industrial & Engineering Chemistry Process Design and Development, 1964. 3(4): p. 289-292.
- [2] Rankin, D.T., et al., Preparation and characterization of oxalate-based neptunium-237 dioxide powder. Am. Ceram. Soc., Bull., 1977. 56(5): p. 478-83, 486.

# Theoretical investigation of the intrinsic oxygen defects in UO<sub>2</sub> (111) and PuO<sub>2</sub> (111) surfaces

W T Lv<sup>1</sup>, B Sun<sup>1</sup>, P F Guan<sup>2</sup>, Y Yang<sup>1,\*</sup>

<sup>1</sup>*LCP, Institute of Applied Physics and Computational Mathematics, Beijing, China*

<sup>2</sup>*Beijing Computational Science Research Center, Beijing, China*

\*e-mail: yang\_yu@iapcm.ac.cn

We studied the formation and distribution behavior of intrinsic oxygen defects in (111) surfaces of UO<sub>2</sub> and PuO<sub>2</sub> by density functional theory (DFT) + *U* combined with the first principle atomistic thermodynamic method. The calculated results indicate that the oxygen interstitial (O<sub>i</sub>) defects are dominant in UO<sub>2</sub>, while the oxygen vacancy (O<sub>v</sub>) and O<sub>i</sub> defects can coexist in PuO<sub>2</sub>. This can be attributed to the different electronic properties of U and Pu elements. An O<sub>v</sub> introduces a deep-level defect state in the band gap of UO<sub>2</sub> acting as a n-type doping, while introduces a shallow-level defect state near the valence-band-maximum (VBM) of PuO<sub>2</sub> as a p-type doping. For an O<sub>i</sub>, its electronic states hybridize with neighboring uranium atoms and results in negligible changes in the band structure of UO<sub>2</sub>. Comparatively an interstitial oxygen atom introduces a deep-level defect state in the band gap of PuO<sub>2</sub>. Moreover, the formation energy of O<sub>v</sub> is found to be sensitive to the surface depth, and O<sub>v</sub> prefer to exist on the sub-surface layer in both UO<sub>2</sub> and PuO<sub>2</sub>. The formation of O<sub>i</sub> is insensitive to the surface depth. The strain effect of formation energy is mainly contributed from the local structural distortion, rather than the electronic hybridization. Through thermodynamic calculation, the strain-modulated formation energy phase diagrams of the oxygen defects have been established over a wide range of temperature and pressure, providing the potential strategy for controlling the type and concentration of intrinsic oxygen defects in UO<sub>2</sub> and PuO<sub>2</sub>. The present study deepens our mechanistic understanding of the role of oxygen defects in the oxidation properties of actinide metals.

# Application of X-ray absorption spectroscopy in support of Pu disposition strategy

Lewis R. Blackburn\*, Aidan A. Friskney, Luke T. Townsend, Latham T. Haigh, Martin C. Stennett and Claire L. Corkhill

<sup>1</sup>*Immobilisation Science Laboratory, University of Sheffield, UK*

<sup>2</sup>*School of Earth Sciences, University of Bristol, UK*

*\*e-mail: lewis.blackburn@sheffield.ac.uk*

The ultimate end-point for all UK-owned separated plutonium (Pu) is a geological disposal facility, either in the form of spent mixed oxide (MOX) fuel or immobilised within the structure of a chemically durable ceramic material [1]. Candidate ceramic wastefoms for Pu include titanate ceramics such as zirconolite or a mixed (Pu,U,Gd)O<sub>2-x</sub> disposal MOX with a suitable neutron absorbing additive such as Gd<sup>3+</sup> to prevent against post closure criticality [2]. The zirconolite phase (ideally CaZrTi<sub>2</sub>O<sub>7</sub>) could feasibly act as a disposal matrix for separated PuO<sub>2</sub> through interdiffusion of Pu<sup>3+/4+</sup> cations within specific lattice sites in the zirconolite structure e.g. CaZr<sub>1-x</sub>Pu<sub>x</sub>Ti<sub>2</sub>O<sub>7</sub> facilitated by either high temperature sintering or by hot isostatic pressing (HIP). Controlled parametric studies have demonstrated, for both routes, that it is feasible to incorporate surrogates (namely Ce, U & Th) and neutron absorbing additives (Gd<sup>3+</sup> and/or Hf<sup>4+</sup>) within both the Ca<sup>2+</sup> and Zr<sup>4+</sup> sites, necessitating the addition of a charge modifier, examples of which include Fe<sup>2+/3+</sup>, Al<sup>3+</sup> and Cr<sup>3+</sup> [3]. X-ray absorption spectroscopy is a powerful element-specific tool to probe oxidation states and coordination environments in materials and can therefore be used to underpin solid solution mechanisms for Pu within candidate wastefom phases. This talk will summarise recent advances in wastefom development with a focus on the application of bulk XAS and HERFD techniques to probe solid solution mechanisms and radiation damage behaviour.

## References

- [1] Nuclear Decommissioning Authority, "Progress on Plutonium Consolidation, Storage and Disposition" 2019.
- [2] Cole et al. "A disposal-MOX concept for plutonium disposition" *Mater. Adv.*, 16, 2024
- [3] Blackburn et al. "Review of zirconolite crystal chemistry and aqueous durability" *Advances in Applied Ceramics*, 120, 2, 69–83, 2021.

## Radiolysis of adsorbed water on PuO<sub>2</sub>

T. COLIN<sup>1\*</sup>, P. ESTEVENON<sup>1</sup>, L. VENAULT<sup>1</sup>, P. MARTIN<sup>1</sup>, L. JOLLY<sup>2</sup>, and P. MOISY<sup>1</sup>

<sup>1</sup> CEA, DES, ISEC, DMRC, Univ Montpellier, Marcoule, France.

<sup>2</sup> CEA-Centre de Valduc, 21120 Is sur Tille, France

\* Thomas.COLIN@cea.fr

In the French nuclear fuel cycle, the plutonium is industrially recycled through the reprocessing of UOx spent fuel. The plutonium is stored in its PuO<sub>2</sub> form inside hermetically sealed containers [1]. The conditioning atmosphere contains air water vapour. Due to plutonium alpha decay, the moisture of the container atmosphere could then adversely affect the storage due to H<sub>2</sub> accumulation, generated by the radiolysis of the water molecules absorbed on the surface of PuO<sub>2</sub> [2].

This work aims to study the radiolysis of adsorbed water on the PuO<sub>2</sub> surface. The first step focus on an overview of the structural characteristics of PuO<sub>2</sub> using Raman spectroscopy, X-Ray Diffraction and thermogravimetric analysis. For powder synthesis, a reactive pathway based on plutonium (IV) peroxide precipitation followed by a calcination was chosen in order to avoid the presence of any carbon species in PuO<sub>2</sub> [3]. In a second step, the evolution of both the gas composition and release amount inside a sealed cell is followed by gas chromatography ( $\mu$ -GC). The influence of the following parameters are studied: atmosphere water content (relative humidity inside the reactor), PuO<sub>2</sub> powder specific surface area and alpha activity (plutonium isotopic composition).

A typical example of the evolution of the amount of H<sub>2</sub> as a function of time is presented in figure 1, which shows a linear evolution around 0.6nmol(H<sub>2</sub>).g(PuO<sub>2</sub>)<sup>-1</sup>.h<sup>-1</sup> at t<50h, leading to a steady state around 1.6  $\mu$ mol(H<sub>2</sub>).g(PuO<sub>2</sub>)<sup>-1</sup> over long timescales. These data were obtained with a 2.5GBq/g PuO<sub>2</sub>, calcined at 280°C, at 60% of relative humidity.

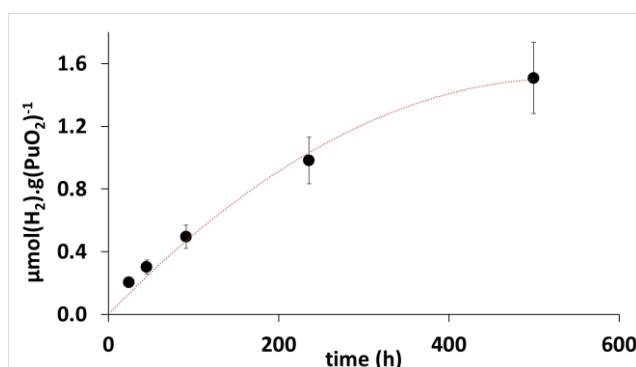


figure 1 : kinetics of hydrogen accumulation from radiolysis of adsorbed water normalized by PuO<sub>2</sub> mass. 1,08g<sub>PuO<sub>2</sub></sub>. 2,5GBq/g<sub>PuO<sub>2</sub></sub>. Calcined at 280°C. Relative humidity : 60%.

### References:

- [1] B. Bonin, « Treatment and recycling of spent nuclear fuel: actinide partitioning – application to waste management », E-DEN. Paris Gif-sur-Yvette. (2008).
- [2] L. Venault, et al. « Dihydrogen H<sub>2</sub> Steady State in  $\alpha$ -Radiolysis of Water Adsorbed on PuO<sub>2</sub> Surface ». Radiation Physics and Chemistry, 162, 136-145 (2019).
- [3] J. A. Leary, “Studies on the preparation, properties, and composition of plutonium peroxide”. Los Alamos Scientific Laboratory of the University of California, LA-1913. (1954).



# Impact of the alkali of background salt on Pu and Np V hydrolysis

G. LASNIER<sup>1\*</sup>, J. AUPIAIS<sup>1</sup>, B. SIBERCHICOT<sup>1,2</sup>

<sup>1</sup>CEA, DAM, DIF, F-91297, Arpajon, France

<sup>2</sup>Université Paris-Saclay, CEA, Laboratoire Matière en Conditions Extrêmes, F-91680 Bruyères-le-Châtel, France

\* e-mail : guillaume.lasnier2@cea.fr

Most of the time, alkaline ions are considered to be spectators of chemical reactions in solution. However, abnormal phenomena found during experimental measurements and problems of reproducibility between different media refute this theory. The hydrolysis of plutonium and neptunium V is a perfect example, with major differences found between sodium chloride and tetramethylammonium chloride. TMA, a cationic analogue of perchlorate anions, is a very large organic cation that does not interfere due to its very large size. The first hydrolysis constant of Np V at zero ionic strength in NaCl [1] medium is  $-11.50 \pm 0.12$  versus  $-8.98 \pm 0.06$  in TMACl [2] medium and the second is  $-24.44 \pm 0.26$  versus  $-19.22 \pm 0.07$ .

This study is performed by Capillary Electrophoresis coupled to an Inductively Coupled Plasma Mass Spectrometer (CE-ICP-MS). To limit carbonation, the media were packaged in vials with a layer of paraffin oil [1]. This study is complemented by Quantum Molecular Dynamics (QMD) in order to better understanding the interactions between the alkalis and the complexes formed.

The results of this study show a strong interaction of light alkalis (lithium and sodium) and a weak interaction of heavy alkalis (potassium, rubidium, caesium) with hydroxo complexes. Figure 1 shows normalised electropherograms of lithium, sodium and heavy alkalis (average of K, Rb, and Cs). Table 1 shows the results obtained at zero ionic strength for plutonium. The hydrolysis constants of neptunium V are very similar. This agrees with literature data, because neptunium and plutonium V are considered to be analogous [3].

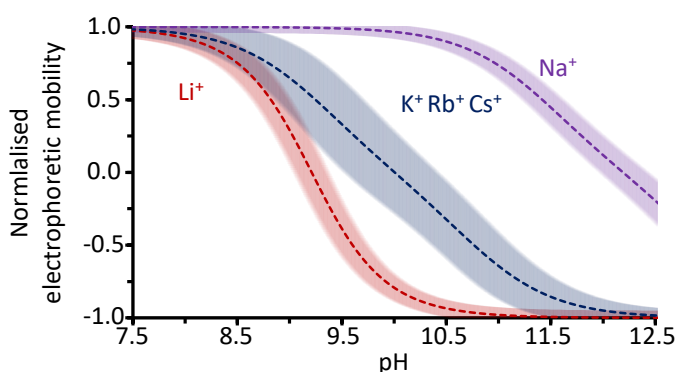


Figure 1: Normalised electrophoretic mobility of plutonium as a function of pH at an ionic strength of  $0.1 \text{ mol L}^{-1}$  in LiCl (red), NaCl (purple) and an average of KCl, RbCl, and CsCl (blue) with their uncertainties at  $k=2$

Table 1: Hydrolysis constants of plutonium at zero ionic strength obtained in this study

Species	Medium	$\text{Log}\beta^0$
$[\text{PuO}_2(\text{OH})]$	LiCl	-8.99 (0.24)
	KCl	-8.96 (0.14)
	RbCl	-9.26 (0.22)
	CsCl	-9.38 (0.20)
$[\text{PuO}_2(\text{OH})_2]^-$	LiCl	-18.74 (0.41)
	KCl	-19.98 (0.66)
	RbCl	-20.51 (0.39)
	CsCl	-20.01 (0.30)

## References

- [1] J. Aupiais, C. Christin, M. Levier, Inorg. Chem., 62, 4533-4539 (2023)
- [2] L. Rao, T. G. Srinivasan, A. Y. Garnov, P. Zanonato, P. D. Bernadato, A. Bismondo, Geochim. Cosmochim. Acta, 68, 4821-4830 (2004)
- [3] NEA, Chemical Thermodynamics of Neptunium and Plutonium, OECD Publishing, Paris

# Comprehensive structural and chemical analysis of secondary phases forming in Cr-doped (U,Ln)O<sub>2±x</sub>

D. Shirokiy,<sup>1</sup> M. Henkes,<sup>1</sup> A. Bukaemskiy,<sup>1</sup> K. O. Kvashnina,<sup>2,3</sup> E. Bazarkina,<sup>2,3</sup> P. Kadin,<sup>3</sup>  
M. Klinkenberg,<sup>1</sup> C. Trautmann,<sup>4</sup> D. Bosbach,<sup>1</sup> and G. L. Murphy,<sup>1</sup>

<sup>1</sup> Institute of Fusion Energy and Nuclear Waste Management, Forschungszentrum Jülich GmbH, 52428 Jülich, Germany

<sup>2</sup> The Rossendorf Beamline at ESRF, The European Synchrotron, CS40220, 38043, Grenoble, Cedex 9, France

<sup>3</sup> Helmholtz Zentrum Dresden-Rossendorf, Institute of Resource Ecology, 01314 Dresden, Germany

<sup>4</sup> GSI Helmholtz Centre for Heavy Ion Research GmbH, 64291 Darmstadt, Germany

\*e-mail: d.shirokiy@fz-juelich.de

Many countries that have used nuclear power a part of their energy supply have faced the issue of spent nuclear fuel (SNF) management and disposal. A variety of these, such as Germany, Finland, and others are inclined to solve this problem by using direct final disposal. The demand for nuclear energy and the need to reduce SNF-generated inventories have highlighted the need for alternative and advanced fuel sources. In this respect, chromium-doped UO<sub>2</sub> is a promising option, as it exhibits a higher performance during irradiation in the reactor than pure UO<sub>2</sub>, enabling a higher burnup and thus reducing the total SNF generation. Despite the high attractiveness, still little is known about the behaviour of Cr in SNF. In particular, the assumptions, that Cr tends to form additional phases with some fission and transmutation products (such as lanthanides (Ln), minor actinides (MA) and Pu), specifically perovskites[1] (Ln/MA/Pu)CrO<sub>3</sub>, have not yet been experimentally verified. The presence of additional phases not only affects the stability of SNF, but also creates localised sources of alpha-radiation and helium bubble formation. To study the secondary phases formed by chromium, we have employed the model system approach and synthesised[2] several samples of Cr-doped (U,Ln)O<sub>2±x</sub> [Ln=Ce, Pr, Gd] and analysed their chemistry using high resolution structural and redox methods. Particularly we used synchrotron X-ray powder diffraction and high-energy resolution fluorescence diffraction X-ray absorption near-edge structure spectroscopy measurements (HERFD-XANES) performed at ROBL BM20 beamline of the European Synchrotron Radiation Facility to determine the presence of described perovskite phase. The data obtained has been complemented by electron paramagnetic resonance analysis. Additionally, perovskite LnCrO<sub>3</sub> [Ln=Ce, Pr, Nd, Gd] pellets were synthesised and exposed to irradiation with swift heavy ions at GSI Helmholtz Centre for Heavy Ion Research to test their radiation damage response. Subsequently, the irradiated pellet surfaces were studied by grazing HERFD-XANES analysis, together with Raman spectroscopy and scanning electron microscopy. In summary, the obtained results make an important contribution to the understanding of the microstructural and chemical stability of spent Cr-doped UO<sub>2</sub> fuel, which is valuable for the science of solid-state chemistry and the nuclear industry in general.

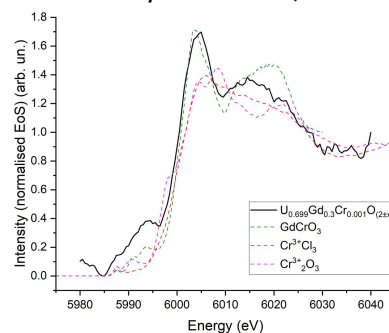


Figure 1: HERFD-XANES Cr K-edge of Cr-doped (Gd,U)O<sub>2±x</sub>

- [1] M. L. Fullarton, et al., *J Mater Chem A*, 2013, **1**, 14633-14640.  
[2] P. Kegler, et al., *Materials*, 2021, **14**.

# Chemical Imaging and Applications Using High Energy Resolution Fluorescence Detection for the Actinides

S. M. Webb<sup>1\*</sup>, N.P. Edwards<sup>1</sup>, and V. Noël<sup>1</sup>

<sup>1</sup>*Stanford Synchrotron Radiation Lightsource, SLAC National Accelerator Center, Menlo Park, CA, United States*

*\*e-mail: samwebb@slac.stanford.edu*

Microscale synchrotron radiation-based x-ray fluorescence (SR-XRF) chemical analyses can provide a unique capability for chemical signature recognition and classification capabilities for actinide micro-particle analysis. SR-XRF is well suited to forensic type analyses of small particles because it is rapid, non-destructive, highly sensitive, has good spatial resolution, and can provide chemical information on the elements that are present when combined with x-ray absorption spectroscopy (XAS). The combination of spatially resolved distribution and chemical information, often known as chemical imaging, effectively provides a “chemical morphology” of the sample of interest and can show how chemical states are distributed within and among a series of particles. This type of measurement is critical for understanding particle origin and history, as the spectroscopy, and its spatial distribution, can provide unique and complementary chemical signatures that may not be elucidated with other forms of measurement.

However, the conventional XAS capability in the near edge region as commonly implemented is often inadequate for systems that require high sensitivity or require a higher detail of spectroscopic information. This can be overcome with the combination of traditional micro SR-XRF and XAS, integrated with a high energy resolution fluorescence detector (HERFD) crystal analyzer. This has been recently implemented at BL 6-2b at SSRL and applied in the determination of the micron-scale oxidation state of uranium in particles. A discussion of the image and data processing techniques that can be applied using spatially resolved HERFD to obtain chemical and structural information, as well as the distribution of phases across different particles at the micro-scale, will also be presented.

# Effects of interfaces Title of presentation or poster (font size 16, bold, centered)

Y. Yang<sup>1\*</sup>

<sup>1</sup>*Institute of Applied Physics and Computational Mathematics, Beijing, China*

<sup>2</sup>*National Key Laboratory of Computational Physics, Beijing, China*

*\*e-mail: yang\_yu@iapcm.ac.cn*

Hydrogen-caused corruptions and irradiation-caused structural damages are two critical degradations that threaten the safe storage and practical applications of uranium. We perform multiscale ab initio calculations and kinetic Monte Carlo (KMC) simulations for the preferential hydriding phenomenon observed on a double-phase U-2.5 wt % Nb alloy, We find that because of different diffusion mechanisms, intrinsic  $\alpha$ -U and  $\gamma$ -U already show different hydrogen accumulation behaviors. The existence of random Nb atoms further inhibits hydrogen accumulation in  $\gamma$ -U.

We also investigate the distribution preference of hydrogen in the  $\alpha$ -U/UO<sub>2</sub> interface. We find that a monolayer of hydrogen atoms firstly assembles right in the interface between  $\alpha$ -U and UO<sub>2</sub>. Through detailed electronic state analysis, it is revealed that the formation of U–H bonds with uranium atoms at the UO<sub>2</sub> side favors this hydrogen atom assembly. The newly formed U–H bonds are similar to the U–O–U superexchange interactions in UO<sub>2</sub>. The incorporation of hydrogen in either  $\alpha$ -U or UO<sub>2</sub> is much higher in energy. After formation of two hydrogen monolayers, following hydrogen atoms have no such preference in the interface area, and tend to distribute inside  $\alpha$ -U.

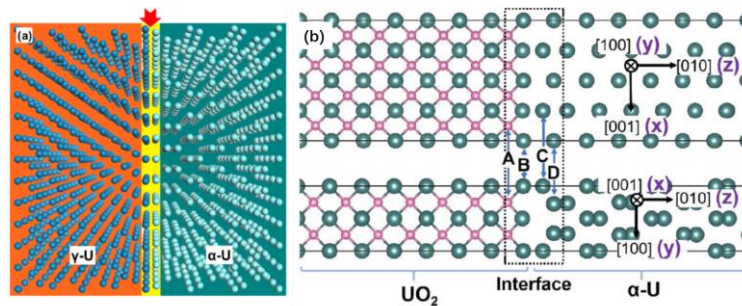


Figure 1: (a) Schematic model for hydrogen diffusions at the phase boundary. (b) The configuration of the  $\alpha$ -U/UO<sub>2</sub> interface for hydrogen distribution from side view.

## References

- [1] Xin-Xin Wang, Hefei Ji, Zi Li, Lijun Zhu, Xianglin Chen, Xiaoyong Yang, Ping Zhang, Peng Shi,\* Xiaolin Wang, Yu Yang,\* and Wenhui Duan, "What is the Role of Nb on Preferential Hydriding of Double-Phased Uranium, Stabilizing  $\gamma$ -U, or Avoiding Hydrogen Aggregation?", J. Phys. Chem. C 125, 9364 (2021).
- [2] X. X. Wang, Z. Li, B. Y. Ao, P. Zhang, P. Wang, Y. Yang\*, "A first-principles study on hydrogen distributions in the  $\alpha$ -U/UO<sub>2</sub> interface", J. Phys.: Condens. Matter 32, 195002 (2020).

# Insights into the structure and redox chemistry of surrogate MIMAS MOX ceramic materials

E. Iwaschko<sup>\*1</sup>, A. Bukaemsky<sup>1</sup>, M. Henkes<sup>1</sup>, L. Amidani<sup>2</sup>, K. Kvashnina<sup>2</sup>, G. Leinders<sup>3</sup>, D. Bosbach<sup>1</sup>, G. Murphy<sup>1</sup>

<sup>1</sup>Research Centre Jülich GmbH (FZJ), Germany

<sup>2</sup>European Synchrotron Radiation Facility (ESRF), France

<sup>3</sup>Belgian Nuclear Research Centre (SCK-CEN), Belgium

\*E-Mail: [e.iwaschko@fz-juelich.de](mailto:e.iwaschko@fz-juelich.de)

MOX (mixed oxide Fuel) is a topical nuclear fuel that has been used in nuclear power plants worldwide, in particular in Germany and France. MOX fuel is a ceramic commonly consisting of a mix of  $\text{UO}_2$  and  $\text{PuO}_2$  with varying Pu concentrations. Amongst other routes, MOX has been commonly produced by what is known as the “MIMAS route” (Micronized Master Blend) [1]. This route is well known to result in a heterogenous material that has microstructural regions of different Pu enrichments [2]. This usually expresses itself in a Pu rich, Pu poor and an intermediate phase [2]. Depending on processing conditions different regions in MOX vary in their Pu enrichment and in their size and distribution. Understanding their chemical properties, in particular the local chemistry and redox states of these regions is critical to ensuring safe and correct eventual disposal of MOX when occurring as spent nuclear fuel (SNF).

In this work, the industrial MIMAS process has been down-scaled to the laboratory level. That way, surrogate MIMAS MOX Pellets have been synthesized using  $\text{CeO}_2$  instead of  $\text{PuO}_2$ . Emphasis has been placed on the influence of the feed  $\text{UO}_2$  powder origin on the structure and chemistry of the final MIMAS MOX ceramic, namely via the precipitation of either Ammonia diuranate (ADU) or Ammonia uranyl carbonate (AUC). These two routes are inspired by the industrial synthesis of MIMAS MOX [1].

High resolution powder synchrotron X-ray diffraction (S-PXRD) measurements performed at the BM20 of the ESRF unveiled discrete but significant phase differences in the surrogate MOX ceramics. SEM-EDS further reveals the contrasting MOX materials that used different precursor materials, highlighting significant heterogeneity. Remarkably, high-energy-resolution fluorescence detected X-ray absorption near edge structure (HERFD-XANES) measurements performed on the U  $M_4$ -edge and Ce  $L_3$ -edge indicate considerable differences in the redox states of the MOX materials, in particular their simultaneous possession of both oxidised and reduced U and Ce respectively. These results subsequently suggest that in actual Pu based MIMAS MOX considerable diversity in redox states are found, but moreover highlight the significance of different synthesis routes in influencing the bulk chemistry of synthesized materials.

## References

- [1] D. Haas, A. Vandergheynst, J. van Vliet, R. Lorenzelli, J.-L. Nigon, Nuclear Technology, 106, 60 (1994).
- [2] R. Delville, M. Verwerft, Microscopy and Microanalysis, 29, 78 (2023).

# Invar effect in Ga/Al alloyed $\delta$ -Pu

Romuald Béjaud<sup>\*1,2</sup>, François Bottin<sup>1,2</sup>, Aloïs Castellano<sup>1,3</sup>, Lucas Baguet<sup>1,2</sup> and Marc Torrent<sup>1,2</sup>

<sup>1</sup>CEA, DAM, DIF, F-91297 Arpajon, France.

<sup>2</sup>Université Paris-Saclay, CEA, LMCE, 91680 Bruyères-le-Châtel, France.

<sup>3</sup>NanoMat/Q-Mat/CESAM and ETSF, Université de Liège Belgium.

\*e-mail: [romuald.bejaud@cea.fr](mailto:romuald.bejaud@cea.fr)

Several long-debated dynamical and elastic unusual properties of  $\delta$ -Pu and its alloys Pu-Ga/Al [1,2] has been captured within an unprecedented unified theoretical framework. This outcome is achieved thanks to machine learning accelerated *ab initio* simulations [3,4] enabling a fine description of strong electronic correlations [5] and explicit temperature effects [6,7,8].

For pure  $\delta$ -Pu, the experimental negative thermal expansion, equilibrium volume and anomalous softening of elastic properties are well reproduced by present simulations within this unified description. We demonstrate that the particular behavior of  $\delta$ -Pu is almost entirely associated with large anharmonic effects and is related to the extreme softening of the phonon spectrum [9].

This simulation procedure has recently been extended to Pu-Ga/Al alloys. Results shows a significant reduction of anharmonic effects with the addition of delatgen elements and also reproduce the famous invar effect of  $\delta$ -Pu alloys, with a thermal expansion going from negative to positive as a function of the Ga/Al content.

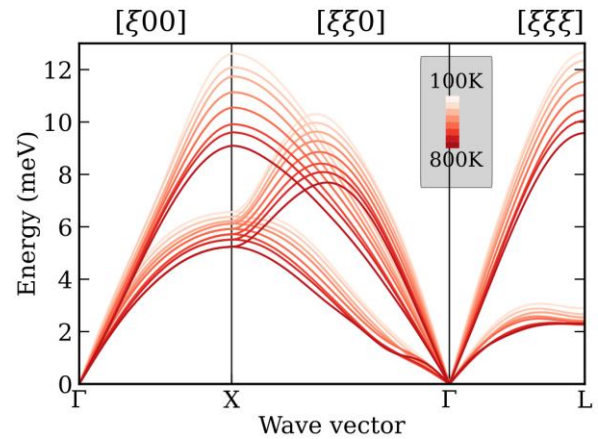


Figure 1: Phonon spectra of  $\delta$ -Pu, using DFT+U +SO MLACS simulations.

## References

- [1] D. Clark, *Plutonium Handbook: Nuclear science and materials science*, Plutonium Handbook (American Nuclear Society, 2019).
- [2] R. Caciuffo, G. H. Lander, and G. van der Laan, *Rev. Mod. Phys.* **95**, 015001 (2023).
- [3] A. Castellano, F. Bottin, J. Bouchet, A. Levitt, and G. Stoltz, *Phys. Rev. B* **106**, L161110 (2022).
- [4] A. Castellano, R. Béjaud, P. Richard, O. Nadeau, C. Duval, G. Geneste, G. Antonius, J. Bouchet, A. Levitt, G. Stoltz, F. Bottin, *Comput. Phys. Commun.* (submitted).
- [5] B. Amadon and B. Dorado, *Journal of Physics: Condensed Matter* **30**, 405603 (2018).
- [6] B. Dorado, F. Bottin, and J. Bouchet, *Phys. Rev. B* **95**, 104303 (2017).
- [7] J. Bouchet and F. Bottin, *Phys. Rev. B* **95**, 054113 (2017).
- [8] F. Bottin, J. Bieder, and J. Bouchet, *Comput. Phys. Commun.* **254**, 107301 (2020).
- [9] F. Bottin, R. Béjaud, B. Amadon, L. Baguet, M. Torrent, A. Castellano and J. Bouchet, *Phys. Rev. B* **109**, L060304 (2024).

# Th-H films: Synthesis and PES study

L. Havela<sup>1\*</sup>, O. Koloskova<sup>1</sup>, F. Huber<sup>2</sup>, T. Gouder<sup>2</sup>

<sup>1</sup>Charles University, Faculty of Mathematics and Physics, Prague, Czech Republic

<sup>2</sup>European Commission, JRC Karlsruhe, Germany

\*e-mail: ladislav.havela@matfyz.cuni.cz

Hydrides of *f*-metals are formed at ambient conditions with maximum H concentration  $RH_3$ . The only exception is Th, yielding (besides  $ThH_2$ ) a higher hydride  $Th_4H_{15}$ , i.e.  $ThH_{3.75}$  [1]. As metal polyhydrides made at ultra-high H pressures, are interesting high  $T_c$  superconductors, it is tempting to explore Th hydrides and their electronic structure. Indeed,  $Th_4H_{15}$  has a superconducting ground states with  $T_c \approx 8$  K [2] enhanced with respect to  $ThH_2$  (1.2 K). We synthesized films by reactive sputtering of Th in atmosphere with progressively increasing H concentration in Ar and performed in situ XPS/UPS study. Two distinct stages could be identified in the spectra, tentatively associated with the two know Th hydrides. XRD and transport studies will follow.

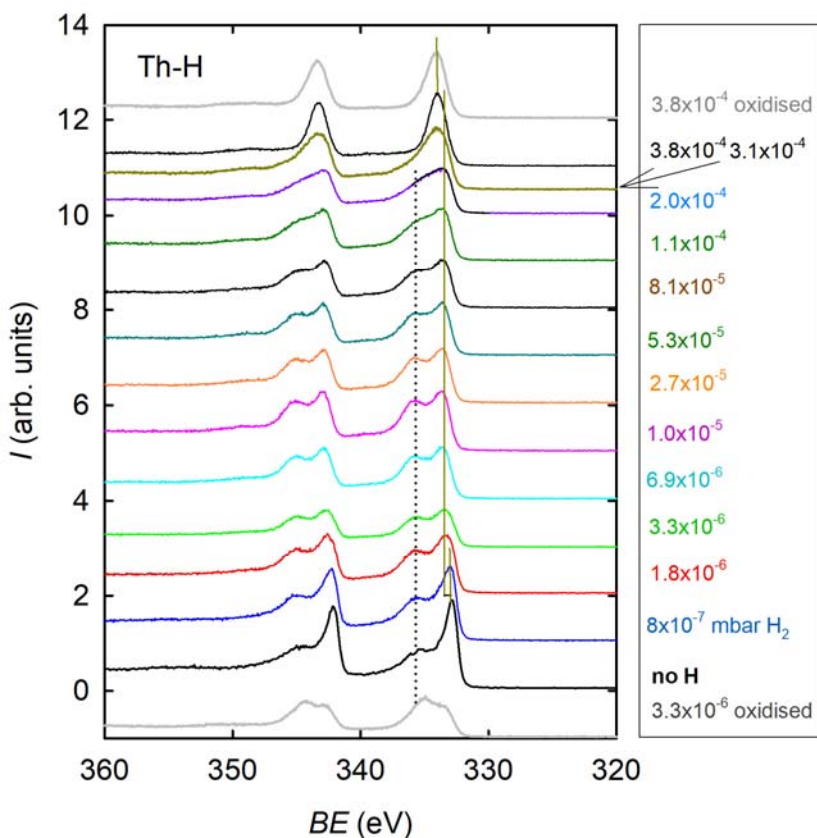


Fig.1: Evolution of the Th-4*f* spectra with increasing partial pressure of  $H_2$  in the sputter gas (Ar). The small shift of the narrow peak (towards higher binding energy) saturates in the  $10^{-5}$  mbar range, where we assume  $ThH_2$ . Going to the  $10^{-4}$  range, the spectra change into a triangular shape. Here we assume  $Th_4H_{15}$ . UPS spectra (not shown here) indicate dramatic reduction of the density of states at the Fermi at the latter stage.

Work supported by the Czech Science Foundation under the project No. 25-16339S and the EU project Access to JRC Physical Research Infrastructures 2022-2-RD-ACTUSLAB-PAMEC.

## References

- [1] see L. Havela, D. Legut, J. Kolorenc, Rep. Prog. Phys. 86, 056501 (2023) and references therein.
- [2] C.B. Satterwaite, D.T. Peterson, J. Less-Common Met. 26, 361 (1972).

# Electronic Structures and Physical Properties of $\alpha$ -Uranium Hydride under Shock Compression

Juan Cui<sup>1,2</sup>, Zhenguo Fu<sup>1,2</sup>, Huan Zheng<sup>1</sup>, Miao Zheng<sup>1</sup>, Dafang Li<sup>1,2</sup>, and Yu Yang<sup>1,2\*</sup>

<sup>1</sup>LCP, Institute of Applied Physics and Computational Mathematics, Beijing 100088, People's  
Republic of China

<sup>2</sup> National Key Laboratory of Computational Physics, Beijing 100088, China

\*e-mail: yang\_yu@iapcm.ac.cn

We investigate the thermophysical properties as well as underlying electronic mechanisms of  $\alpha$ -UH<sub>3</sub> under shock compression up to 200 GPa by performing first-principles molecular dynamics (FPMD) simulations. We obtain its principal Hugoniot derived from the equation of state (EOS) and compare that with available experimental data of UH<sub>3</sub> and other promising metal hydrides used for hydrogen storage. With respect to the pair correlation function (PCF), we depict the chemical picture of the shocked UH<sub>3</sub> and show the dissociation process under shock compression. Besides, a systematic study of electrical transport properties, optical reflectivity, density of states and electron localization functions under shock compression provides a comprehensive insight into the structures and properties of shocked UH<sub>3</sub>, which is expected to facilitate the understanding of uranium hydrides for their applications in nuclear industry.



# Low temperature physics and materials science of elemental uranium thin films and alloys

C. Bell<sup>1\*</sup>, R. S. Springell<sup>1</sup>, L. Harding<sup>1</sup>, G. H. Lander<sup>1</sup>, S. A. Hussain<sup>1</sup>, K Brewer<sup>1</sup>, L. Onuegbu<sup>1</sup>, R. Nicholls<sup>1</sup>, J. Bouchet<sup>2</sup>, S. Giblin<sup>3</sup>

<sup>1</sup>School of Physics, University of Bristol, Bristol BS8 1TL, United Kingdom

<sup>2</sup>CEA, DES, IRESNE, DEC, SESC, LM2C, F-13108 Saint-Paul-Lez-Durance, France

<sup>3</sup>School of Physics and Astronomy, Queen's Buildings, Newport Road, Cardiff, CF24 3AA, United Kingdom

\*e-mail: cb13399@bristol.ac.uk

Thin films offer a myriad of ways of controlling and tuning states of matter. We can apply epitaxial strain, vary the dimensionality, and combine different order parameters together using proximity effects to name but a few of the possibilities [1]. In this talk I will briefly describe two case studies of engineering structural and electronic states with thin films. First, I will show an intriguing study of a topotactic phase transition in elemental U between an epitaxy-induced metastable hexagonal-close-packed phase, and the bulk ground-state, the orthorhombic structure [2]. Second, I will introduce using alloys of U and Nb to study the use of spin-orbit physics to generate novel superconducting order parameters in polycrystalline films [3].

## References

- [1] Springell *et al.*, *Advances in Physics* **71**, 87 (2022).
- [2] Nicholls *et al.*, *Phys. Rev. Materials* **6**, 103407 (2022).
- [3] Hussain *et al.* (in preparation).

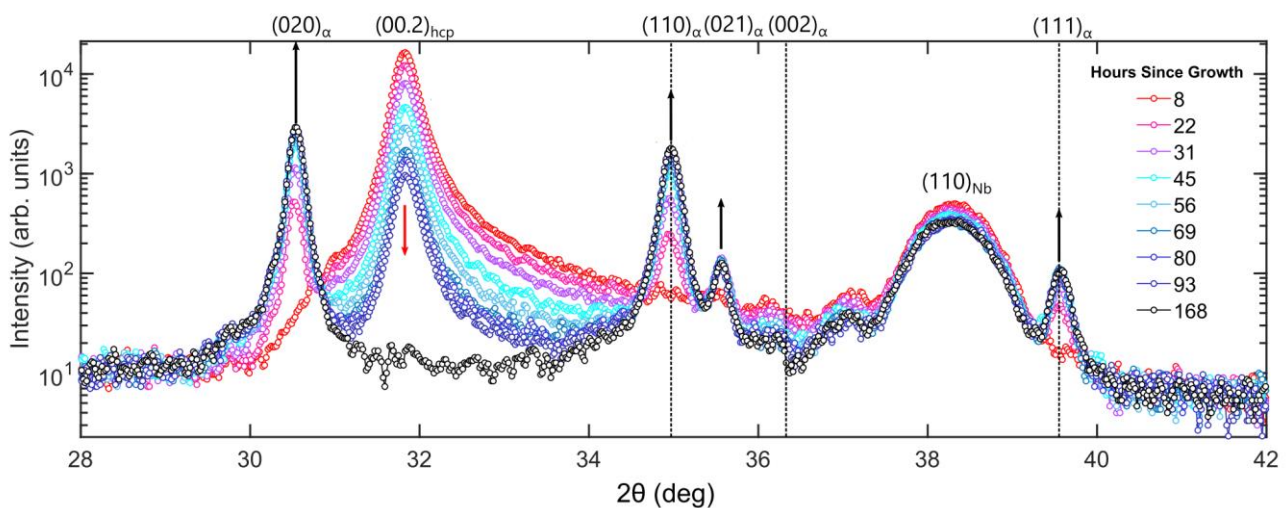


Figure 1: Specular scans of a 1400 Å hexagonal-close-packed U film grown onto a polycrystalline Cu{111} surface over the first seven days following growth. Arrows indicate the direction of growth/decay of the Bragg peaks. The dashed line represents the position of the bulk U orthorhombic (002) reflection. Taken from Ref. [2].

# Uranium hydrides with substitutions: thin films studies

O. Koloskova<sup>1\*</sup>, E. Tereshina-Chitrova<sup>1</sup>, T. Gouder<sup>2</sup>, and L. Havela<sup>3</sup>

<sup>1</sup> Institute of Physics, Czech Academy of Sciences, Czech Republic

<sup>2</sup> European Commission, Joint Research Centre (JRC), Germany

<sup>3</sup> Charles University, Faculty of Mathematics and Physics, Czech Republic

\*e-mail: koloskova@fzu.cz

Uranium hydrides, recognized as the first known ferromagnets with magnetism driven purely by 5f states, have been under investigation for over 50 years and still reveal unexpected phenomena. Notably, their relatively high Curie temperature (165 K [1]) does not align with the moderate uranium atom distances (0.360 nm for  $\alpha$ -UH<sub>3</sub> and 0.331 nm for  $\beta$ -UH<sub>3</sub>), raising questions about the applicability of Hill physics. Furthermore, UH<sub>2</sub> [2], synthesized exclusively in thin film form with a longer interatomic distance ( $d_{U-U} = 0.378$  nm), exhibits a lower Curie temperature (120 K) and magnetic moment (0.8  $\mu_B$ ) compared to trihydrides (1  $\mu_B$ ).

Studies of thin films with exceptionally clean surfaces have enabled high-quality XPS/UPS data acquisition, revealing that polar bonds between U-6d and 7s states and H-1s states play a crucial role in uranium hydride magnetism. Supporting this observation, bulk studies of (UH<sub>3</sub>)<sub>1-x</sub>T<sub>x</sub> (T: transition metals such as Mo, Zr, Nb, etc. [3]) demonstrate an enhancement of the transition temperature due to an elevated effective H/U ratio. However, in thin film form, these values are reduced. This discrepancy may arise from the higher instability of H atoms in films, caused by a combination of substitution effects and the highly energetic deposition process. To achieve higher Curie temperatures, it is essential to augment the H content.

One proposed approach involves substituting Th while maintaining the  $\beta$ -UH<sub>3</sub> crystal structure, as one of thorium hydrides (e.g., Th<sub>4</sub>H<sub>17</sub>) can accommodate more than three hydrogen atoms per thorium atom. Preliminary results from these studies will be presented, including XPS analyses of the electronic structure in comparison with physical properties (magnetization and resistivity) and the crystal structure of thin films.

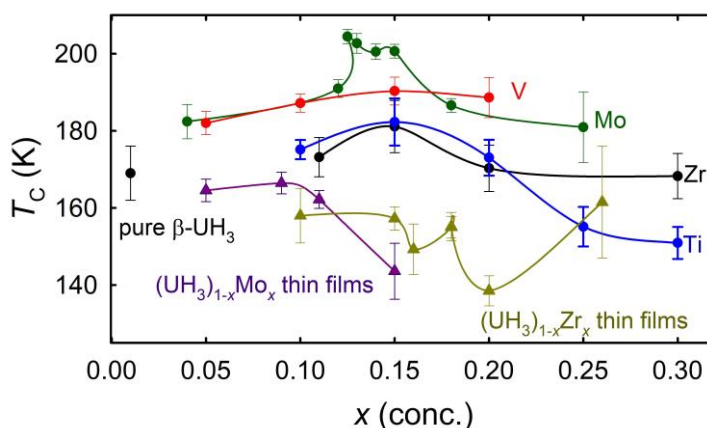


Figure 1: Comparison of concentration dependences of thin films and bulk samples with various T-metal substitutions. Data for bulk samples were adopted from [3].

Work supported by the Czech Science Foundation under the project No. 25-16339S and the EU project Access to JRC Physical Research Infrastructures 2022-2-RD-ACTUSLAB-PAMEC.

## References

- [1] L. Kývala *et al.*, J. Nucl. Mat., 567, 153817 (2022).
- [2] L. Havela *et al.*, Inorg. Chem., 57, 14727 (2018).
- [3] O. Koloskova *et al.*, J. Al. Comp., 856, 157406 (2021).

# Innovative Lexan-Aerogel detector for fission track for Nuclear Forensics

BabayewRami<sup>1,2</sup>, Yaacov Yehuda-Zada<sup>1,2</sup>, Galit Bar<sup>3</sup>, Elgad Noam<sup>1,2</sup>, Last Mark<sup>4</sup>, Jan Lorincik<sup>5</sup>,

Itzhak Orion<sup>2</sup>, Shay Dadon<sup>1</sup>, Aryeh Weiss<sup>6</sup>, Galit Katarivas Levy<sup>7</sup>, Halevy Itzhak<sup>2</sup>

<sup>1</sup> Physics Department, Nuclear Research Center Negev, Beer-Sheva, Israel

<sup>2</sup> Nuclear Engineering, Faculty of Engineering Sciences, Ben Gurion University of the Negev, Israel

<sup>3</sup> Department of Solid-State Physics, Soreq Nuclear Research Center, Yavne, Israel

<sup>4</sup> Department of Software and Information Systems Engineering, Faculty of Engineering Sciences, Ben Gurion University of the Negev, Israel

<sup>5</sup> Nuclear Fuel Cycle Department, Research Centre Řež, Hlavní130, Husinec, Czech Republic

<sup>6</sup> Bar Ilan University, Ramat Gan P.O.B. 90000 5290002 Israel

<sup>7</sup> Dept. of Biomedical Engineering, Faculty of Engineering Sciences Ben-Gurion University of the Negev, Beer-Sheva, Israel

\*e-mail: [halevy.itzhak.dr@email.com](mailto:halevy.itzhak.dr@email.com)

Innovative Lexan-Aerogel detector for fission track was developed.

From the event of fission, the energetic fission products are traveling with the three parameters energy, geometry and absorption on the path ( $dE/dx$ ).

The idea behind the new detector is to add distance to the path without adding too much absorption. By sol gel technique we achieved this goal, it is aerogel that has solid structure but its absorption is very low. We can prepare the aerogel in wide range of densities, 0.05-0.8 gr/cm<sup>3</sup>.

It was important to find an aerogel that is not activated in the flux of the nuclear reactor.

We used the TRIM [1] software to instigate the path of the fission products and the energy loss.

We simulated also the fission product stars by our Trainer [2] software. Results of different width of aerogel 0-65 $\mu$ m are shown in figure 1. Results of different penetration in our Lexan-Aerogel detector depending on the width of aerogel 0-65 $\mu$ m are shown in figure 2.

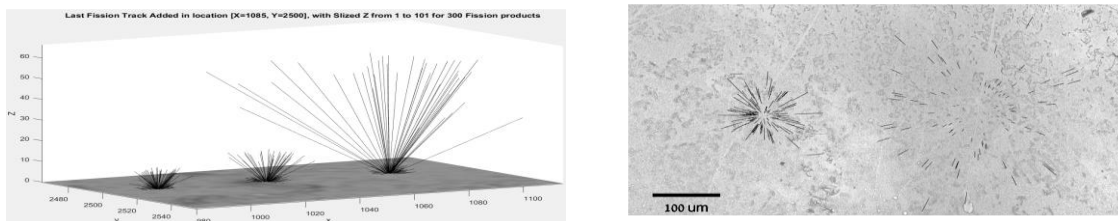


Figure 1: FT in different width of aerogel 0-65 $\mu$ m is shown in simulation and microscope

## References

[1] Rami Babayew, Yaacov Yehuda-Zada, Noam Elgad, Lorincik Jan, Orion Itzhak, Aryeh Weiss, Galit Katarivas Levy, Itzhak Halevy; Nuclear forensics – Fission track Analysis – Simulation for training. Journal of Radioanalytical and Nuclear Chemistry, Volume 333, pages 3359–3375, (2024)

# Structural incorporation of U(V) as a dominant U stabilization pathway during Fe(II)-promoted recrystallization of Fe-oxyhydroxysulfates

L. Kononova<sup>1\*</sup>, M. Åström<sup>1</sup>, D. Prieur<sup>2,3</sup>, E. Bazarkina<sup>2,3</sup>, K. Kvashnina<sup>2,3</sup>, N. Chen<sup>4</sup>, and C. Yu<sup>1</sup>

<sup>1</sup>Linnaeus University, Sweden

<sup>2</sup>The European Synchrotron, France

<sup>3</sup>Helmholtz-Zentrum Dresden-Rossendorf, Germany

<sup>4</sup>Canadian Light Source, Canada

\*e-mail: liubov.kononova@lnu.se

Oxidation of sulfide-bearing soils and rocks releases acidic sulfate-rich solutions with elevated levels of U(VI) to adjacent ecosystems. This process also results in the formation of Fe(III) oxyhydroxysulfates (e.g., schwertmannite and jarosite) that can adsorb considerable U(VI) and thus limit its mobilization/dispersion [1]. However, these U(VI)-bearing oxyhydroxysulfates are unstable and can recrystallize to more stable Fe(III) oxides (e.g., lepidocrocite and goethite), especially under circumneutral conditions in the presence of Fe(II). These recrystallization processes and co-linked reactions between Fe(II) and U(VI), like the systems with ferrihydrite, Fe(II), and U(VI) [2], represent a key but largely unexplored pathway for U retention/stabilization in these settings.

Here, we conducted two batch experiments by reacting U(VI)-sorbed schwertmannite (U-SCH, 0.2% U) and jarosite (U-JA, 0.03% U), with 0, 1, 3, and 50 mM Fe(II) at near-neutral pH for 1 hour to 2 weeks in an anaerobic chamber. The XRD analysis revealed complete transformation of U-SCH to goethite within 2 weeks, while U-JA only partially transformed to goethite even at the highest Fe(II) concentration. The edge energies of U L<sub>3</sub>-edge XANES spectra of the reacted U-SCH and U-JA were intermediate between surface-sorbed uranyl and UO<sub>2</sub> (Figure 1), suggesting a potential predominance of U(V). ITFA analysis of the U M<sub>4</sub>-edge HERFD-XANES data [3] confirmed the strong dominance of U(V), comprising 55–71% in U-SCH and 27–57% in U-JA. The remaining U was primarily U(VI), with a small fraction (up to 8%) as U(IV).

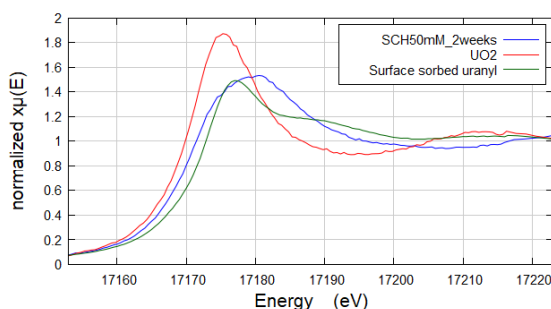


Figure 1. U L<sub>3</sub>-edge XANES spectra of the reacted U-SCH and reference spectra for surface-sorbed uranyl and UO<sub>2</sub>

## References

- [1] C. Yu, U. Lavergren, P. Peltola, H. Drake, B. Bergbäck, and M. E. Åström, "Retention and transport of arsenic, uranium and nickel in a black shale setting revealed by a long-term humidity cell test and sequential chemical extractions," *Chem. Geol.*, vol. 363, pp. 134–144, Jan. 2014, doi: 10.1016/j.chemgeo.2013.11.003.
- [2] M. S. Massey *et al.*, "Competing retention pathways of uranium upon reaction with Fe(II)," *Geochim. Cosmochim. Acta*, vol. 142, pp. 166–185, Oct. 2014, doi: 10.1016/j.gca.2014.07.016.
- [3] K. O. Kvashnina and S. M. Butorin, "High-energy resolution X-ray spectroscopy at actinide M<sub>4,5</sub> and ligand K edges: what we know, what we want to know, and what we can know," *Chem. Commun.*, vol. 58, no. 3, pp. 327–342, 2022, doi: 10.1039/D1CC04851A.

## New insight to U(V) stability in ancient titanate minerals

L. M. Mottram<sup>1</sup>, A. A. Friskney<sup>1</sup>, L. Harding<sup>2</sup>, K. Kvashnina<sup>3,4</sup>,

E. F. Bazarkina<sup>3,4</sup> and C. L. Corkhill<sup>5\*</sup>

<sup>1</sup>*Department of Materials Science and Engineering, The University of Sheffield, UK*

<sup>2</sup>*School of Physics, The University of Bristol, UK*

<sup>3</sup>*Helmholtz-Zentrum Dresden-Rossendorf (HZDR), Institute of Resource Ecology, Germany*

<sup>4</sup>*The Rossendorf Beamline at ESRF – The European Synchrotron, France*

<sup>5</sup>*School of Earth Science, The University of Bristol, UK*

*\*e-mail: c.corkhill@bristol.ac.uk*

Naturally-occurring radioactive accessory minerals, containing a significant proportion of U and Th, are of interest in the development of safe disposal strategies for actinide-containing radioactive wastes generated through civil nuclear energy and nuclear military operations. Two key examples of these wastes are U-containing spent nuclear fuel and inventories of separated PuO<sub>2</sub> derived from spent nuclear fuel reprocessing, both of which require safe immobilisation over timescales of many hundreds of thousands of years. The eventual disposal solution for such actinide-bearing radioactive wastes is in a geological disposal facility, up to 1 km below the surface of the Earth. In this environment, the eventual release of U or Pu to the geosphere and biosphere will be controlled by the dissolution of waste by groundwater. To mitigate against this, and to build a robust post-closure safety case for disposal to the satisfaction of the environmental safety regulators, it is necessary to develop innovative, durable materials for actinide immobilisation.

A suite of naturally occurring titanate minerals have been identified as being excellent templates for actinide immobilisation materials, having retained most of their U/Th inventories for up to 1 billion years, despite undergoing hydrothermal alteration and becoming metamict as a result of self-alpha radiation damage. Studying naturally-occurring specimens of these minerals, including titanate pyrochlore [(Ca,U)Ti<sub>2</sub>O<sub>7</sub>], zirconolite [(Ca,U)ZrTi<sub>2</sub>O<sub>7</sub>] and, to a lesser extent, brannerite [UTi<sub>2</sub>O<sub>6</sub>] and thorutite [ThTi<sub>2</sub>O<sub>6</sub>], can give insight to the long-term behaviour of actinide-containing radioactive waste materials in geological disposal environments.

While these minerals have attracted attention from researchers for a number of decades, advances in analysis techniques have enabled new insights into the speciation of U in these minerals. In particular, a combination of X-ray spectroscopic techniques, including High Energy Resolution Fluorescence Detected X-ray Absorption Near Edge Spectroscopy (HERFD XANES) at the U M<sub>4</sub>-edge, in both bulk and macro-focus mode, and micro-focused Extended X-ray Absorption Fine Structure ( $\mu$ -EXAFS) at the U L<sub>3</sub>- and U L<sub>1</sub>-edges have been used to evidence novel U speciation and local coordination in these exotic radio-minerals. These results lay the foundations for the development of an entirely new range of materials for actinide immobilisation, with particular relevance to the UK's 140 tonne inventory of civil separated plutonium.

# Uranium retention by chukanovite an Fe(II) hydroxycarbonate corrosion product of canisters in deep geological repositories

C. Soto-Ruiz<sup>1\*</sup>, U. Alonso<sup>1</sup> and T. Missana<sup>1</sup>

<sup>1</sup>CIEMAT, Avda. Complutense 40, Madrid (Spain), 28040

\*e-mail: Carla.Soto@ciemat.es

The deep geological repository (DGR) is the best solution for confining high-level radioactive waste (HLRW). DGRs are multibarrier systems, where a carbon steel container, confining the waste, is surrounded by a compacted bentonite barrier and placed in an adequate geological formation. The purpose of DGRs is to delay radionuclide migration to the biosphere until their radiation is inoffensive. The radiation emitted by the waste together with the saline pore water in the clay, contribute to the corrosion of the canister, which form corrosion products at the canister/bentonite interface.

Chukanovite,  $\text{Fe}_2(\text{OH})_2(\text{CO}_3)$ , a Fe (II) hydroxycarbonate is a corrosion product found in this environment, if reducing conditions are present and the carbonate content is significant [1], [2], [3].

The objective of this research is to study the uranium ( $^{233}\text{U}(\text{VI})$ ) retention by chukanovite and to evaluate possible redox effects. To the best of our knowledge no previous studies on this issue are available in the literature.

The chukanovite was synthesized under anoxic controlled conditions and thoroughly characterized, confirming that the material is entirely composed by Fe(II) (Figure 1).

Batch sorption isotherms were carried out with two different electrolytes ( $\text{NaHCO}_3$  and  $\text{NaCl}$ ) at an ionic strength of 0.1 M and the equilibrium pH (7-8).

Uranium presents high sorption in chukanovite ( $K_d \sim 1 \cdot 10^3$  to  $1 \cdot 10^4 \text{ mL} \cdot \text{g}^{-1}$ ), approximately on order of magnitude higher in  $\text{NaCl}$  than in  $\text{NaHCO}_3$ . Different retention mechanisms are responsible of uranium retention in both systems that will be discussed.

This study was co-funded by the European Union under Grant Agreement n° 101166718 (EURAD2) and by the Spanish Ministry of Science and Innovation (ACOMER Project PID2022-138402NB-C22).

## References

- [1] E. Erdős, H. Altorfer, Mater. Corros., 27, 304-312 (1976).
- [2] V. Pandarinathan, K. Lepková, W. Van Bronswijk, Corros. Sci. 85, 26-32 (2014).
- [3] J. Duboscq, M. Abdelmoula, C. Rémazeilles, M. Jeannin, R. Sabot, P. Refait, J. Phys. Chem. Solids, 138, 109310 (2020).

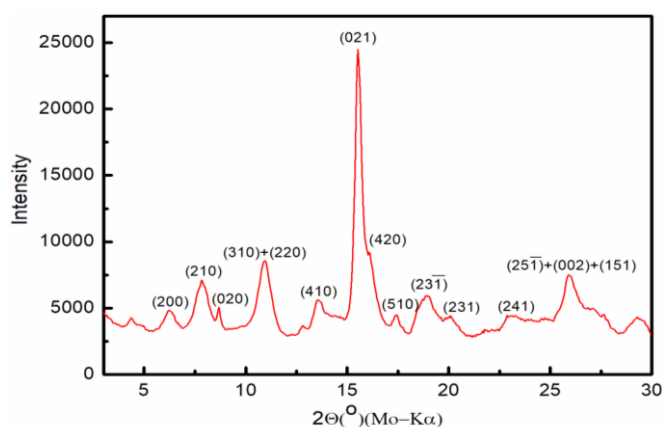


Figure 1. X-ray diffractogram under anoxic conditions of the chukanovite synthesized.

# Revealing the crystal chemistry and dissolution kinetics of doped uranium dioxide nuclear fuel

L. M. Harding<sup>1\*</sup>, E. Lawrence Bright<sup>2,3</sup>, C. Bell<sup>1</sup>, J. Laverock<sup>4</sup>, T.B. Scott<sup>1</sup>, A. Adamska<sup>5</sup>, C. Corkhill<sup>6</sup>, and R. Springell<sup>1</sup>

<sup>1</sup>*School of Physics, University of Bristol, United Kingdom*

<sup>2</sup>*The Rossendorf Beamline (ROBL), European Synchrotron Radiation Facility, Grenoble, France*

<sup>3</sup>*Institute of Resource Ecology, Helmholtz-Zentrum-Dresden-Rossendorf, Dresden, Germany*

<sup>4</sup>*School of Chemistry, University of Bristol, United Kingdom*

<sup>5</sup>*Sellafield Ltd, Warrington, United Kingdom*

<sup>6</sup>*School of Earth Sciences, University of Bristol, United Kingdom*

\*e-mail: [lottie.harding@bristol.ac.uk](mailto:lottie.harding@bristol.ac.uk)

Metal-oxide dopants are used to improve microstructural behaviour in UO<sub>2</sub>. Understanding the role dopants have on the corrosion of UO<sub>2</sub> is vital for predicting behaviours in long-term storage facilities. Inconsistency in the synthesis of bulk doped phases has resulted in contradicting findings using U M<sub>4</sub>-edge HERFD-XANES [1,2] regarding the crystal chemistry. Thin films offer a significant advantage to this problem, as systematic ternary phases can be engineered to explore the role of dopants in homogeneous single crystals [3]. We present the structural and chemical characterisation of Al-, Cr-, and Ti-doped (0 – 15 mol %) [001]-UO<sub>2</sub> epitaxial films. In-situ XRD and U M<sub>4</sub>-edge XES has been conducted in an aqueous environment at BM20, ESRF, inducing radiolysis and revealing the corrosion chemistry and dissolution kinetics of doped-UO<sub>2</sub>.

## References

- [1] H. Smith *et al.*, *Comms Chem.*, 5, (2022)
- [2] G. Murphy *et al.*, *Nat. Comms.*, 14, (2023)
- [3] R. Springell *et al.*, *Adv. In Phys.*, 71 (2022)

# Probing the local disorder in $U_3O_7$ and $U_3O_8$ by neutron total scattering

A. Vieyra-Huerta<sup>1,2\*</sup>, G. Leinders<sup>1</sup>, H. Fischer<sup>3</sup>, G. Baldinozzi<sup>4</sup>, D. Lamoen<sup>2</sup>, M. Verwerft<sup>1</sup>

<sup>1</sup>Belgian Nuclear Research Centre (SCK CEN), Institute for Nuclear Energy Technology, Belgium

<sup>2</sup>EMAT, Department of Physics, University of Antwerp, Belgium

<sup>3</sup>Institut Laue-Langevin, France

<sup>4</sup>Université Paris-Saclay, CentraleSupélec, CNRS, SPMS, France

\*e-mail: [alejandro.vieyra.huerta@sckcen.be](mailto:alejandro.vieyra.huerta@sckcen.be)

The behavior of nuclear fuel to oxidation and corrosion is a key topic for the safety assessment of nuclear (interim) storage facilities.  $U_4O_9$ ,  $U_3O_7$ , and  $U_3O_8$  compounds are part of the series of oxides that form under oxidation of  $UO_2$  [1]. Currently, many of these structures are well known [2,3], but some discrepancies exist between the results obtained by standard diffraction techniques, mainly sensitive to the long-range order of these structures, and the electronic structure and the short-range order probed by techniques such as XAFS, NIXS, RIXS, and PDF analysis [4,5].

Due to oxidation, the atomic environments distort from the pristine cubic coordination of  $UO_2$  into cuboctahedral oxygen clusters, which form a defect pattern leading to the long-range modulations observed in  $U_4O_9$  and  $U_3O_7$  [2,3]. As the degree of oxidation increases further, pentagonal bipyramid or octahedral environments are formed in  $U_3O_8$ . For all compounds, neutron powder diffraction proved indispensable to refine the crystal structures [2,6,7]. Interestingly, in  $U_3O_7$ , which is the predecessor of  $U_3O_8$ , the cuboctahedral coordination environments appear severely distorted from regular geometry, but a transition to the pentagonal bipyramidal environments typical of  $U_3O_8$  is not apparent in the long-range model. This opens some questions about the relationship with the  $U_3O_8$  structure, which remains under investigation. To probe the local structures and examine the structural relationships in more detail, we have performed neutron total scattering experiments on  $U_3O_7$  and  $U_3O_8$  at several temperatures between 6K and 300K. Results of the data set processing will be presented and discussed.

## References

- [1] J.D. Higgs, B.J. Lewis, W.T. Thompson, Z. He, *Journal of Nuclear Materials*, 366 (2007) 99.
- [2] R.I. Cooper, B.T.M. Willis, *Acta Crystallographica Section A*, 60 (2004) 322.
- [3] G. Leinders, R. Delville, J. Pakarinen, T. Cardinaels, K. Binnemans, M. Verwerft, *Inorganic Chemistry*, 55 (2016) 9923.
- [4] S.D. Conradson, *et al.*, *Physical Review B*, 88 (2013) 115135.
- [5] G. Leinders, R. Bes, K.O. Kvashnina, M. Verwerft, *Inorganic Chemistry*, 59 (2020) 4576.
- [6] B.O. Loopstra, *Journal of Inorganic & Nuclear Chemistry*, 39 (1977) 1713.
- [7] G. Leinders, G. Baldinozzi, C. Ritter, R. Saniz, I. Arts, D. Lamoen, M. Verwerft, *Inorganic Chemistry*, 60 (2021) 10550.



# Magneto-elastic and multipolar interactions in $U_xTh_{1-x}O_2$

S. Adnan<sup>1</sup>, Z. Hua<sup>2</sup>, Puspa Upreti<sup>3</sup>, Shuxiang Zhou, Sabin Regmi<sup>2</sup>, Krzysztof Gofryk<sup>2</sup>, J Matthew Mann<sup>4</sup>, David H Hurley<sup>2</sup>, Michael E Manley<sup>3</sup>, and M. Khafizov<sup>1\*</sup>

<sup>1</sup>The Ohio State University, USA

<sup>2</sup>Idaho National Laboratory, USA

<sup>3</sup>Oak Ridge National Laboratory, USA

<sup>4</sup>Air Force Research Laboratory, USA

\*e-mail: khafizov.1@osu.edu

We investigate phonon-spin interaction in  $U_xTh_{1-x}O_2$  using thermal transport, magnetization, and phonon linewidth measurements. Single crystal spanning  $0 < x < 1$  U composition were fabricated using hydrothermal method. Thermal conductivity was measured over 77 - 300 K range. Conductivity of  $ThO_2$  exhibits temperature trends consistent with phonon mediated thermal transport limited by 3-phonon interactions.  $UO_2$  conductivity has a strong suppression at low temperature governed by phonon-spin interaction. Small concentration of U added to  $ThO_2$  immediately suppresses conductivity beyond what is expected from a Rayleigh-type phonon scattering by substitutional impurity. The suppression is best captured with a resonant scattering mechanism. Resonant frequency and intensity were determined based on a model that uses first-principles derived phonon and phonon-phonon interactions and considers interaction between phonons and paramagnetic ions with a spin  $S=1$ . Measured resonant scattering parameters as function uranium concentration are shown in Figure 1 [1]. Resonant frequency and intensity exhibit strong dependence on uranium concentration. Magnetization measurement on a selected samples show a departure from Curie-Weiss law consistent with previous measurements and attributed to magnetoelastic interactions. Phonon linewidth was measured using inelastic X-ray scattering to confirm the thermal transport model.

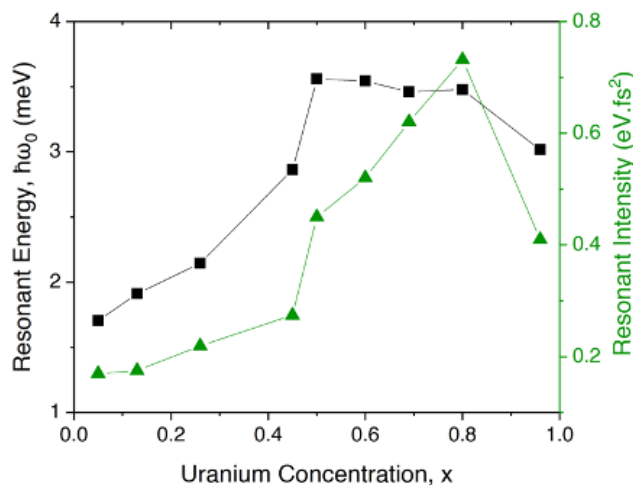


Figure 1: Parameters summarizing the phonon-spin interaction obtained from analysis of low temperature thermal conductivity in  $U_xTh_{1-x}O_2$ .

Current hypothesis is that the resonant frequency corresponds to a cross-over between phonon and paramagnon dispersions. Our measurement serves as a way to measure paramagnons and assess the strength of spin exchange and magnetoelastic interactions in  $U_xTh_{1-x}O_2$ . The resonant frequency exhibits two regimes. On high uranium side, the resonant frequency is weakly dependent on uranium concentration, but on low uranium concentration side, the resonant frequency gradually increasing with increasing x. These two distinct regimes can be attributed to a difference in the strength of spin exchange interactions.

References: [1] S. Adnan et al., <https://doi.org/10.48550/arXiv.2412.05448>.

# Examining the uranium valence states from anomalous diffraction

G. Leinders<sup>1\*</sup>, I. Arts<sup>2</sup>, R. Bes<sup>3</sup>, K. Kvashnina,<sup>4,5</sup> O. G. Grendal<sup>6</sup> and M. Verwerft<sup>1</sup>

<sup>1</sup>Belgian Nuclear Research Centre (SCK CEN), Institute for Nuclear Energy Technology, Belgium

<sup>2</sup>EMAT & NanoLab Center of Excellence, Dept. of Physics, University of Antwerp, Belgium

<sup>3</sup>Department of Physics and Helsinki Institute of Physics, University of Helsinki, Finland

<sup>4</sup>Rossendorf Beamline, European Synchrotron Radiation Facility (ESRF), France

<sup>5</sup>Institute of Resource Ecology, Helmholtz Zentrum Dresden Rossendorf (HZDR), Germany

<sup>6</sup>Department of Materials Science and Engineering, Norwegian University of Science and Technology, Norway

\*e-mail: gregory.leinders@sckcen.be

Uranium finds its main application as nuclear fuel in commercial power generation and research reactors. However, because of its wide range of possible valence states and complex coordination chemistry, the physico-chemical properties of uranium are being studied in many other application fields as well [1]. Uraniumdioxide (UO<sub>2</sub>) exhibits a simple fluorite structure with cubic coordination of tetravalent cations. UO<sub>2</sub> is quite susceptible to oxidation, leading to structural phase transformations and the occurrence of mixed-valence compounds such as U<sub>4</sub>O<sub>9</sub>, U<sub>3</sub>O<sub>7</sub> and U<sub>3</sub>O<sub>8</sub>. The first group of oxides (U<sub>4</sub>O<sub>9</sub> and U<sub>3</sub>O<sub>7</sub>) are structurally closely related to a fluorite-type lattice, but the excess anions form clusters and develop a long-range periodical order. A transformation from the fluorite-type structure to a layered structure occurs when oxidation progresses from U<sub>3</sub>O<sub>7</sub> to U<sub>3</sub>O<sub>8</sub>, which makes the U<sub>3</sub>O<sub>7</sub> phase an interesting structure to unravel.

The uranium valence distribution in these mixed-valence oxides has been investigated extensively, using a variety of experimental, empirical, and theoretical methods, such as X-ray absorption spectroscopy, X-ray photoelectron spectroscopy, bond-valence sum, and electronic structure calculations. However, the results were not always consistent [2], e.g. two different distributions have been reported for U<sub>3</sub>O<sub>8</sub>: [ $\frac{1}{3} \times \text{U(IV)} + \frac{2}{3} \times \text{U(VI)}$ ] and [ $\frac{2}{3} \times \text{U(V)} + \frac{1}{3} \times \text{U(VI)}$ ]. Nowadays, consensus has been reached regarding the latter case, supported by results from HERFD-XANES measurements [2]. For the U<sub>3</sub>O<sub>7</sub> phase, a ratio of [ $\frac{1}{3} \times \text{U(IV)} + \frac{2}{3} \times \text{U(V)}$ ], without a substantial contribution of U(VI), was pointed out from similar XAS measurements [3]. However, a more complicated charge distribution scheme, including a small contribution of U(VI), can be assigned to specific cation sites in U<sub>3</sub>O<sub>7</sub>, taking into account that the crystal structure comprises an expanded cell containing 60 uranium and 140 oxygen atoms (U<sub>60</sub>O<sub>140</sub>) [4]. To better address these discrepancies, we have performed diffraction anomalous fine structure (DAFS) experiments, aimed at obtaining site-specific information on the chemical state of uranium. A newly developed analysis routine was recently reported and applied on experimental datasets of UO<sub>2</sub> and KUO<sub>3</sub> [5]. In this contribution, we will present our progress on the evaluation of the more complex systems U<sub>3</sub>O<sub>7</sub> and U<sub>3</sub>O<sub>8</sub>.

## References

- [1] A.R. Fox, *et al.*, Nature, 455 (2008) 341.
- [2] K.O. Kvashnina, *et al*, Physical Review Letters, 111 (2013) 253002.
- [3] G. Leinders, *et al*, Inorganic Chemistry, 56 (2017) 6784.
- [4] G. Leinders, *et al*, Inorganic Chemistry, 60 (2021) 10550.
- [5] G. Leinders, *et al*, Journal of Applied Crystallography, 57 (2024) 284.

# New insights into the $\text{UO}_2$ oxidation process from in situ HERFD at the U $M_4$ edge

E.E. Bazarkina<sup>1,2\*</sup>, S. Bauters<sup>1,2</sup>, Y. Watier<sup>3</sup>, S. Weiss<sup>1</sup>, S.M. Butorin<sup>4</sup> and K.O. Kvashnina<sup>1,2</sup>

<sup>1</sup> Institute of Resource Ecology, Helmholtz Zentrum Dresden-Rossendorf (HZDR), Germany

<sup>2</sup>The Rossendorf Beamline at ESRF, France

<sup>3</sup>ESRF, The European Synchrotron, France

<sup>4</sup>Condensed Matter Physics of Energy Materials, X-ray Photon Science, Department of Physics and Astronomy, Uppsala University, PO Box 516, SE-75120 Uppsala, Sweden

\*e-mail: elena.bazarkina@esrf.fr

Despite the high importance of the oxidation of  $\text{UO}_2$ , many aspects of the U and O state evolution during this process remain unclear because of complex kinetics and several possible oxidation scenarios. In the U-O system, the relation among structure, U-O composition and U oxidation state is particularly complex [1, 2, 3]. In this point of view, the HERFD XANES at U  $M_4$  edge provides unique information about the oxidation state of U while the structural characteristics are less important [1, 3]. However, the in-situ high-temperature spectroscopy measurements at U  $M_4$  edge are challenging because of the low energies involved, i.e. 3.7 keV for the incident beam and 3.3 eV for the emitted fluorescence. To perform such novel measurements at high temperatures at the ROBL beamline at ESRF [4, 5], a special optical cell was designed (figure 1). A single experimental run was performed by heating slowly the  $\text{UO}_2$  exposed to the air up to 550°C, keeping this T, cooling down, and verifying the stability of the oxidation product. The spectra show pre-oxidation changes related to the mobility of oxygen atoms in  $\text{UO}_2$  at temperatures below 350°C and the oxidation processes starting above 350°C. The comparison of the spectra obtained in situ with the spectra of known U-O phases (e.g.  $\text{U}_4\text{O}_9$ ,  $\text{U}_3\text{O}_7$ ,  $\text{U}_3\text{O}_8$  and  $\text{UO}_3$ ), the Principle Component Analysis coupled with Iterative Transformation Factor Analysis, all show that the distribution of U oxidation states and formation of new structures are interposed. The evolution is not linear in time with several distinct stages. Work is currently in progress to describe the driving mechanisms during different stages of oxidation.

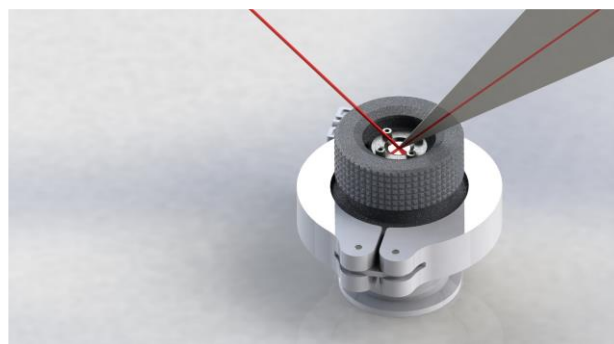


Figure 1: The heating cell for in-situ HERFD measurements at U  $M_4$  edge.

## References

- [1] K.O. Kvashnina et al., Physical Review Letters, 111, 253002 (2013).
- [2] G. Leiders et al., Inorganic Chemistry, 56, 6784 (2017).
- [3] K.O. Kvashnina and S. Butorin, Chemical Communications, 58, 327 (2022).
- [4] A.C. Scheinost et al., Journal of Synchrotron Radiation, 28, 333 (2021).
- [5] K. O. Kvashnina, A.C. Scheinost, Journal of Synchrotron Radiation, 23, 836 (2016).

# Luminescence and Circularly Polarized Luminescence of Molecular Complexes of Actinides (Am to Es)

Gaël Ung<sup>1\*</sup>

<sup>1</sup>University of Connecticut, USA; Lawrence Berkeley National Laboratory, USA.

\*e-mail: [gael.ung@uconn.edu](mailto:gael.ung@uconn.edu)

Circularly polarized luminescence (CPL) is the preferential emission of right- or left-handed circularly polarized light. Because of the core-like nature of 4f orbitals, the split between energy levels of 4f-elements is larger through spin-orbit coupling than through crystal field splitting. In 4f-elements, each luminescent transition between spin-orbit coupling term levels is associated with a specific transition type, resulting in different relative CPL strengths. More importantly, CPL spectroscopy allows for better distinction of the individual components resulting from crystal field splitting, though these transitions' selection rules are not well understood.

We will show that by employing appropriate ligands, luminescent molecular complexes of americium, curium, berkelium, californium, and einsteinium can be obtained. Additionally, by utilizing chiral ligands, CPL spectra of transplutonium elements (Am and Cm) can be observed.



*Figure 1: Picture of a luminescent curium complex in solution.*

# Lanthanide nanoparticles and MOFs heterostructures boosting NIR-II imaging-guided photodynamic therapy

Qi-Xian Wang,<sup>1</sup> Xiang-Fei Yang,<sup>1</sup> Zhen Qin,<sup>1</sup> Jun Chen<sup>1</sup>

<sup>1</sup> Institute of Materials, China Academy of Engineering Physics, Sichuan Province, 621908, China, e-mail: 15921963121@163.com

Lanthanide nanoparticles NaLnF<sub>4</sub> can convert low-energy near-infrared light into high-energy visible light through upconversion process, which are promising light converter<sup>[1]</sup>. Heterostructures of NaLnF<sub>4</sub> and porphyrinic metal-organic frameworks (MOFs) have been reported as a promising platform for near-infrared (NIR)-driven photodynamic therapy (PDT), while the energy transfer from NaLnF<sub>4</sub> to MOFs greatly decreased the upconversion emissions. To develop NaLnF<sub>4</sub> and MOFs heterostructures with significantly improved PDT and imaging simultaneously is important to track their location to implement therapy accurately<sup>[2]</sup>.

Herein, we constructed Er<sup>3+</sup>-doped NaLnF<sub>4</sub>@MOF core@shell nanoparticles to integrate NIR-driven PDT and NIR-II imaging. NaLnF<sub>4</sub> nanoparticles are designed with upconversion and NIR emission simultaneously under a single 980 nm excitation, where the upconversion luminescence (UCL) overlaps well with the absorption of Zr-based porphyrin MOF, enabling efficient energy transfer from NaLnF<sub>4</sub> to the MOF shell to generate <sup>1</sup>O<sub>2</sub>. And the NIR luminescence, which gave out under a lower excitation power than that of UCL, could be used to track the location and distribution of the heterostructures via NIR-II imaging. Moreover, anti-programmed death-ligand 1 (α-PD-L1) immunotherapy was introduced synergistically to improve antitumor immunity efficacy. The combination of NaLnF<sub>4</sub>@MOF and α-PD-L1 not only inhibited primary tumors but also suppressed distant one, leading to an effective tumor inhibition rate of 95%. This work provides an integrated nanopatform for boosting NIR-II imaging-guided PDT/immunotherapy efficacy toward tumor treatment.

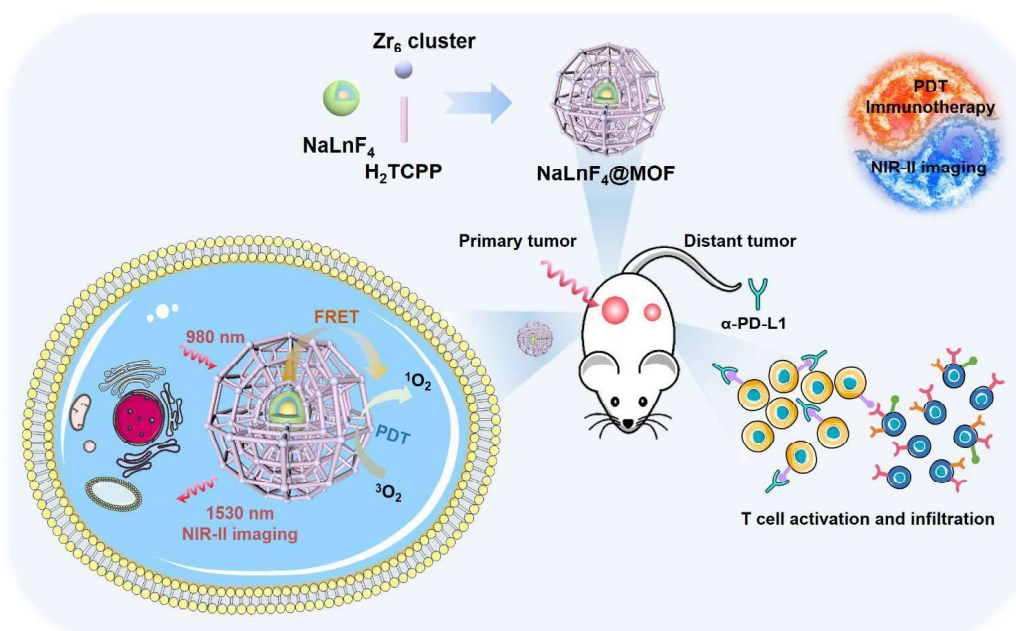


Fig. 1. Schematic illustration of NaLnF<sub>4</sub>@MOF heterostructured nanoparticles for NIR-driven photodynamic immunotherapy and NIR-II imaging

## References

- [1] Q.X. Wang *et al.*, *Nano Today* **43**, 101439 (2022).
- [2] G. Hong, *et al.*, *Nat. Biomed. Eng.* **1**, 0010 (2017).



# Experimental Characterization and Theoretical Modelling of X-ray Absorption Spectra of Protactinium(V) Complexes

T. Shaaban<sup>1</sup>, C. Le Naour<sup>2</sup>, H. Oher<sup>2</sup>, T. Aubert<sup>2</sup>, P. L. Solari<sup>3</sup>, T. Burrow<sup>3</sup>, M. Hunault<sup>3</sup>, A.S.P. Gomes<sup>1</sup>, F. Réal<sup>1</sup>, V. Vallet<sup>1</sup>, M. Maloubier<sup>2</sup>

<sup>1</sup>Université de Lille, CNRS, UMR 8523 – PhLAM – Physique des Lasers, Atomes et Molécules, F-59000 Lille, France.

<sup>2</sup>Université Paris-Saclay, CNRS/IN2P3, IJCLab, 91405 Orsay, France.

<sup>3</sup>Synchrotron Soleil, Saint-Aubin, F-91192 Gif-sur-Yvette, France.

\*e-mail: tamara.shaaban@univ-lille.fr

The physical and chemical properties of solvated actinide complexes, including their speciation, bond nature with the surrounding environment, and thermodynamic and spectroscopic properties, hold significant implications for societal and industrial applications. Among the actinides, protactinium ( $Z=91$ ) remains unique because, depending on its oxidation state, it can behave as an "f element" (Pa(IV)) or a "d element" (Pa(V)). In solution, Pa(V) dominates because Pa(IV) is unstable and can be directly oxidized to Pa(V) unless a strong reducing agent is present [1]. Pa(V) can exist in solution as  $\text{Pa}^{5+}$ , and in some specific solutions, it will form  $\text{PaO}^{3+}$  [2, 3]. Apparently, it does not form the actinyl moiety  $\text{PaO}_2^+$ , which is not the case for its heavier neighbor elements, uranium, neptunium, and plutonium. To identify the absence or presence of the mono-oxo bond in Pa(V) complexes, one can employ spectroscopic techniques such as X-ray spectroscopies, which have played a crucial role in actinide characterization [4].

An experimental campaign at the MARS beamline of SOLEIL in February 2024 analyzed protactinium samples using HERFD-XANES, RIXS, and EXAFS to investigate electronic and structural properties. Intriguing spectral features were observed (see Figure 1), notably the similarity between oxalate and fluoride solutions, raising questions about the mono-oxo bond formation in oxalic acid suggested in prior studies [5]. Complementary quantum theory analyses were employed to explore these findings.

This work is accompanied by theoretical modeling of the XANES spectra using relativistic Time-Dependent Density Functional Theory (TD-DFT) [6] at the  $L_3$  and  $M_4$  edges of the structural models obtained from the EXAFS fitting. Additionally, these calculations allow us to investigate the nature of transitions which the excitations are occurring.

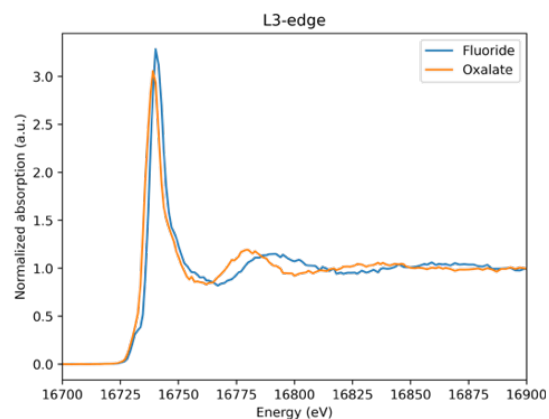


Figure 1: HERFD-XANES  $L_3$  edge spectra of  $\text{Pa}^{(V)}$  in hydrofluoric and oxalic acids.

## References

- [1] N. Banik et al., Dalton Trans. 45, 453-457 (2015).
- [2] C. Le Naour et al., Inorg. Chem. 44, 9542-9546 (2005).
- [3] T. Shaaban et al., Chem. Eur. J., e202304068 (2024) ; Ibid, Chem. Comm. In press, (2024).
- [3] C. Den Auwer et al., EurJIC 21, 3843-3859 (2003).
- [4] M. Mendes et al., Inorg. Chem. 49, 9962-9971 (2010).
- [5] W. Misael et al., Inorg. Chem. 62, 11589-11601 (2023).

# Probing actinide electronic structure using high-energy resolution X-ray spectroscopy

Clara L. Silva<sup>1,2</sup>, L. Amidani<sup>1,2\*</sup>, and K. Kvashnina<sup>1,2\*</sup>

<sup>1</sup>*The Rossendorf Beamline at ESRF – The European Synchrotron, Grenoble, France*

<sup>2</sup>*Helmholtz-Zentrum Dresden-Rossendorf (HZDR), Institute of Resource Ecology, Dresden, Germany*

\**e-mail: kristina.kvashnina@esrf.fr*

Actinide systems continue to raise many unanswered questions on topics involving the number of electrons in valence states, the degree of f-electron localization, and the character of their chemical bonding. Their partially filled 6d and 5f valence shells are responsible for most of their complex behaviour. Understanding the intricate electronic structure of actinides requires the use of advanced experimental and theoretical techniques. Among the experimental approaches, resonant inelastic X-ray scattering (RIXS) and XANES in the high-energy fluorescence detection mode (HERFD-XANES) at the actinide  $M_{4,5}$  edge have proven to be powerful techniques to investigate their electronic structure [1–4]. Here, we report on recent progress in the X-ray spectroscopy of 5f electron systems across the series  $AnCl_4(DME)_2$  (DME = dimethoxyethane, An = Th, U, Np, Pu). RIXS and HERFD-XANES at the An  $M_{4,5}$  edge provide detailed information on its local electronic structure. Comparative analysis by changing the actinide ion allows for a systematic study of bonding trends across the series, focusing on the influence of the 5f electron occupancy. The interpretation of the data is supported by electronic structure calculations based on crystal field multiplet theory, which provide a deeper insight into the description of the nature of the spectral features.

## References

- [1] Kvashnina, K. O., Butorin, S. M., Martin, P. & Glatzel, P. *Phys. Rev. Lett.* 111, 253002 (2013).
- [2] Amidani, L. et al. Probing the Local Coordination of Hexavalent Uranium and the Splitting of 5f Orbitals Induced by Chemical Bonding. *Inorg. Chem.* 60, 16286–16293 (2021).
- [3] Kvashnina, K. O. & Butorin, S. M. High-energy resolution X-ray spectroscopy at actinide  $M_{4,5}$  and ligand K edges: what we know, what we want to know, and what we can know. *Chem. Commun.* 58, 327–342 (2022).
- [4] Silva, C. L., Amidani L., Retegan, M., Weiss, S. Bazarkina, E. F., Graubner, T., Kraus, F., Kvashnina, K. O., *Nat Commun.* 15, 6861 (2024).



# Advanced x-ray spectroscopy study of Pu(III-VI) aqua ions

Harry Ramanantoanina<sup>1\*</sup>, Sven Schenk<sup>1</sup>, Cédric Reitz<sup>2</sup>, David Fellhauer<sup>1</sup>, Hanna Kaufmann-Heimeshoff<sup>1</sup>, Tim Prüssmann and Tonya Vitova<sup>1</sup>

<sup>1</sup>*Institute for Nuclear Waste Management, Karlsruhe Institute for Technology, D-76021 Karlsruhe, Germany*

*\*e-mail: [harry.ramanantoanina@kit.edu](mailto:harry.ramanantoanina@kit.edu)*

Understanding the relationship between bonding properties and bond stability of Pu in various oxidation states is crucial for comprehending their environmental behavior. Pu naturally exists in four oxidation states (III, IV, V, VI), which dictate its chemical properties and environmental fate. [1] Despite experimental challenges, investigating Pu chemistry, especially in aqueous solutions, is crucial for understanding interactions with ligands and chemical stability; it has also significance for nuclear waste management, fuel reprocessing, and environmental cleanup. In this presentation, we study plutonium in aqueous solution, with special focus on the bonding interaction between Pu and water ligand. We prepared Pu aqueous solutions with different oxidation states [2] and analyzed them using advanced techniques such as Pu  $M_{4,5}$ -edge core-to-core and valence-band resonant inelastic x-ray scattering (RIXS) both at the experimental [3,4] and theoretical levels. [5] Besides, we developed computational method, calculating RIXS maps with the ligand-field density-functional theory (LFDFT) model. [5] This allows us to obtain ligand-field parameters (Slater-Condon integrals, spin-orbit coupling constant and ligand-field potential) without scaling factors or empirical corrections. The results show very good agreement between experiments and theory, facilitating our spectral interpretation. This joint experiment-theory effort provides insights into Pu ion coordination chemistry, and its local electronic structure, complementing standard UV-visible spectroscopy and nuclear magnetic resonance studies. We also aim at extracting long-sought details on the Pu-ligand bonding interaction, bond-covalency and stability relationship, shedding light on the Pu solvation dynamics, and informing future studies on Pu ion stability under various environmental conditions and oxidation state monitoring. This work received funding from the European Research Council (ERC) under the European Union's Horizon 2020 research and innovation program (N. 101003292).

## References

- [1] D.L. Clark, S.S. Hecker, G.D. Jarvinen and M.P. Neu, Plutonium. In: L.R. Morss, N. Edelstein, and J. Fuger, (eds). 2008, Springer, Dordrecht.
- [2] A. Tasi, X. Gaona, D. Fellhauer, M. Böttle, J. Rothe, K. Dardenne, D. Schild, M. Grivé, Mireia, E. Colàs, J. Bruno, K. Källström, M. Altmaier, and H. Geckeis, *Radiochim. Acta*, 106, 259-279 (2018).
- [3] T. Vitova, I. Pidchenko, D. Fellhauer, P.S. Bagus, Y. Joly, T. Prüssmann, S. Bahl, E. Gonzalez-Robles, J. Rothe, M. Altmaier, M.A. Denecke and H. Geckeis, *Nat. Commun.*, 8, 16053 (2017).
- [4] T. Vitova, I. Pidchenko, D. Fellhauer, T. Prüssmann, S. Bahl, K. Dardenne, T. Yokosawa, B. Schimmelpfennig, M. Altmaier, M. Denecke, J. Rothe and H. Geckeis, *Chem. Commun.*, 54, 12824 (2018).
- [5] H. Ramanantoanina, *Computation*, 10, 70 (2022).

# A journey through the interpretation of uranyl $M_{4,5}$ edges HERFD-XANES

L. Amidani<sup>1,2\*</sup>, K. Kvashnina<sup>1,2</sup>

<sup>1</sup>*The Rossendorf beamline, Grenoble, France*

<sup>2</sup>*Institut of Resource Ecology, HZDR, Dresden, Germany*

*\*e-mail: lucia.amidani@esrf.fr*

HERFD-XANES at the An  $M_{4,5}$  edges is recognized as an invaluable tool to gain insight in the An electronic structure and it is increasingly explored to gain insight into the nature of the An bond. Very few information can be retrieved from the spectra without the support of theoretical calculations, which have therefore a prominent role in the interpretation of HERFD-XANES data. In recent years, several theoretical approaches tried their hand at reproducing HERFD-XANES data at the  $M_{4,5}$  edges. Most often, the uranyl spectrum is among the cases that any methodology tries to reproduce, which makes the uranyl HERFD-XANES the most calculated spectrum in the actinide field. It is therefore interesting to look at uranyl to understand how different theories perform in the challenge of reproducing HERFD-XANES spectroscopy.

In this talk, I propose a journey through the calculations of the uranyl  $M_{4,5}$  HERFD-XANES to compare how different theoretical methodologies reproduce the data and how their findings are connected to the nature of An bonding.

# Evolution of the Eu L<sub>3</sub> edge RIXS spectra across the paramagnetic–ferromagnetic transition in EuS

J. Kolorenč

*Institute of Physics of the Czech Academy of Sciences, Na Slovance 2, 182 00 Prague, Czech Republic*

*e-mail: kolorenc@fzu.cz*

Recently, we described a mechanism of how two different sets of electronic excitations appear in the valence-to-core RIXS spectrum of europium sulfide measured at the Eu L<sub>3</sub> edge [1]. One set of excitations is composed of a hole in the S 3p bands and an electron excited to the extended Eu 5d band states, the other set is made up from a hole in the Eu 4f states and an electron in localized Eu 5d states bound to the 4f hole by its Coulomb potential. The delocalized excitations arise from the dipole-allowed 5d to 2p emissions, whereas the localized excitations result from the dipole-forbidden (but quadrupole-allowed) 4f to 2p emissions. Although explicitly demonstrated only in EuS, we expect that analogous behavior is observable also in other gaped Eu compounds containing Eu<sup>2+</sup> ions, like halides.

The study [1] discussed only the paramagnetic phase of EuS. In this contribution, we theoretically analyze how the spectral features corresponding to the localized 4f–5d excitons should change across the transition into the low-temperature ferromagnetic phase, and whether the expected changes are prominent enough to be detectable in the experiment. The theoretical estimates are obtained in a simple Eu<sup>2+</sup> ionic model where the 5d states experience a cubic crystal field. Although the model seems crude, it should reflect the reality reasonably well given the localized character of the excitations in question.

## References

[1] L. Amidani, J. J. Joos, P. Glatzel, J. Kolorenč, The magnetic exciton of EuS revealed by resonant inelastic x-ray scattering, [arXiv:2310.18096](https://arxiv.org/abs/2310.18096) (2023).

# Probing U multiplet excitations with high resolution M<sub>4,5</sub>-edge RIXS

M. Sundermann,<sup>1,2</sup> D.S. Christovam,<sup>1</sup> A. Marino,<sup>1</sup> H. Gretarsson,<sup>2</sup> B. Keimer,<sup>3</sup> L. H. Tjeng,<sup>1</sup> A. Severing<sup>1,4</sup>

<sup>1</sup>Max-Planck Institute for Chemical Physics of Solids, Dresden, Germany

<sup>2</sup>DESY/PETRA-III, Hamburg, Germany

<sup>3</sup>Max-Planck Institute for Solid State Research, Stuttgart, Germany

<sup>4</sup>Institute of Physics II, University of Cologne, Cologne, Germany

\*e-mail: [severing@ph2.uni-koeln.de](mailto:severing@ph2.uni-koeln.de)

It is challenging to describe the electronic structure of U-based intermetallic compounds due to the complex interplay of 5*f* band formation and correlation effects [1]. However, the limitations of a single-Slater-determinant approach are not apparent from experiment. For example, x-ray absorption (XAS) spectra are broad, obscuring atomic-like multiplet structures [2], while core-level PES spectra typically show a broad main emission line with, at most, one satellite [3]. These factors often lead to conflicting interpretations of U intermetallic compounds' x-ray data [4-9].

Valence band resonant inelastic x-ray scattering (RIXS) is the method of choice to detect *ff* or multiplet excitation. RIXS at the U M<sub>4,5</sub>-edges (M<sub>4,5</sub> XAS: 3*d*<sup>10</sup>5*f*<sup>*n*</sup> → 3*d*<sup>9</sup>5*f*<sup>*n*+1</sup>) offers a high signal-to-background ratio, but energy resolution has historically been limited at the M<sub>4,5</sub>-edges in the tender x-ray regime. The IRIXS spectrometer at beamline P01, DESY/PETRA-III now achieves unprecedented energy resolutions of 50meV at the U M<sub>5</sub> edge (see Fig. 1).

Valence band M<sub>4,5</sub>-edge RIXS is particularly suited for uranium intermetallic compounds [10,11]. For U-U distances beyond the Hill limit, multiplet excitations persist despite the strong 5*f* covalence. These multiplet excitations (5*f*<sub>0</sub><sup>*n*</sup> → 5*f*<sub>*i*</sub><sup>*n*</sup>) serve as fingerprints of the leading configuration, revealing the formal valence, while broad charge transfer scattering (5*f*<sub>0</sub><sup>*n*</sup> → 5*f*<sub>*j*</sub><sup>*n*+*m*</sup>  $\underline{L}_j^m$ ) indicates the presence of covalence

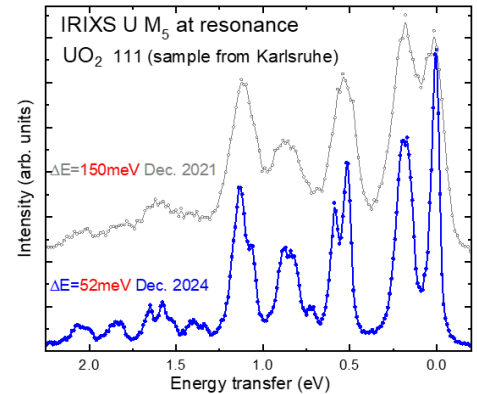


Fig. 1: Demonstration of the enhanced energy resolution of the IRIXS spectrometer at DESY/PETRA III, illustrated using M<sub>5</sub>-edge RIXS data of UO<sub>2</sub>, measured at resonance.

## References

- [1] A. Marino *et al.*, Phys. Research **6**, 033068 (2024) and references therein
- [2] F.de Groot & A. Kotani, *Core Level Spectroscopy of Solids*, CRC Press, Boca Raton, (2008).
- [3] S.-i. Fujimori *et al.*, Phys. Rev. B **91**, 174503 (2015).
- [4] S.-i. Fujimori *et al.*, J. Phys. Soc. Jpn. **88**, 103701 (2019) and J. Phys. Soc. Jpn. **90**, 015002 (2021)
- [5] L. Miao *et al.*, Phys. Rev. Lett. **124**, 076401 (2020)
- [6] S.M. Thomas *et al.*, Sci. Adv. **6** eabc8709 (2020)
- [7] A. B. Shick *et al.*, Phys. Rev. B **103**, 125136 (2021)
- [8] S. Liu *et al.*, Phys. Rev. B **106**, L241111 (2022)
- [9] F. Wilhelm *et al.* Commun. Phys. **6**, 96 (2023)
- [10] A. Marino *et al.*, Phys. Rev. **108**, 045142 (2023) &
- [11] D. S. Christovam *et al.*, Phys. Rev. Research **6**, 033299 (2024)

# Using experimental actinide chemistry to solve technical challenges in spent fuel and nuclear material management within the Nuclear Decommissioning Authority Group

E. M. B. MacCormick<sup>1\*</sup>, C. R. T. Smylie<sup>1</sup>, R. Bernard<sup>2</sup>, H. M. Steele<sup>2</sup>, R. Orr<sup>3</sup>, E. K. Gibson<sup>1</sup>,

J. H. Farnaby<sup>1</sup>

<sup>1</sup>University of Glasgow, Glasgow, UK,

<sup>2</sup>Sellafield Ltd, Cumbria, UK

<sup>3</sup>National Nuclear Laboratory, Cumbria, UK

\*e-mail: [e.maccormick.1@research.gla.ac.uk](mailto:e.maccormick.1@research.gla.ac.uk)

During the reprocessing of spent nuclear fuel, plutonium is separated from waste fission products.<sup>1</sup> The plutonium material is stored in the form of dioxide ( $\text{PuO}_2$ ) powders in sealed packages.<sup>2</sup> Interim  $\text{PuO}_2$  storage presents technical challenges. These include the possibility of adventitious reactions of  $\text{PuO}_2$  with atmospheric and other gases, for example the radiolysis of water generating  $\text{H}_2$ .<sup>3</sup> Additionally, the chemical composition and the properties of the  $\text{PuO}_2$  have also been observed to change during storage.<sup>1</sup> In this work interim storage conditions were replicated through reactivity studies with atmospheric gases and  $\text{AnO}_2$  ( $\text{An} = \text{U}, \text{Th}$ ) nanoparticles. The aim of this work is to establish structure-property relationships to gain a better understanding of this chemistry. This data will contribute to the retreatment and storage solutions needed for the future management of the UK's civil plutonium. Reactivity studies with  $\text{H}_2$ , water, and other atmospheric gases will give insight into the absorbed species and the surface chemistry.<sup>4</sup> Structure-property relationships will be investigated using X-ray Absorption Spectroscopy (XAS) and Inelastic Neutron Scattering (INS).

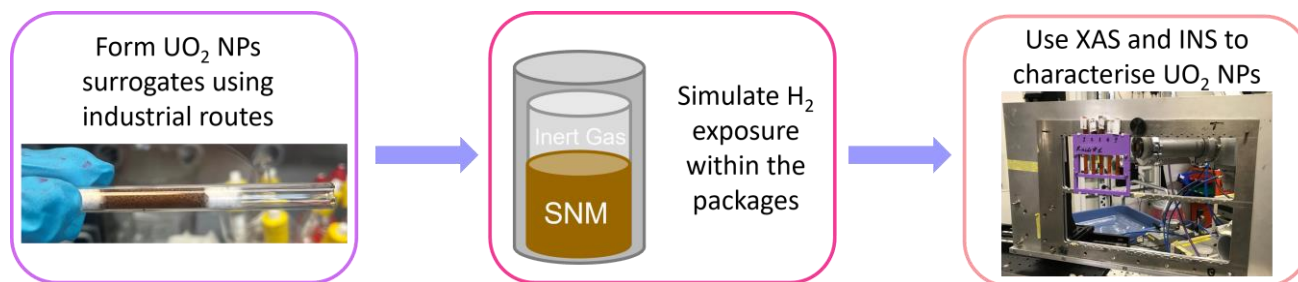


Figure 1: Workflow procedure from forming  $\text{UO}_2$  NPs, simulating  $\text{H}_2$  exposure, characterising the NPs using XAS and INS

## References

- [1] N. C Hyatt, NPj Materials Degredation, 2020, **4**, 28.
- [2] Nuclear Decommissioning Authority, *Progress on plutonium consolidation, storage and disposition*, March 2019.
- [3] H. E. Sims, K. J. Webb, J. Brown, D. Morris and R. J. Taylor, *Journal of Nuclear Materials*, 2013, **437**, 359-364.
- [4] J. Leduc, M. Frank, L. Jürgensen, D. Graf, A. Raauf and S. Mathur, *ACS Catalysis*, 2019, **9**, 4719-4741

# Freezing Pu(IV) Hexanuclear Clusters in the Formation of Plutonium Oxide Nanoparticles

M. Viro<sup>1\*</sup>, M. Cot-Auriol<sup>1</sup>, S. Dourdain<sup>1</sup>, T. Dumas<sup>2</sup>, C. Tamain<sup>2</sup>, D. Menut<sup>3</sup>,  
M. Hunault<sup>3</sup>, P. L. Solari<sup>3</sup>, Philippe Moisy<sup>2</sup>, Sergey I. Nikitenko<sup>1</sup>

<sup>1</sup> ICSM, Univ Montpellier, CEA, CNRS, ENSCM, Marcoule, France.

<sup>2</sup>CEA, DES, ISEC, DMRC, Univ Montpellier, Marcoule, France.

<sup>3</sup>Synchrotron SOLEIL, MARS beamline, Gif-sur-Yvette, France.

\*e-mail: [matthieu.virot@cea.fr](mailto:matthieu.virot@cea.fr)

The formation of plutonium oxide nanoparticles in aqueous solution is a pivotal process with implications across various fields, including nuclear waste management, environmental safety, and industrial applications.[1-3] Understanding the mechanisms underlying the formation of these nanostructures is crucial for improving strategies related to the safe storage of radioactive elements and mitigating their environmental impact. Furthermore, such knowledge opens pathways for the development of nanomaterials with tailored advanced properties for specific technological applications. Recent studies have strongly suggested that Pu(IV) oxo-hydroxo clusters play a central role as key intermediates in the formation of colloidal PuO<sub>2</sub> nanoparticles.[4] These transient species may act as precursors for the final nanoparticle structures, offering a unique opportunity to probe their formation and control the physicochemical properties of the resulting PuO<sub>2</sub> nanoparticles.

This presentation will summarize recent insights into the formation mechanism of colloidal PuO<sub>2</sub> nanoparticles in aqueous solutions. Deconvolution studies of Vis-NIR absorption spectra during nanoparticle formation have revealed intermediate species. Additionally, the use of aqueous solutions containing organic ligands (DOTA, acetate and glycine) to arrest the reaction during Pu(IV) hydrolysis has enabled the stabilization of intermediates exhibiting distinct fingerprints. Synchrotron-based X-ray scattering and absorption techniques provided a detailed description of their structural and electronic properties, which align with Pu(IV) hexanuclear oxo-hydroxo core structures stabilized by the respective organic ligands. Beyond the experimental challenge of characterizing these nanostructures in dilute conditions—particularly using SAXS—this work underscores the contribution of hexameric polynuclear Pu(IV) species to the formation mechanism of PuO<sub>2</sub> nanoparticles in aqueous conditions. It represents a significant step toward understanding the formation mechanisms of PuO<sub>2</sub> nanoparticles. The insights gained contribute substantially to the broader field of actinide chemistry and ongoing efforts to develop innovative solutions in environmental and technological contexts.

## References

- [1] Gerber et al. *Nanoscale*, 2020.
- [2] Baumann et al. *Nanomaterials*, 2023
- [3] M. Viro et al. *Nanoscale advances*, 2022.
- [4] M. Cot-Auriol et al. *Chemical Communications*, 2022.

# The role of structure and redox in the solid-state chemistry of Ce doped UO<sub>2</sub> nanoparticles

K. D. Stuke\*<sup>1</sup>, N. Huittinen<sup>2,3</sup>, M. Henkes<sup>1</sup>, C. Schreinemachers<sup>1</sup>, P. Kegler<sup>1</sup>, A. Rossberg<sup>3,4</sup>, L. Amidani<sup>3,4</sup>, K. Kvashnina<sup>3,4</sup>, D. Bosbach<sup>1</sup> and G. L. Murphy<sup>1</sup>

<sup>1</sup> Research Centre Juelich GmbH, 52428 Jülich, Germany

<sup>2</sup>Institute of Chemistry and Biochemistry, Freie Universität Berlin, 14195 Berlin, Germany

<sup>3</sup>Helmholtz-Zentrum Dresden-Rossendorf (HZDR), 01328 Dresden, Germany

<sup>4</sup>The European Synchrotron Radiation Facility (ESRF), 38000 Grenoble, France

\*e-mail: [k.stuke@fz-juelich.de](mailto:k.stuke@fz-juelich.de)

Mixed Oxide (MOX) nuclear fuel is a topical nuclear fuel that consists of a mixture of UO<sub>2</sub> and PuO<sub>2</sub> and is used currently to fuel many nations' nuclear energy programs. After a burn-up period of approximately 45 Gwd/Th<sub>u</sub>, the fuel structure goes considerable heterogenization and deconstruction. The formed structure is known as the *high burn-up structure* (HBS). The HBS regions of the fuel exhibit increased porosity compared to UO<sub>2</sub> and occur as nanomaterials. A detailed investigation of these materials regarding their formation and thermal stability is necessary to support use of nuclear fuel and further for its eventual disposal within a final geological nuclear repository.<sup>[1]</sup> The complexity of spent nuclear fuel (SNF) challenges its direct investigation, in which model system studies are often enacted in order to expediate research efforts and further focus on single effects often using high resolution methods.

Following this line of investigation cerium doped UO<sub>2</sub> based nanomaterial compounds were synthesized using an adapted hydrothermal method and subsequently investigated in the context of their chemistry in relation to the HBS of SNF.<sup>[2]</sup> Synthesized materials were characterized using powder X-ray diffraction measurements to examine phase purity but also determine approximate nanostructure sizing. Subsequent *Scanning electron microscopy* as well as *energy dispersive X-Ray spectroscopy* (SEM-EDX) measurements were used to validate the nanostructure assignment and further established the incorporation of cerium within the materials. *High Energy Resolution Fluorescence Detected X-ray absorption near-edge structure* (HERFD-XANES) measurements were carried out at BM20 at the European Synchrotron Radiation Facility (ESRF), to determine the local structure and redox changes to the nanoparticles. Measurements performed on the U-M<sub>4</sub> edge and Ce-L<sub>3</sub> edge revealed surprising diversity in the Ce and U redox states where U<sup>+4</sup>, U<sup>+5</sup>, U<sup>+6</sup> and Ce<sup>+3</sup>, Ce<sup>+4</sup> were identified, although the compounds occur as single-phase structure from PXRD measurements. The origin of this behavior is reckoned to the unique nanostructure of the materials and their ability to form oxidized layers upon air exposure with subsequent chemical transport of Ce and U cations. These hypotheses were subsequently tested using extended X-ray absorption near edge structure measurements in addition to thermogravimetric analysis and in situ high temperature PXRD. The results of this work will be discussed in relation to the chemistry of UO<sub>2</sub> nanomaterials vs. micromaterials in addition to their relevance to HBS nuclear fuel chemistry.

## References

- [1] V. V. Rondinella, T. Wiss, *Materials Today*, Volume 13, Issue 12, Pages 24-32, **2010**.
- [2] R. Zhao, L. Wang, *Royal Society of Chemistry*, Volume 16, 2645-2651, **2014**.

# Electrophoretic techniques: Setting up characterization tools for radioactive nanoparticles

F. Gignac<sup>1\*</sup>, J. Aupiais<sup>1</sup>

<sup>1</sup>CEA, DAM, DIF, F-91297 Arpajon, France

\*e-mail: [fanny.gignac@cea.fr](mailto:fanny.gignac@cea.fr)

Currently, there is significant interest in studies concerning radioactive nanoparticles present in the environment, as it is suspected that these particles may act as vectors for the migration of radionuclides. In order to understand the behavior of these nanoparticles in the environment, it is necessary to characterize them, including their size and charge.

The objective of this study is to characterize PuO<sub>2</sub> nanoparticles, thanks to Taylor dispersion analysis (TDA) and capillary isoelectric focusing (cIEF). These two techniques were realized on a capillary electrophoresis (CE) coupled with inductively coupled plasma mass spectrometry (ICP-MS). TDA is a technique for measuring hydrodynamic radius, which has already proven its effectiveness in determining the size of gold nanoparticles [1] or super paramagnetic iron oxide nanoparticles (SPION) [2]. This method is complementary to technique already used like dynamic light scattering (DLS) or transmission electron microscopy (TEM). cIEF method allows the determination of the isoelectric point (pI) of nano-objects. This technique would allow for a better understanding of the physicochemical behavior of colloids under environmental conditions, such as pH. This has already been used in the measurement of pI of proteins, with or without radioactive elements [3], and appears promising for the analysis of nanoparticles.

We were first interested in the development of TDA on model nanoparticles, such as gold nanoparticles. This allowed us to establish the method on the instruments. We observed a significant difference between the reference size and the hydrodynamic size measured by TDA. Preliminary results were then obtained on ThO<sub>2</sub> nanoparticles synthesized in a dry process. We observed a strong aggregation of these nanoparticles, which was confirmed by analyses performed using Scanning electron microscopy (SEM). This may be the result of aggregation during the dispersion of the particles in deionized water. However, PuO<sub>2</sub> nanoparticles are synthesized through a liquid process, it is possible to expect a minimal phenomenon of aggregation.

In parallel, a preliminary study was conducted on the coupling of cIEF and ICP-MS. An optimization phase for the coupling was carried out and preliminary results on ThO<sub>2</sub> nanoparticles were obtained. These results suggest that the sample focusing has been successfully achieved, which is promising for the continuation of the study. This subject remains challenging, however, because the isoelectric point markers that would allow to realize a range of pI calibration standards are not compatible with ICP-MS measurements because they are not detectable. Then, it is considered to use protein-actinide interactions as a marker, for which the pI is known, such as actinide-transferrin, for example [3].

[1] U. Pyelle, A. Jalil, C. Pfeiffer, B. Pelaz, W. Parak, J. Colloid Interface Sci., 450, 288-300 (2015)

[2] S. Balog, D. Urban, A. Molisevic, F. Crippa, B. Rothen-Rutishauser, A. Petri-Flink, J. Nanoparticles Res., 297, 19-29 (2017)

[3] F. Brulfert, J. Aupiais, Dalton Trans, 47,9915-10300 (2018).



## **MARS beamline: an x-ray toolbox serving actinide science**

M.O.J.Y. Hunault\*, T. G. Burrow, P. Piau, W. Breton, D. Menut, and P.-L. Solari

*Synchrotron SOLEIL, L'Orme des Merisiers, Saint-Aubin, BP48, 91190 Gif-sur-Yvette, France*

*\*e-mail: Myrtille.hunault@synchrotron-soleil.fr*

The MARS (Multi-Analyses on Radioactive Samples) beamline, built in partnership with the CEA, at Synchrotron SOLEIL (France) has been open to the international community since 2010 and is fully devoted to advanced structural and chemical characterizations of radioactive matter (solid or liquid) using hard X-rays in the 3-35 keV energy range [1,2]. Today, the maximum total equivalent activity present at the beamline at once is 185 GBq, thus allowing the analysis of nuclear spent fuel [3]. Currently, different types of experiments are available: X-ray absorption spectroscopy (XANES and EXAFS), X-ray emission spectroscopy (XES) and beyond, Transmission X-ray diffraction (TXRD), High-Resolution X-ray diffraction (HRXRD), Small Angle and Wide Angle X-ray Scattering (SAXS/WAXS) are also available.[4] These techniques can be combined with imaging techniques based on X-ray microbeam raster scanning techniques or tomography reconstruction protocols.

This contribution presents recent experimental achievements in the field of nuclear science. In particular, the application of combined XANES, EXAFS and SAXS to investigate plutonium clusters, full characterization of a massive radial piece of spent nuclear fuel and selected examples of RIXS studies of actinide compounds.

### References

- [1] B. Sitaud, et al., *Journal of Nuclear Materials*, 425, 238–243 (2012)
- [2] I. Llorens, et al. *Radiochimica Acta*, 102, 957–972 (2014)
- [3] V. Klosek et al. *Journal of Nuclear Materials*, 586, 154660 (2023)
- [4] T. Dumas et al. *J Synchrotron Radiation*, 29, 30–36 (2022)

# Fission Product Speciation in $U_{1-y}Pu_yO_{2-x}$ SIMMOx Using Synchrotron Techniques

R. Caprani<sup>1</sup>, P. Martin<sup>1</sup>, D. Prieur<sup>2,\*</sup>, J. Martinez<sup>1</sup>, F. Lebreton<sup>1</sup>,  
K. Kvashnina<sup>2</sup>, E. F. Bazarkina<sup>2</sup>, N. Clavier<sup>3</sup>

<sup>1</sup> CEA, DES, ISEC, DMRC, Univ Montpellier, Marcoule, France

<sup>2</sup> Helmholtz Zentrum Dresden Rossendorf (HZDR), Dresden, Germany

<sup>3</sup> Institut de Chimie Séparative de Marcoule, Univ Montpellier, CEA, CNRS, ENSCM, Marcoule, France

\*[d.prieur@hzdr.de](mailto:d.prieur@hzdr.de)

Mixed Oxides (MOx) fuels are widely used in Pressurized Water Reactors (PWRs) for nuclear fuel cycles and waste management. Understanding the secondary phases formed from irradiation by-products, primarily Fission Products (FPs), is crucial for ensuring fuel safety during reactor operation and reprocessing.

We developed  $U_{1-y}Pu_yO_{2-x}$  SIMfuel (SIMMOx) to study FP speciation in MOx fuel, with synthesized samples mimicking irradiated MOx containing 24 wt.% Pu and a burnup of 13 at.%. Using a multi-scale approach, we characterized the structural, microstructural, and atomic properties to gain detailed insights into FP behavior.

Our results revealed that soluble FPs (Ce, La, Nd, Y, Sr, Zr) induce slight oxidation of actinides within the  $U_{1-y}Pu_yO_{2-x}$  matrix, impacting its stability. In metallic FP-bearing samples, we observed partial segregation among metallic FPs (Mo, Pd, Rh, Ru) with distinct crystallographic structures. Notably, the addition of Ba led to a speciation shift, forming perovskite inclusions and significantly altering the oxidation state of FPs like Mo. These changes highlight the complex interplay of FPs in irradiated fuel matrices.

Overall, our study establishes SIMMOx as a robust model for investigating FP interactions in MOx fuels, providing new insights into their effects on fuel properties and informing strategies for reactor safety and fuel reprocessing.

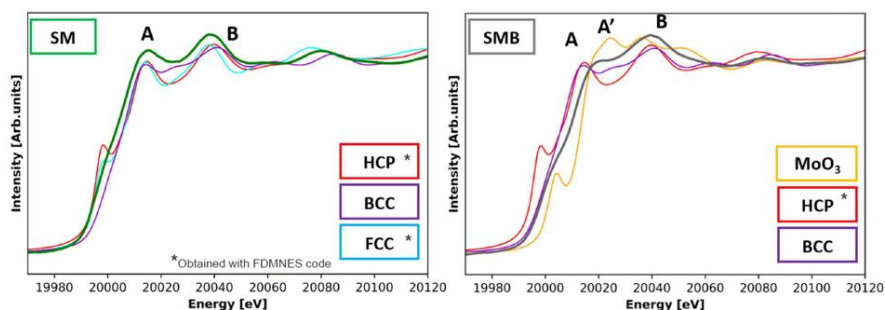


Figure 1: Influence of Ba on the speciation of Mo in Ba-bearing SIMMOX (right)

## References

[1] R. Caprani, PhD thesis, 2023.

[2] R. Caprani et al., J. Nucl. Mater., vol. 585, p. 154607 (2023).

# The Coordination Chemistry of U<sup>4+</sup> in Aqueous Solutions: Challenges and Insights from Spectroscopy and Theory

G. Raposo-Hernández<sup>1</sup>, R. R. Pappalardo<sup>1</sup>, F. Réal<sup>2</sup>, V. Vallet<sup>2</sup>, and E. Sánchez Marcos<sup>1</sup>

<sup>1</sup>Department of Physical Chemistry, University of Seville, 41012-Seville, Spain

<sup>2</sup>Université de Lille, CNRS, UMR 8523-PhLAM, Physique des Lasers, Atomes et Molécules, F-59000 Lille, France

\*e-mail: [florent.real@univ-lille.fr](mailto:florent.real@univ-lille.fr)

The aqueous U<sup>4+</sup> ion is a key species in the chemistry of uranium, with significant implications for nuclear fuel processing, environmental chemistry, and radiochemistry. Indeed, the safety assessment of a future repository, as well as the remediation of various uranium mining and milling legacies, requires a better understanding of cation interactions with potential ions (thermodynamic database, structures, etc.) and its speciation diagram.

At low pH, techniques such as EXAFS and UV-Vis spectroscopy have been instrumental in studying U<sup>4+</sup> hydrolysis and structural properties. However, these methods often yield conflicting results. For instance, EXAFS studies [1,2,3] report consistent U<sup>4+</sup>-water distances (2.41-2.42Å) but show wide variation in coordination numbers, ranging from 8 up to almost 11, depending on solvent and concentration. This inconsistency creates uncertainty regarding the coordination environment of U<sup>4+</sup> at low pH and in a diluted solution, which theoretical approaches has not completely solved [4,5,6]. While UV-vis spectroscopy can differentiate U<sup>4+</sup> from its hydrolyzed species, it provides limited insights into coordination number [7,8,9].

This study presents a comprehensive examination of the physico-chemical properties of U<sup>4+</sup> in aqueous solution, using a combination of highly accurate relativistic quantum calculations with statistical approach. By integrating these approaches, we aim to resolve discrepancies between EXAFS and UV-Vis data, offering a more unified understanding of U<sup>4+</sup> behavior at low pH.

## References

- [1] H. Moll, M. A. Denecke, F. Jalilehvand, M. Sandström, and I. Grenthe, *Inorg. Chem.*, **38** (8), 1795–1799, (1999)
- [2] C. Hennig, J. Tutschku, A. Rossberg, G. Bernhard, and A. Scheinost. *Inorg Chem.* **44**(19):6655-6661 (2005).
- [3] A. Uehara, T. Fujii, H. Matsuura, N. Sato, T. Nagai, K. Minato, H. Yamana, and Y. Okamoto. *Proceedings in Radiochemistry*, **1**(1), 161-165 (2011).
- [4] R. Atta-Fynn, D. F. Johnson, E. J. Bylaska, E. S. Ilton, G.K. Schenter, and W. A. De Jong. *Inorg. Chem.* **51** (5), 3016–3024 (2012).
- [5] R.J. Frick, A. B. Pribil, T. S. Hofer, B.R. Randolph, A. Bhattacharjee, and B. M. Rode. *Inorg. Chem.*, **48** (9), 3993–4002 (2009).
- [6] E. Acher, M. Masella, V. Vallet, and F. Réal. *Phys. Chem. Chem. Phys.*, **22** (4), 2343–2350 (2020).
- [7] K. Opel, S. Weiß, S. Hübener, H. Zänker, and G. Bernhard. *Radiochimica Acta*, **95** (3), 143–149 (2007).
- [8] S. Lehmann, H. Foerstendorf, T. Zimmermann, M. Patzschke, F. Bok, V. Brendler, T. Stumpf, and R. Steudtner. *Dalton Trans.*, **48** (48), 17898–17907 (2019).
- [9] W. Cha, H.-K. Kim, H. Cho, H.-R Cho, E.C. Jung, and Y. Lee. *RSC Adv.* **10** (60), 36723–36733 (2020).

# Development of a spent PWR MOx fuel using the SIMMOx approach

M. BERNAR<sup>1\*</sup>, P. MARTIN<sup>1</sup>, J. MARTINEZ<sup>1</sup>, L. MARCHETTI<sup>1</sup> and S. SZENKNECT<sup>2</sup>

<sup>1</sup> CEA, DES, ISEC, DMRC, Univ Montpellier, Bagnols-sur-Cèze, Site de Marcoule, France

<sup>2</sup> ICSM, Univ de Montpellier, CEA, CNRS, ENSCM, Bagnols-sur-Cèze, Site de Marcoule, France

\* Mickael.BERNAR@cea.fr

In France, the UOx spent fuel irradiated in Pressurised Water Reactor (PWR) is reprocessed to recover uranium and plutonium through the PUREX process. The final waste from this process contains fission products (FPs), such as platinum-group metals (Rh, Ru, Pd), which are now considered recoverable materials [1]. These FPs are more abundant in irradiated MOx (U,Pu)O<sub>2</sub> but this fuel is not currently reprocessed. The aim is therefore to develop an enhanced route allowing the recovering of Rh, Ru, Pd during MOx spent fuel reprocessing. To achieve this goal, the first step is to have a comprehensive understanding of these fission products behaviors. Given the high radiotoxicity of MOx spent fuel, studying such materials remains limited.

This study aims to develop a manufacturing route for a model material with the same microstructure and physicochemical properties as irradiated PWR MOx fuel with an initial plutonium content of 11 wt% and burnup of 45 GW/d/t<sub>hm</sub>. Our strategy is based on the development of a SIMMOx material [2] consisting on a fresh (U,Pu)O<sub>2</sub> doped with precursors of 12 fission products during fabrication. The fission products used belong to 3 groups described by Kleykamp [3] based on their behavior in irradiated fuel: FPs soluble in the (U,Pu)O<sub>2</sub> (Ce, Nd, La, Y, Zr), FPs present in metallic secondary phase (Rh, Ru, Pd, Tc, Mo) and FPs forming secondary oxide phase (Ba, Sr, Zr, Mo). The first step of this study involves manufacturing dense (U,Pu)O<sub>2</sub> pellets doped with fission product precursors using the industrial MIMAS process for MOx fuel fabrication. The second step consists of characterizing the manufactured material through different characterization methods to assess its representativeness. The manufacturing process resulted in dense pellets with less than 5% porosity. Optical imaging of a polished pellet face (Figure 1 (a)) revealed white and gray (highlight by blue circles) precipitates. The latter are consistent with the metallic cluster (white) and oxide perovskite phase (gray) observed in irradiated fuel [3]. The cationic distribution was analyzed using Raman spectrometry [4]. Figure 1 (b) displays a Raman map illustrating the intensity of the predominant line at about 1150 cm<sup>-1</sup>, often referred as characteristic UO<sub>2</sub> line. This map reveals three distinct phases: plutonium-rich clusters in blue ( $\approx$  26 wt% Pu), uranium-rich clusters in red (close to 0 wt% Pu), and a phase with intermediate plutonium content in green ( $\approx$  11 wt% Pu). This cationic distribution is typical of MOx PWR fuel [5]. The coupling of optical imaging and  $\mu$ -Raman spectroscopy over the same area, as illustrated in Figure 1, shows that fission product inclusions are localized within the plutonium-rich clusters.

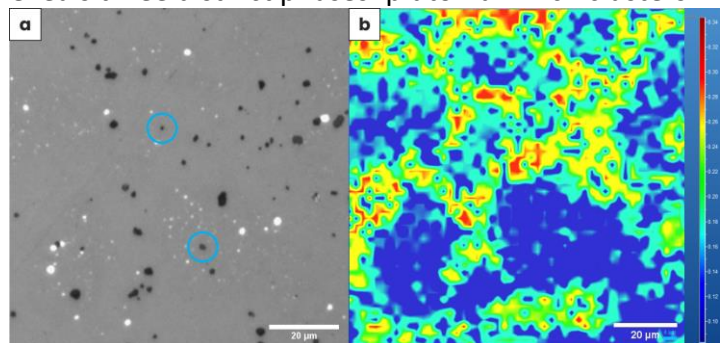


Figure 1. Optical imaging (a), 2LO intensity  $\mu$ -RAMAN mapping (b) of one sample polished face

## References

- [1] S. Bourg *et al.*, Prog. Nucl. Ener., 94, 2017, pp. 222-228.
- [3] H. Kleykamp, Nucl. Tech., vol. 80, 1988, pp. 412-422.
- [5] H. Bernard, J.Nucl. Mater., vol. 166, 1989, pp. 105-111.

- [2] R. Caprani *et al.*, J. Nucl. Mater., vol. 585, 2023, pp. 154607.
- [4] O. Kahraman *et al.*, J. Appl. Phys., vol. 132, 2022, pp. 115106.

# Radiation Stability and Structural Chemistry of $(\text{Zr}_{0.95}^{241}\text{Am}_{0.05})_{1-x}\text{Nd}_x\text{O}_{2-x0.5}$ Phases

G. L. Murphy<sup>1</sup>, S. Gilson<sup>2</sup>, K. Popa<sup>3</sup>, Tonya Vitova,<sup>4</sup> Damien Prieur,<sup>2</sup> O. Valu<sup>3</sup>, J.-Y. Colle<sup>3</sup>, O. Walter<sup>3</sup>, and N. Huittinen<sup>3,5</sup>

*1 Institute of Fusion Energy and Nuclear Waste Management (IFN-2), Forschungszentrum Jülich GmbH, 52428 Jülich, Germany*

*2 Institute of Resource Ecology, Helmholtz-Zentrum Dresden-Rossendorf, 01328 Dresden, Germany*

*3 European Commission, Joint Research Centre (JRC), Karlsruhe, Germany*

*4 Karlsruhe Institute of Technology (KIT), Institute for Nuclear Waste Disposal (INE), P.O. 3640, D-76021 Karlsruhe, Germany*

*5 Institute of Chemistry and Biochemistry, Freie Universität Berlin, 14195 Berlin, Germany*

*\*e-mail: g.murphy@fz-juelich.de*

The radiation and structural stability of Zircaloy cladding material that houses spent nuclear fuel (SNF) is an important factor when considering the storage and eventual disposal of SNF in a geological repository. It is known that on the surface of the cladding, oxidized zirconia ( $\text{ZrO}_2$ ) phases are inherently present. Following fuel swelling and rim contact, the zirconia layer on the interior surface can interact with SNF elements, leading to the formation of phases such as pyrochlore and zirconates among others. These phases act as the first intermediate barrier between SNF and the metallic cladding and consequently are important to consider in safety design, particularly for release of radionuclides (RNs). A pertinent RN that contributes significantly to the radiological hazard of SNF, is the isotope Am-241. The chemistry of Am is largely unique, being able to readily dissociate between its tetravalent and trivalent states in oxides, making it difficult to investigate via surrogate studies. Furthermore, Am-241 has a relatively short  $t_{1/2}$  of 432 years and decays via alpha emission (5.486 MeV), resulting in significant ensuing radiation damage in host materials. Consequentially, understanding the radiation stability and structural chemistry of host material phases incorporating Am-241 is pertinent for safe disposal of SNF. As a part of the European Commission ActUsLab program, we have investigated several zirconium oxide polymorphs, including but not limited to Nd-pyrochlore and zirconia, doped with 5 mol% Am-241. The particular focus of the investigation is to understand the thermal and radiation stability of the different oxide polymorphs when Am-241 is incorporated. Phases were subsequently analyzed via X-ray absorption near edge structure measurements, variable temperature X-ray powder diffraction, Raman spectroscopy in addition to electron microscopy. This presentation will highlight these results obtained regarding the structural chemistry of Am incorporated  $\text{ZrO}_2$  phases in addition to radiation response from self-irradiation that has occurred for over 1.5 years from the presence of Am-241.

# Synthesis of polynuclear neodymium structures as a model for actinide clusters

Maëva Munoz<sup>1\*</sup>, Christelle Tamain<sup>1</sup>, Matthieu Viro<sup>2</sup>, Valérie Vallet<sup>3</sup> and Dominique Guillaumont<sup>1</sup>

<sup>1</sup>CEA, DES, ISEC, DMRC, Univ Montpellier, Marcoule, France. <sup>2</sup>ICSM, Univ Montpellier, CEA, CNRS, ENSCM, Marcoule, France. <sup>3</sup>Laboratoire PhLAM, UMR CNRS 8523, Université des Sciences et Technologies de Lille, Villeneuve d'Ascq, France

\*maeva.munoz@cea.fr

Actinide chemistry is significantly influenced by the formation of polynuclear species, which have attracted considerable interest over the past decades. These species hold potential applications in waste management, fuel reprocessing and even biological systems. The polynuclear species of actinides (i.e., actinides clusters) discussed here materialize as molecules containing multiple metal centers connected by oxo and/or hydroxo groups. This forms the core of the cluster, often described by its nuclearity,  $N$ , which represent the number of actinide atoms within the cluster. These entities arise via condensation reactions (referred to as ololation and oxolation reactions) occurring in aqueous conditions and are surface-stabilized by organic or inorganic ligands.

In the solid state, various polynuclear species of actinides have been identified from XRD crystal structures, with various nuclearities ranging from 2 to 38. However, the hexamer consisting of 6 actinide atoms ( $An_6$ ) is frequently observed.<sup>[1]</sup> This nuclearity has been studied and stabilized several times in the form of the  $[An_6O_4(OH)_4]^{12+}$  core in the presence of carboxylate ligands for neptunium, uranium, thorium and plutonium in solution.<sup>[2, 3, 4]</sup> Our group has also studied the formation of plutonium hexameric clusters under various conditions and has revealed similarities in UV-Vis spectra associated with this nuclearity.<sup>[1, 4, 5]</sup> However, it remains difficult to identify these polynuclear species in solution since spectral fingerprints related to other nuclearities are not yet known.

The first objective of this study is to develop reliable spectroscopic databases, in order to help the identification of polynuclear species in solution. Initially, we focused on a model system using neodymium(III), selected as an analogue for plutonium(III). This work begins with the synthesis of Nd(III) single crystals characterized by X-ray diffraction (SCXRD) for which specific spectra were collected using UV-visible spectroscopy. Ligands and chemical conditions were selected to synthesize clusters with nuclearities differing from  $N=6$ , while also studying the impact of the distance between the donor atoms of the ligands on the formation and stability of the clusters. This approach will then be applied to plutonium with the aim of simplifying the identification of its different clusters in solution. This approach will pave the way to the understanding of the mechanisms involved in the formation of polynuclear species.

## References

- [1] Knope, K. E. *Chem. Rev.*, **2013**, *113* (2), 944–994.
- [2] Takao, K. *Inorg. Chem.*, **2012**, *51* (3), 1336–1344.
- [3] Takao, S. *Eur. J. Inorg. Chem.*, **2009**, *2009* (32), 4771–4775.
- [4] Tamain, C. *Eur. J. Inorg. Chem.*, **2016**, *2016* (22), 3536–3540.
- [5] Chupin, G. *Inorg. Chem.*, **2022**, *61* (12), 4806–4817.
- [6] Cot-Auriol, M. *Chem. Commun.*, **2022**, *58* (94), 13147–13150.

# Chemical footprints of thorium, uranium, and lanthanum in molten LiF-BeF<sub>2</sub> explored through molecular dynamic simulation technology

X. Li, Y. Gong\*

Key Laboratory of Thorium Energy, Shanghai Institute of Applied Physics, Chinese Academy of Sciences, Shanghai, China

\*e-mail: lixuejiao@sinap.ac.cn; gongyu@sinap.ac.cn

The Chemical forms and transport properties of thorium, uranium, and lanthanum ions in molten LiF-BeF<sub>2</sub> are systemically studied via first-principles and machine-learning potential molecular dynamic simulations. The densities, viscosities, diffusion coefficients, densities of electronic states, coordination numbers, and cluster structures of molten LiF-BeF<sub>2</sub>-ThF<sub>4</sub> (FLiBeTh), LiF-BeF<sub>2</sub>-UF<sub>4</sub> (FLiBeU), and LiF-BeF<sub>2</sub>-LaF<sub>3</sub> (FLiBeLa) in figure 1 are analyzed in detail. Studies have shown that the density and thermal expansion coefficient of molten FLiBeTh are higher than those of FLiBeU in the temperature range of 873-1073 K. Besides, the FLiBeTh has the narrowest band gap and more active Th electrons, which is one of the reasons for the more diverse and stable bonding structures and lower diffusion coefficients of Th ion. In addition, the quantitative relationships between these properties and LaF<sub>3</sub> concentration are also investigated. Furthermore, the concept of Be-F tetrahedron stress index is proposed in molten fluorides, where the proportion of zero order structure is a strongly correlated parameter for the diffusion coefficient. Overall, the understanding and characterization of fuel salt structure and property are underscored and the relationships between microstructure and diffusivity performance are established.

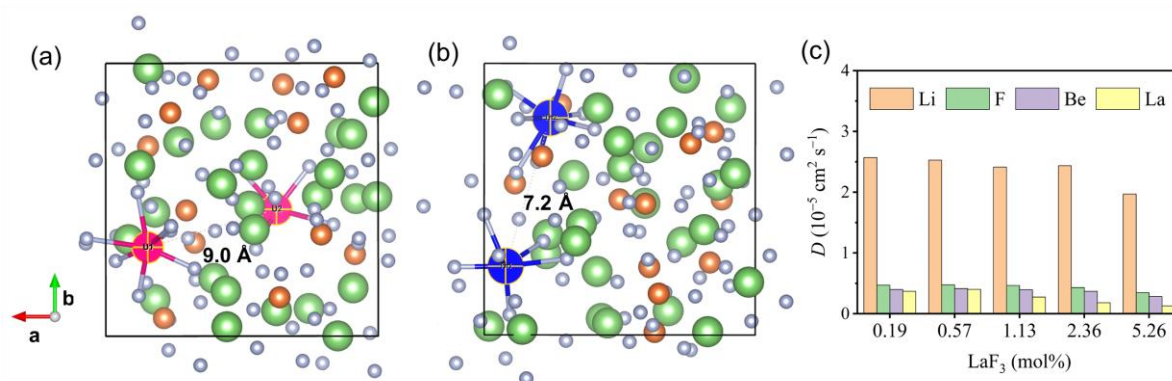


Figure 1: Initial configurations of molten (a) FLiBeU and (b) FLiBeTh, and (c) Ionic self-diffusion coefficients of FLiBeLa with different LaF<sub>3</sub> concentration (color-code: green-Li, orange-Be, gray-F, pink-U, blue-Th)

## References

- [1] X. Li, T. Xu, and Y. Gong, Phys. Chem. Chem. Phys., 26, 12044 (2024).
- [2] X. Li, R. Cui, Y. Song, and Y. Gong, J. Nucl. Mater., 599, 155201 (2024).

# Complexation of Protactinium(V) with Chlorides in aqueous solution: Thermodynamic and Structural Insights

M.Maloubier\*, T. Shaaban<sup>2</sup>, H. Oher<sup>1</sup>, V. Vallet<sup>2</sup>, F. Réal<sup>2</sup>, B. Siberchicot<sup>3</sup>, and C. Le Naour<sup>1</sup>

<sup>1</sup> *Université Paris-Saclay, CNRS/IN2P3, IJCLab, 91405 Orsay, France*

<sup>2</sup> *Université de Lille, CNRS, UMR 8523 – PhLAM – Physique des Lasers, Atomes et Molécules, F-59000 Lille-France*

<sup>3</sup> *CEA, DAM, DIF, F-91297 Arpajon, France ; and Université Paris-Saclay, CEA, Laboratoire Matière en Conditions Extrêmes, F-91680 Bruyères-le-Châtel, France.*

*\*e-mail: melody.maloubier@ijclab.in2p3.fr*

Protactinium(V) stands out among the actinides(V) for its peculiar chemical behavior, characterized by the absence of the actinyl moiety in condensed phase compounds. Instead, Pa(V) has a short mono-oxo bond, experimentally observed in oxalic and sulfuric media. However, the stability of this bond is uncertain and can disappear upon complexation, as observed with fluoride ions [1]. Interestingly, the experimentally measured Pa-O bond length in oxalate complexes (1.75 Å) differs significantly from the theoretical prediction of ~1.85 Å [2], highlighting the challenges of accurately modelling the behavior of Pa(V). The study of Pa(V) is further complicated by its remarkable propensity for hydrolysis and polymerization even in acidic conditions, and the difficulty in isolating significant amounts of this actinide, making it difficult to handle and investigate.

In this study, we investigate the complexation of Pa(V) with chloride ions, using X-ray absorption spectroscopy (XAS) to probe its chemical environment in different concentrations of hydrochloric acid. Chlorides, with their weak ligating properties, are expected to stabilize the mono-oxo bond in Pa(V) chloride complexes [3]. While thermodynamic studies have predicted the likely chemical forms of these complexes, they remain controversial and their structural details have remained elusive until now [4].

Using EXAFS analysis, we identified two distinct structures of Pa(V)-chloride complexes at 3M and 12M HCl. In addition, the EXAFS spectra adjustments with structures obtained by theoretical calculations reveal, for the first time a Pa-O bond length around 1.83 Å, aligning more closely with theoretical calculations [1,2,3]. This finding confirms the persistence of an oxo bond in Pa(V) chloride systems, advancing our understanding of protactinium chemistry. These results not only reconcile experimental observations with theoretical predictions but also provide a basis for future investigations into the coordination chemistry of Pa(V).

## References

- [1] M. Mendes, S. Hamadi, C. Le Naour, J. Roques, A. Jeanson, C. Den Auwer, P. Moisy, S. Topin, J. Aupiais, C. Hen-nig, and M.V. Di Giandomenico, *Inorg. Chem.* 49, 9962-9971 (2010).
- [2] H. Oher, J. Delafoulhouze, E. Renault, V. Vallet and R. Maurice, *Phys. Chem. Chem. Phys.* 25, 10033-10041 (2023).
- [3] T. Shaaban, F. Réal, R. Maurice and V. Vallet, *Chem. Eur. J.* 30, e202304068 (2024).
- [4] R. Muxart, R. Guillaumont, A. Pacault, and G. Pannetier, *Compléments au nouveau traité de chimie minérale.* (1974).



# Molecular Compounds of Actinide(IV) Oxalate: Structure and Bond Characterization

C. Tamain<sup>1\*</sup>, M. Autillo<sup>1</sup>, D. Guillaumont<sup>1</sup>, L. Guerin<sup>1</sup>, R. Wilson<sup>2</sup>, C. Berthon<sup>1</sup>

<sup>1</sup> CEA, DES, ISEC, DMRC, Univ Montpellier, Marcoule, France

<sup>2</sup> Chemical Sciences and Engineering Division, Argonne National Laboratory, Lemont, IL 60439, USA

\*e-mail: christelle.tamain@cea.fr

Oxalic acid is a very commonly used ligand for the quantitative recovery of actinides during the reprocessing of spent fuel. Numerous studies have focused on the structural characterization of polymeric phases containing actinides in various oxidation states, with varying dimensions ranging from linear structures to three-dimensional networks [1]. Despite these many structural studies and the interest in this ligand, there have been few attempts to describe the actinide-oxalate bond due to (i) the absence of molecular monomeric An(IV) oxalate compounds; (ii) the limited number of isomorphous An(IV) oxalate compounds along the actinide series; and (iii) the difficulty in treating polymeric compounds with DFT (Density Functional Theory) calculations, whereas monomeric compounds are perfect candidates.

Recently, we synthesized and characterized isomorphous molecular oxalate compounds,  $[An(C_2O_4)_5][Co(NH_3)_6]_2 \cdot 4H_2O$ , for the series of actinide(IV) ions from thorium to plutonium (An = Th, U, Np, Pu). These complexes feature five non-bridging bidentate oxalates in the actinide coordination sphere, providing the opportunity to probe the actinide-oxalate bond (Figure 1). To analyze the properties of this bond, structural studies were complemented by vibrational spectroscopy (Raman and IR) and DFT calculations. These results were compared to An(IV) hexanitrate complexes,  $[(C_2H_5)_4N]_2An^{IV}(NO_3)_6$ , also obtained for the same actinides, which similarly feature only oxygen donors in the actinide coordination sphere but with a higher coordination number (12 instead of 10 for the oxalate compounds).

The bond analysis of these compounds confirms that the actinide-oxygen bond is predominantly ionic for both families, with a slight increase in covalence from thorium to uranium, but little variation between uranium and plutonium. Charge transfer increases with the coordination number, but the covalence effects remain weak and similar for both oxalates and nitrates.

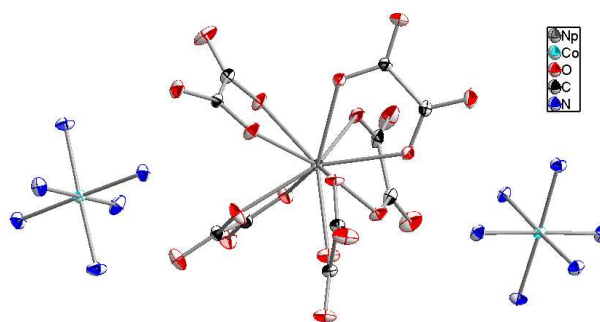


Figure 1: Structure of  $[An(C_2O_4)_5][Co(NH_3)_6]_2 \cdot 4H_2O$  (An=Th, U, Np, Pu).

## References

[1] F. Abraham, B. Arab-Chapelet, M. Rivenet, C. Tamain, S. Grandjean, Actinide oxalates, solid state structures and applications. *Coord. Chem. Rev.*, 266-267, 28-68 (2014).

# A DFT+DMFT look at the Magnetic Properties of $\delta$ Plutonium

F. Gendron<sup>1,2,\*</sup> and B. Amadon<sup>1,2</sup>

<sup>1</sup>CEA, DAM, DIF, F-91297 Arpajon, France

<sup>2</sup>Université Paris-Saclay, CEA, Laboratoire Matière en Conditions Extrêmes,  
91680 Bruyères-le-Châtel, France

\*e-mail: frederic.gendron@cea.fr

The rationalization of the electronic and magnetic properties of metallic plutonium is still subject to debate nowadays from an ab-initio perspective. Elemental plutonium contains a partially filled 5f shell that should lead to strong electron correlation effects, and therefore, to a sizable local moment. However, experimentally no evidence of ordered nor disordered local moments has been characterized in metallic plutonium. Indeed, alloyed  $\delta$ -Pu exhibits a nearly temperature-independent magnetism at low temperatures that is characteristic of a non magnetic ground state. In this presentation we will discuss the calculated electronic structure and magnetic susceptibilities obtained using the combination of density functional theory and dynamical mean field theory (DFT+DMFT).[1] We will show that the experimental trends are principally reproduced by this approach as the spin-orbit coupling, the crystal-field interaction and the dynamical fluctuations are taken into account simultaneously. The calculated DMFT susceptibilities are characteristic of a Kondo system where the local moment is screened by the conduction electrons. The energy scale of this effect is found to be sensitive to the different approximations used in the DMFT approach.

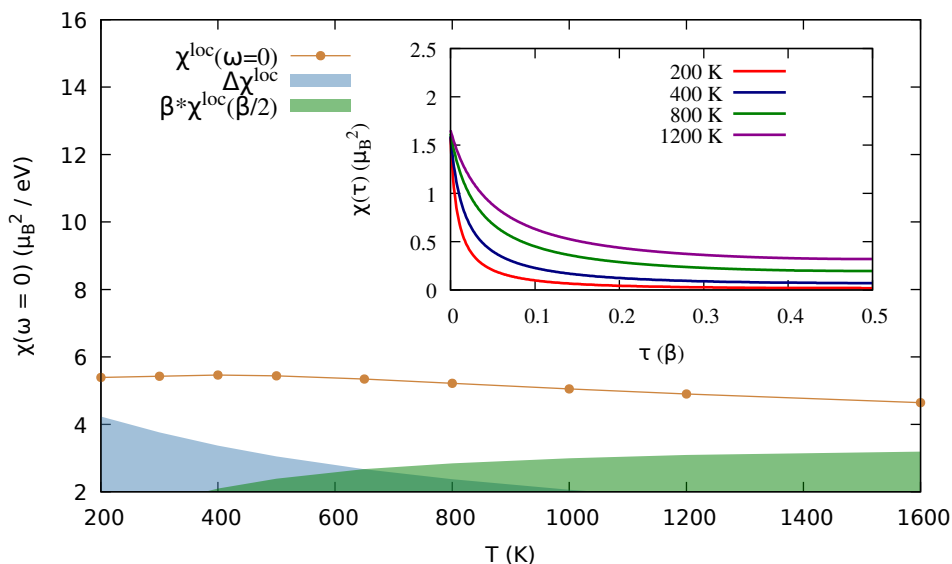


Figure 1: Static  $\chi(\omega=0)$  and dynamical  $\chi(\tau)$  local magnetic susceptibilities of the  $\delta$ -Pu as a function of the temperature.

## References

[1] B. Amadon, Phys. Rev. B, 94, 115148 (2016)

# Magnetic Structure Changes Under External Stimuli in UO<sub>2</sub>: High-Field and Strain-Induced Transitions

E.A. Tereshina-Chitrova<sup>1\*</sup>, L. V. Pourovskii<sup>2,3</sup>, S. Khmelevskiy<sup>4</sup>, D. Gorbunov<sup>5</sup>, L. Horak<sup>6</sup>, R. Caciuffo<sup>7</sup>

<sup>1</sup>*Institute of Physics ASCR, 182 21 Prague, Czech Republic*

<sup>2</sup>*CPHT, CNRS, 91120 Palaiseau, France*

<sup>3</sup>*Collège de France, Université PSL, 75005 Paris, France*

<sup>4</sup>*VSC Research Center, Technical University of Vienna, 1040 Vienna, Austria*

<sup>5</sup>*HLD-EMFL, 01328 Dresden, Germany*

<sup>6</sup>*Faculty of Mathematics and Physics, Charles University, 121 16 Prague, Czech Republic*

<sup>7</sup>*Istituto Nazionale di Fisica Nucleare, 16146 Genova, Italy*

\*e-mail: teresh@fzu.cz

UO<sub>2</sub>, beyond its critical role as a nuclear fuel, is a complex magnetic material that poses significant challenges to both experimental and theoretical investigations due to the intricate interplay of spin-phonon interactions, multipolar ordering, and Jahn-Teller effects [1]. Crystallizing in a face-centered cubic (*fcc*) lattice, UO<sub>2</sub> exhibits magnetic frustration arising from the energy degeneracy of three antiferromagnetic (AFM) states, which leads to the establishment of a  $3\mathbf{k}$  transverse AFM order below the Néel temperature  $T_N = 30.8$  K. Previous studies have highlighted complex magnetoelastic phenomena in UO<sub>2</sub> [2,3].

In this work, we demonstrate how external stimuli, such as high magnetic fields and strain, resolve the magnetic frustration and induce the magnetic structure changes of UO<sub>2</sub> using both single crystals and thin films. For single-crystalline UO<sub>2</sub>, ultrasound velocity measurements under pulsed magnetic fields up to 65 T reveal a crossover in  $\Delta v/v$  near 50 T, consistent with *ab initio* predictions of a  $3\mathbf{k}$ -to- $2\mathbf{k}$  magnetic transition [4]. Our results indicate that above 50 T, the structure remains antiferromagnetic in the (*x,y*) plane but becomes ferromagnetic in the *z* direction, with a further transition to the  $1\mathbf{k}$  structure predicted at approximately 104 T.

Interestingly, high magnetic fields are not required to stabilize alternative magnetic structures when strain is applied to UO<sub>2</sub> along the [001] direction, as e.g. in thin films. We predict a  $3\mathbf{k} \rightarrow 1\mathbf{k}$  transition induced by tetragonal distortion in UO<sub>2</sub> thin films [5]. Our findings demonstrate that the  $1\mathbf{k}$  and  $2\mathbf{k}$  AFM orders, which compete with the  $3\mathbf{k}$  ground state in the frustrated UO<sub>2</sub> lattice, can be effectively tuned through external stimuli, offering new perspectives on the complex relationship between magnetism and lattice distortions in UO<sub>2</sub>.

## References

- [1] G. H. Lander and R. Caciuffo, J. Phys.: Condens. Matter 32, 374001 (2020).
- [2] O. G. Brandt and C.T.Walker, Phys. Rev. Lett. 18, 11 (1967).
- [3] M. Jaime et al., Nat. Commun. 8, 99 (2017).
- [4] E.A. Tereshina-Chitrova et al., Phys. Rev. B 110, 224417(2024).
- [5] E. A. Tereshina-Chitrova et al., Adv. Funct. Mater. 34, 2311895 (2024).

## Magnetic properties of mixed actinide oxides

Eric. Colineau<sup>1\*</sup>, Jean-Christophe Griveau<sup>1</sup>, Laura Martel<sup>1</sup>, Karin Popa<sup>1</sup>, Sorin-Octavian Vălu<sup>1</sup>, Ondrej Beneš<sup>1</sup>, Jean- François Vigier<sup>1</sup>, Morgane Rochedy<sup>1</sup>, Anna Smith<sup>2</sup>, Rudy J.M. Konings<sup>1,2</sup>, and Rachel Eloirdi<sup>1</sup>

<sup>1</sup>European Commission, Joint Research Centre (JRC), Karlsruhe, Germany

<sup>2</sup>Delft University of Technology, Faculty of Applied Sciences, Radiation Science & Technology Department, Delft, The Netherlands

\*eric.colineau@ec.europa.eu

The physical properties of actinide-based mixed oxides - in particular thorium, uranium, neptunium, plutonium and americium – are of large technological and safety interest for nuclear power and non-power applications : their use for nuclear fuels is well-known, but they are also used or considered for many other applications like for example plutonium-238 oxide or uranium-doped americium-241 oxide for deep space exploration [1].

In addition, these materials are also very interesting from a fundamental science point of view : Although they are insulators with localized 5f electrons, crystal field theory is not sufficient to explain their magnetic properties including for example multipolar order.

UO<sub>2</sub> develops dipolar magnetic order at low temperatures with moments ( $m_U = 1.74\mu_B$ ) ordering into a type-I antiferromagnetic structure below  $T_N = 30.8K$  [2]. NpO<sub>2</sub> also orders magnetically, at  $T_N = 25K$ , but the dipolar moment is vanishing and the primary order parameter is a rank-5 multipole (triakontadipole). In addition, induced antiferroquadrupolar (AFQ) ordering is observed in both UO<sub>2</sub> (transverse) and NpO<sub>2</sub> (longitudinal) [2]. Thorium does not possess 5f electrons and its oxide ThO<sub>2</sub> displays a diamagnetic behaviour. PuO<sub>2</sub> displays a temperature-independent paramagnetism, because the ground state of the Plutonium ion is a non-magnetic singlet [3]. However, first-principle calculations predict a ferro- or antiferro-magnetic ground state, not observed experimentally and a possible “hidden order” has been postulated [4]. Finally, AmO<sub>2</sub> shows an antiferromagnetic transition at 8.5K [5] whereas CmO<sub>2</sub> presents a Curie-Weiss behaviour [6].

In the present study, we will report on the magnetic properties of mixed oxides involving thorium, uranium, neptunium, plutonium and americium.

### References

- [1] J.-F. Vigier, D. Freis, P. Pöml, D. Prieur, P. Lajarge, S. Gardeur, A. Guiot, D. Bouëxière, and R.J.M. Konings, *Inorganic Chemistry* 57, 4317 (2018)
- [2] L. Martel, A. Hen, Y. Tokunaga, F. Kinnart, N. Magnani, E. Colineau, J.-C. Griveau, and R. Caciuffo, *Phys. Rev. B* 98, 014410 (2018)
- [3] P. Santini, R. Lémanski, and P. Erdős, *Magnetism of actinide compounds*, *Advances in Physics*, 48:5, 537-653 (1999)
- [4] J.T. Pegg, A.E. Shields, M.T. Storr, A.S. Wills, D.O. Scanlon, and N.H. de Leeuw, *Phys. Chem. Chem. Phys.* 20, 20943 (2018)
- [5] D. G. Karraker, *J. Chem. Phys.* 63, 3174 (1975)
- [6] L.R. Morss, J.W Richardson, C.W. Williams, G.H. Lander, A.C. Lawson, N.M. Edelstein, and G.V. Shalimoff, *Journal of the Less-Common Metals* 156, 273 – 289 (1989)

# Connecting High Field and High Pressure Superconductivity in $\text{UTe}_2$

D. Braithwaite<sup>1</sup>, T. Vasina<sup>1</sup>, D. Aoki<sup>2</sup>, G. Seyfarth<sup>3</sup>, J.-P. Brison<sup>1</sup>, C. Marcenat<sup>1</sup>, A. Pourret<sup>1</sup>, G. Lapertot<sup>1</sup> and G. Knebel<sup>1</sup>

<sup>1</sup>Univ. Grenoble Alpes, CEA, Grenoble-INP, IRIG, Pheliqs, 38000 Grenoble, France

<sup>2</sup>IMR, Tohoku University, Oarai, Ibaraki 311-1313, Japan

<sup>3</sup>Univ. Grenoble Alpes, INSA Toulouse, Univ. Toulouse Paul Sabatier, EMFL, CNRS, LNCMI, Grenoble 38042, France

\*e-mail: Daniel.braithwaite@cea.fr

The existence of multiple superconducting phases induced by either pressure[1] or magnetic field[2] is one of the most striking features of superconductivity of  $\text{UTe}_2$ , among the many unusual superconducting properties of this system. I will show thermodynamic measurements of the superconducting phase diagram combining pressure and magnetic fields up to 30T. We find that the ambient pressure, high field, superconducting phase evolves continuously with pressure to join the high pressure, zero field superconducting phase[3]. This proves that these two phases are one and the same, and must have the same order parameter. This imposes new constrictions for theoretical models for the superconducting mechanisms and order parameters in this extraordinary system.

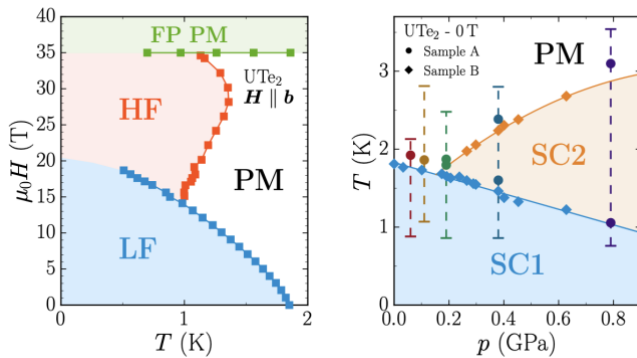


Figure 1. Multiple superconducting phases in  $\text{UTe}_2$  under field (left) or pressure (right) adapted from references [2] and [1]. In this work we show that the superconducting HF and SC2 phases are in fact identical.

## References

- [1] D. Braithwaite et al. Commun Phys **2**, 147 (2019)
- [2] A. Rosuel et al. PRX **13**, 011022 (2023)
- [3] T. Vasina et al. [arXiv:2410.17733](https://arxiv.org/abs/2410.17733) (2024)

# Perpendicular magnetic anisotropy in a single Dy adatom ferrimagnet

A. B. Shick<sup>1\*</sup>, F. Maca<sup>1</sup>, and D. Legut<sup>2</sup>

<sup>1</sup>FZU-Institute of Physics, Czech Academy of Sciences, Prague, the Czech Republic

<sup>2</sup>IT4Innovations, VSB-Technical University of Ostrava, Ostrava, the Czech Republic

\*e-mail: shick@fzu.cz

Rare-earth atom adsorption on suitable surfaces is a viable pathway for creating atomic scale magnetic information storage in the most fundamental unit of matter. Dysprosium (Dy) exhibits a large magnetic anisotropy and can be protected against quantum tunneling in a uniaxial crystal field [1]. Among possible substrates graphene (Gr)/Ni(111) has been set forward as the optimal scaffold where to deposit adatoms.

We address the electronic and magnetic structure, and the magnetic anisotropy of Dy@Gr/Ni(111) making use of the DFT+U(HIA) methodology [2], and 3x3x1 supercell model (see Fig1A) with 36 Ni-atoms, and the layer of graphene with 18 C atoms on the top of Ni surface. The Dy adatom is placed in the hollow position.

The  $f$ -shell  $n_{4f} = 9.9$  occupation corresponds to Dy<sup>2+</sup> valence. The values of spin  $M_S=3.5\mu_B$ , orbital  $M_L=5.1\mu_B$ , and total  $M_J=8.6\mu_B$  magnetic moments are noticeably different from the atomic second Hund's rule. There is almost zero moment on Gr atoms. The Ni substrate moment of  $-19.8\mu_B$  is anti-aligned to the Dy 4*f*-shell moment.

The spin-resolved 5*d*- and 4*f*-projected DOS of Dy are shown in Fig. 1B together with the partial DOS for the graphene C-atoms. It indicates a significant n-doping due to the charge transfer to graphene, and the metallic character of Dy@GR/Ni(111). The calculated  $M_{4,5}$ -edge XAS and XMCD spectra are shown in Fig1C. They can be used to make a comparison of our predictions with the experimental data.

The magnetic anisotropy energy (MAE) is calculated from the many-body ground state energy difference for different directions of the magnetization,  $E[100] - E[001] = 11.3$  meV and  $E[010] - E[001] = 9.6$  meV. This large and positive MAE can be important for the ultra-high density magnetic recording.

Financial support was provided by the Czech Science Foundation (GACR) Grant No. 24-11992S.

## References

- [1] A. Singha *et al.*, *Nat. Comm.* 12, 4179 (2021).
- [2] A. B. Shick, E. Belsch, A. I. Lichtenstein, *Phys. Rev. B* 108, L180408 (2024).

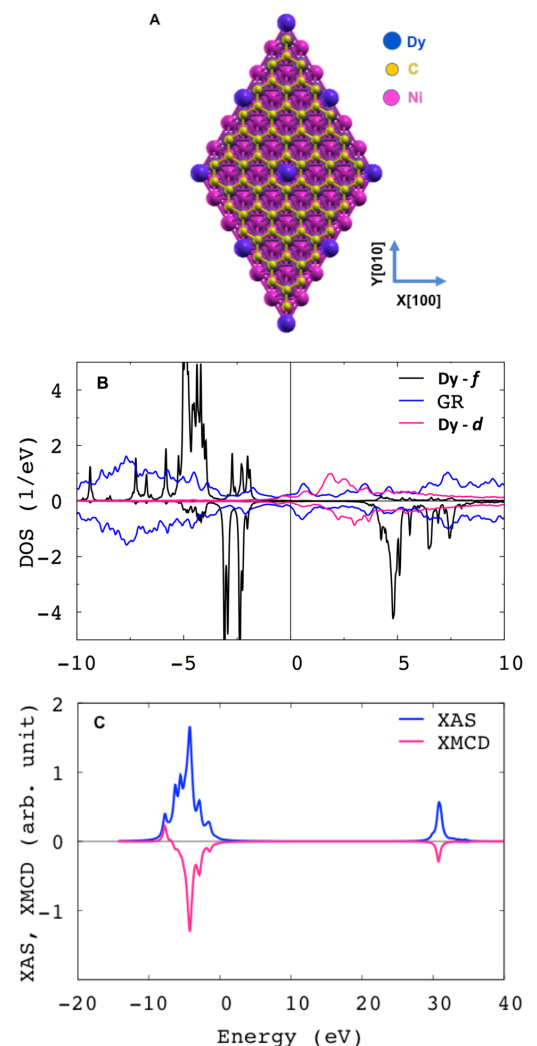


Figure 1: Supercell model for Dy@Gr/Ni (A); Dy 5d, 4f Dy and Gr DOS (B); the  $M_{4,5}$  edge XAS and XMCD spectra (normal incidence).

# Exploring New Uranium Materials Containing Kagome Networks

Midori Amano Patino<sup>1,4</sup>, Valentin Taufour<sup>2</sup>, Stephane Raymond<sup>3</sup>, Georg Knebel<sup>1</sup>, Gerard Lapertot<sup>1</sup>, Daniel Braithwaite<sup>1</sup>, Jean-Pascal Brison<sup>1</sup>, Elise Pachoud<sup>4</sup>, Klaus Hasselbach<sup>4</sup>

<sup>1</sup>Univ. Grenoble Alpes, CEA, Grenoble INP, IRIG, Pheliqs, 38000 Grenoble, France

<sup>2</sup>University of California Davis, Department of Physics and Astronomy, California, U.S.

<sup>3</sup>Univ. Grenoble Alpes, CEA, IRIG, MEM, MDN, Grenoble, France

<sup>4</sup>Univ. Grenoble Alpes, Institut Néel, CNRS, Grenoble, France

[Midori.AMANO-PATINO@cea.fr](mailto:Midori.AMANO-PATINO@cea.fr) / [Midori.AMANO-PATINO@neel.cnrs.fr](mailto:Midori.AMANO-PATINO@neel.cnrs.fr)

In recent years, Kagome metals have attracted significant attention due to their distinctive electronic band structures, which feature Dirac points, van Hove singularities, and a flat band [1,2]. These characteristics drive electronic instabilities and give rise to non-trivial topological effects, observed across various Kagome metal families. Prominent examples of Kagome metals include  $AV_3Sb_5$  ( $A = K, Rb, Cs$ ) exhibiting superconductivity [4],  $Fe_3Sn_2$  with signatures of low-energy Weyl fermions and associated topological Fermi arc surface [5], and  $ScV_6Sn_6$  exhibiting charge density wave [6]. Within this context, the  $RV_6Sn_6$  family, where  $R$  is a rare-earth element, has garnered considerable interest [7]. In these materials, the  $R$  sites form triangular 2D lattices that alternate with Kagome networks of non-magnetic vanadium sites. The Fermi surface is predominantly influenced by the  $d$ -orbitals of the Kagome lattice, while the localised  $f$ -orbitals of the rare-earth elements introduce magnetic degrees of freedom, resulting in a complex interplay with the Kagome network's physics. A particularly interesting case arises when uranium is incorporated into these systems. The  $5f$  electrons of uranium exhibit dual behaviour, being both localised and itinerant, which fosters non-trivial interactions. These interactions can lead to phenomena such as heavy fermion behaviour, Kondo effects, and unconventional superconductivity [8,9].

Building on this idea, the novel compound  $UV_6Sn_6$  has been successfully synthesised at CEA-Grenoble, and single crystals have been grown. Measurements of specific heat, magnetisation, and resistivity reveal incommensurate magnetic spin ordering that locks into an antiferromagnetic ground state. To further understand this state, we conducted neutron diffraction experiments and discovered that the crystallographic structure of  $UV_6Sn_6$  is intriguingly complex.

## References

- [1] J. Khatua, et al. *Physics Reports* **1041**, 1 (2023).
- [2] H. Kim, et al., *Commun Phys* **6**, 1 (2023).
- [3] X.-G. Wen, *Science* **363**, eaal3099 (2019).
- [4] S. D. Wilson and B. R. Ortiz, *Nat Rev Mater* **9**, 420–432 (2024).
- [5] Z. Ren et al., *Npj Quantum Mater.* **7**, 109 (2022).
- [6] Y. Hu et al., *Nat Commun* **15**, 1658 (2024).
- [7] X. Xu, et al. *Rep. Prog. Phys.* **86**, 114502 (2023).
- [8] W. Suski, *Phys. Solid State* **41**, 733 (1999).
- [9] J. G. Checkelsky, *Nat Rev Mater* **9**, 509 (2024).

# Tracing quasiparticle dynamics and hybridization dynamics in PuCoGa<sub>5</sub>

Haiyan Lu<sup>1</sup>

<sup>1</sup> Institute of Materials, China Academy of Engineering Physics, 621908, Jianguyou, China, e-mail: hyluphys@163.com

In this study, we systematically investigated the evolution of correlated electronic states in the plutonium-based unconventional superconductor PuCoGa<sub>5</sub> upon temperature using the embedded dynamical mean-field theory merged with density functional theory<sup>[1-2]</sup>. The reproducibility of theoretical total density of states and experimental photoemission spectra for PuCoGa<sub>5</sub> guarantees the reliability of calculation. The mixed-valence nature of PuCoGa<sub>5</sub> leads to intriguing quasiparticle dynamics and hybridization dynamics. Our findings reveal the presence of Dirac fermions and a temperature-driven localized-itinerant crossover of 5*f* states. As the temperature decreases, the low-energy quasiparticle resonances develop gradually, while the high-energy quasiparticle resonances exhibit quite different behaviors with an initial increase and subsequent decrease. Furthermore, we identified a characteristic temperature of approximately 290 K for the onset of hybridization gaps, which is much lower than the coherence temperature 580 K for 5*f* electrons. These results can provide valuable insight on the the electronic structures, quasiparticle dynamics, and hybridization processes in 5*f* correlated electron systems.

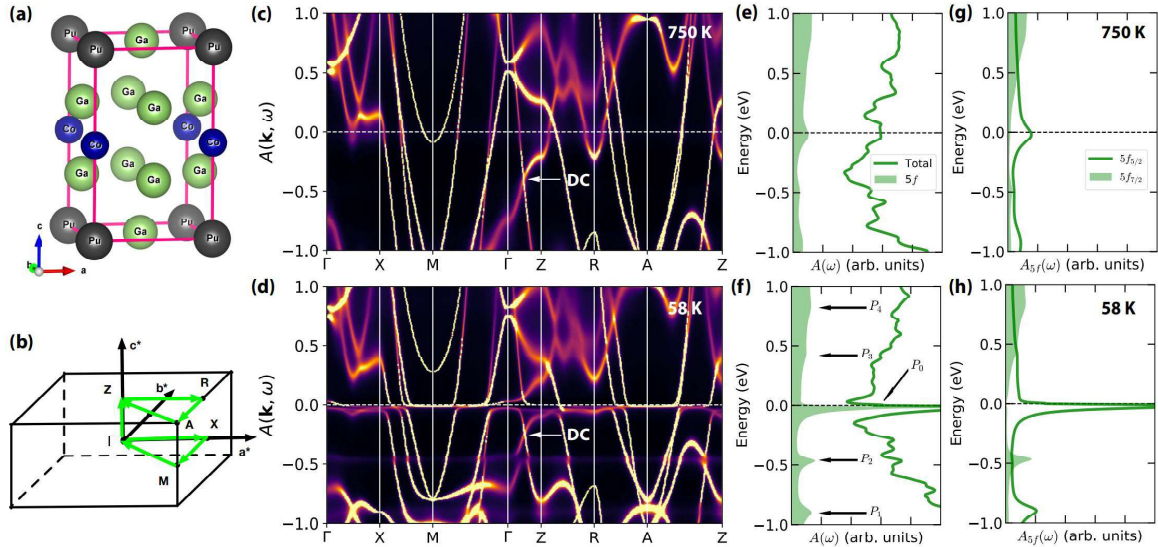


Fig. 1. Temperature-dependent electronic structures of PuCoGa<sub>5</sub>. (a) Crystal structure and (b) first Brillouin zone of PuCoGa<sub>5</sub>. (c)-(d) Quasiparticle band structures at 750 K and 58 K. Along the  $\Gamma$ -Z line, the Ga2-pz and Ga1-s orbitals cross with each other, which leads to a Dirac cone, as indicated by white arrow. (e)-(f) Total density of states  $A(\omega)$  and partial 5*f* density of states  $A_{5f}(\omega)$  at 750 K and 58 K. Here, the labels P0, P1, P2, P3, and P4 denote the peaks of quasiparticle multiplets. (g)-(h) Partial 5*f* density of states split by spin-orbit interactions at 750 K and 58 K

## References

- [1] Li Huang\* and Haiyan Lu†, *Phys. Rev. B* **109**, 205132 (2024).
- [2] Haiyan Lu\* and Li Huang, *Phys. Rev. B* **108**, 165109 (2023).



# $U_{13}Pd_{47}Ge_{25}$ : a quasicrystalline Tsai-type approximant with spin-glass behaviour

Magdalena Majewicz<sup>1</sup>, Maria Szlawska<sup>1</sup>, Valérie Demange<sup>2</sup>, Thierry Guizouarn<sup>2</sup>, Mathieu Pasturel<sup>2</sup>

<sup>1</sup> Institute of Low Temperature and Structure Research, Polish Academy of Sciences, 50-422 Wrocław, Poland

<sup>2</sup> Univ Rennes, CNRS, ISCR – UMR6226, ScanMAT – UAR2025, F-35000 Rennes, France

e-mail: mathieu.pasturel@univ-rennes.fr

Since their discovery by Shechtman *et al.* in 1984 [1], quasicrystals and their approximants have attracted considerable scientific interest, not only for their exceptional crystallographic properties, but also for their wide range of chemical and physical properties and related applications [2].

The cubic  $YCd_6$  structure-type and its derivatives form a well-known family of 1/1 Tsai-type quasicrystal approximants [3]. While many  $4f$  element-based intermetallics belong to this family, examples with actinides are much scarcer, with only  $NpCd_6$  and  $PuCd_6$  appearing in databases. In the course of our investigation on the U-Pd-Ge system, we discovered the formation of the ternary  $U_{13}Pd_{47}Ge_{25}$  phase [4] adopting this structure type. Examination of the crystal structure by X-ray and electron diffractions confirms the presence of a pseudo-5-axis originating from the stacking of endohedral clusters (fig 1).

The crystallographic details of this germanide (*i.e.* triangular network of U1, large cage around U2, mixed occupancy of two Pd/Ge sites) are favourable for the occurrence of magnetic frustration. Consequently, spin-glass like features are evident in the magnetic properties (fig. 1), specific heat and electrical resistivity of this material. Furthermore, these physical properties are influenced by the crystallographic disorder.

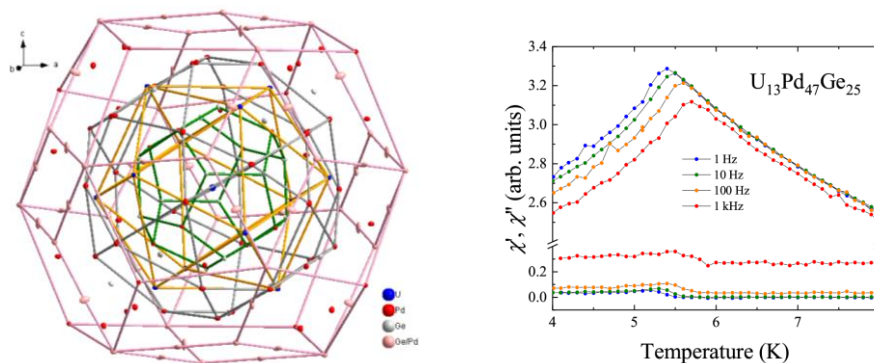


Figure1 Description of  $U_{13}Pd_{47}Ge_{25}$  crystal structure as a stacking of endohedral clusters, and temperature dependence of its ac susceptibility measured at several frequencies.

## References

- [1] D. Shechtman *et al.*, *Phys. Rev. Lett.* **53**, 1951 (1984).
- [2] E. Macia Barber, *Appl. Sci.-Basel* (2019). doi:10.3390/app9102132
- [3] C. P. Gómez, S. Lidin, *Phys. Rev B* **68**, 024203 (2003).
- [4] M. Majewicz *et al.* *J. Alloys Compd.* **1010**, 177541 (2025)

# Low Temperature Ground State Properties of 4f and 5f based phosphate compounds [RE or An]PO<sub>4</sub> with RE= Ce, Sm (sc) and An=<sup>239</sup>Pu, <sup>241</sup>Am.

Jean-Christophe Griveau\*, Karin Popa, Olaf Walter, Eric Colineau and Laura Martel

*European Commission, Joint Research Centre (JRC), Karlsruhe, Germany*

*\*jean-christophe.griveau@ec.europa.eu*

Phosphate materials have been extensively studied in the last decades due to the variety of use in advanced domains related to their 4f electronic structure such as ionic conductors, catalysts, luminescent materials, etc. [1]. They have also been considered for their structural and chemical stability for embedding nuclear materials. Monazite, apatite or double monophosphates for instance have been thoroughly studied as matrices for immobilization of nuclear waste [2].

Few basic properties of these systems at low temperature (<77K) have been reported on pure lanthanide-based phosphates especially magnetic susceptibility or heat capacity [3,4]. Nevertheless, this knowledge is crucial to establish fundamental models of their ground state from a theoretical point of view as for modeling potential applications [5]. Here we present results on CePO<sub>4</sub>, SmPO<sub>4</sub>, <sup>239</sup>PuPO<sub>4</sub> and <sup>241</sup>AmPO<sub>4</sub>. Main features of RE compounds have been previously reported - SmPO<sub>4</sub> and CePO<sub>4</sub> - but not in single crystal form or not at extreme conditions such as low temperature (T= 0.37 K) or under magnetic field (B= 14 T). DC and AC magnetization measurements (M/H,  $\chi$ ) using a Quantum Design MPM-3 (7T) magnetometer and Heat Capacity (C<sub>p</sub>) determined by hybrid relaxation technics in PPMS 14T have been performed on single crystals and bulk samples.

We do not observe any hint of magnetic transition below 77 K for CePO<sub>4</sub> reported as an antiferromagnet [6]. Strong Schottky anomalies due to crystal field effect are observed for SmPO<sub>4</sub> and CePO<sub>4</sub> in heat capacity and magnetic susceptibility, contrary to Van Vleck ground state compound EuPO<sub>4</sub> [7]. For all these systems, LaPO<sub>4</sub> is used as a pure phonon compound reference. For actinide-based compounds we did performed complementary measurement by heat capacity to clarify the antiferromagnetic order at T<sub>N</sub> ≈ 3.9 K for <sup>239</sup>PuPO<sub>4</sub> and its dependence with magnetic field [8]. At the lowest temperature achieved on <sup>241</sup>AmPO<sub>4</sub> sample in heat capacity [8], namely 17 K, we do not observe any hint of any magnetic anomaly nor Schottky signature, in agreement with published magnetic susceptibility measurements [9]. Extending these studies – especially thermodynamics ones - to CmPO<sub>4</sub> [10] would be of a great interest especially considering long-term storage of nuclear wastes.

## References

- [1] L. Martel et al, Solid State Nucl. Magn. Reson., 2020, **105**, 101638.
- [2] M. R. Rafiuddin et al, ACS Omega, 2022, **7**, 44, 39482–39490.
- [3] S. Neumeier et al., Radiochimica Acta, 2017, **105**, 11, 961.
- [4] Handbook on the Physics and Chemistry of Rare Earths, 1984, **9**, 237.
- [5] J. Diwu et al, Inorg. Chem., 2012, **51**, 12, 6906–6915.
- [6] J.T. Ellis et al., 1985, ORNL—6128, Watson, D.M. (Ed.). USA
- [7] L. Martel et al, Phys. Rev. B **100**, 2019, 054412.
- [8] K. Popa et al, Inorg. Chem. 2020, **59**, 9, 6595–6602.
- [9] L. Martel et al, J. Phys. Chem. C 2021, **125**, 40, 22163–22174.
- [10] F. Weigel et al., Inorg. Chim. Acta, 1984, **94**, 1-33, 31

## List of posters

1	Rami Babayew	An Innovative Approach to Isotopic Fingerprinting in Nuclear Forensics: Leveraging LEXAN® SSNTDs and Aerogel for Enhanced FTA Analysis
2	Romuald Béjaud	<i>Ab initio</i> study of point defect diffusion in $\delta$ -Pu.
3	François Bottin	Machine learning assisted <i>ab initio</i> simulations for actinides
4	Jacob Alan Branson	Evaluating 5 <i>f</i> Orbital Covalency in $UX_6^-$ (X = F, Cl) with U M-edge Resonant Inelastic X-ray Scattering
5	Daphné Cette	Materials research for the development of Americium-based RTGs and RHUs used in space missions
6	Xiuting Chen	Gas-phase syntheses and structures of organothorium complexes
7	Eric Colineau	ActUsLab (Actinide User Laboratory)
8	Claire Corkhill	An investigation of $(U_{(1-(x+y))}Th_xGd_y)O_{2-\delta}$ solid solutions as a function of synthesis method: Supporting disposal of the UK's plutonium
9	Shanmukh Veera Venkata U. Devanaboina	Stabilization of $\alpha$ -UH <sub>3</sub> in U-Hf Hydrides: Effects on Structure and Magnetism
10	Noam Elgad	Utilization of Deep Learning for Star Segmentation and Classification using Semi-Automated Adaptive Threshold methodology
11	Sébastien Faure	Influence of Pu(IV) and Pu(VI) on the extraction properties of anion exchange resins
12	Leo Gilliver	Underpinning National Nuclear Safety via the Safe Storage of Legacy Nuclear Waste
13	António Pereira Gonçalves	Novel Uranium Hybrid Materials
14	António Pereira Gonçalves	New Uranium Carbides for ISOL targets
15	Jiaolai Jiang	SERS detection of trace uranium at application scenarios
16	Hanna Kaufmann-Heimeshoff	Resonant inelastic X-ray scattering tools to count 5 <i>f</i> electrons of actinides and probe bond covalency
17	Eleanor Lawrence Bright	Accessing single-crystal U <sub>4</sub> O <sub>9</sub> and U <sub>3</sub> O <sub>7</sub> using topotactic oxidation
18	Jason Ross	8-Hydroxyquinoline as a potential Ligand for Actinide Decorporation
19	Mustapha Gida Saleh	Dissolution of unirradiated MOX fuel in the presence of metallic iron
20	Rui Song	Interstitial-Oxygen doping induced Insulator-Metal transition and structure phase transition in UO <sub>2+x</sub>
21	William Thomas	Under pressure to uncover a record Tc in uranium - Synthesis and electrical transport of new uranium hydride phases
22	Qi-Xian Wang	Lanthanide nanoparticles and MOFs heterostructures boosting NIR-II imaging-guided photodynamic therapy

# An Innovative Approach to Isotopic Fingerprinting in Nuclear Forensics: Leveraging LEXAN® SSNTDs and Aerogel for Enhanced FTA Analysis

Babayew Rami<sup>1,2</sup>, Yaacov Yehuda-Zada<sup>1,2</sup>, Galit Bar<sup>3</sup>, Elgad Noam<sup>1,2</sup>, Last Mark<sup>4</sup>, Jan Lorincik<sup>5</sup>, Itzhak Orion<sup>2</sup>, Shay Dadon<sup>1</sup>, Aryeh Weiss<sup>6</sup>, Galit Katarivas Levy<sup>7</sup>, Halevy Itzhak<sup>2</sup>

<sup>1</sup> Engineering Department, Nuclear Research Center Negev, Beer-Sheva, Israel

<sup>2</sup> Unit of Nuclear Engineering, Faculty of Engineering Sciences, Ben Gurion University, Israel

<sup>3</sup> Department of Solid-State Physics, Soreq Nuclear Research Center, Yavne, Israel

<sup>4</sup> Department of Software and Information Systems Engineering, Ben Gurion University, Israel

<sup>5</sup> Nuclear Fuel Cycle Department, Centre Řež, Hlavní 130, Řež 250 68, Husinec, Czech Republic

<sup>6</sup> Bar Ilan University, Ramat Gan P.O.B. 90000 5290002 Israel

<sup>7</sup> Dept. of Biomedical Engineering, Ben-Gurion University, Beer-Sheva, Israel

This research aims to advance isotopic identification capabilities in nuclear forensics by enhancing the resolution of fission track data. Initially, we developed classical image processing algorithms to assess the feasibility of isotopic identification through unique fission track characteristics of fissile materials on LEXAN® Solid State Nuclear Track Detectors (SSNTD). Our current focus is on achieving improved isotopic separation through two innovative approaches:

1. **Integration of Aerogel:** We incorporate aerogel as a low-attenuation spacer to enhance track clarity.
2. **Penetration Depth Analysis:** We systematically examine the penetration depths of fission products within the detector.

Additionally, we are investigating the potential use of fluorescent aerogel as a standalone detector, which could eliminate the need for chemical etching typically required in Fission Track Analysis (FTA) procedures.

Our research employs three primary methods:

1. **GEANT4 Monte Carlo** Simulations (version 10.6, "QGSP\_BERT\_HP" physics library) to generate realistic physical data, focusing on aerogel widths of 50nm-30µm.
2. **FTA Trainer Application:** A custom-developed tool [1] for generating visual SSNTD track data based on GEANT4 simulations.
3. **TRIM (SRIM 2008) Simulations:** Modeling fission product interactions across various fissile isotopes within the new detector configuration.

Initial findings indicate that incorporating aerogel significantly improves track clarity and detection efficiency compared to LEXAN®. TRIM simulations reveal variations in penetration depths of fission products due to differences in kinetic energy and physical characteristics.

The integration of aerogel enhances detection sensitivity, facilitating more precise characterization of fission products and aiding isotopic separation through classical image processing techniques. While promising, further research is needed to optimize the detection system's performance, potentially leading to more accurate and efficient identification methods for nuclear materials.

## References

[1] **Babayew, R.**, Yehuda-Zada, Y., Elgad, N. *et al.*, Simulation tools for improvement of the fission track analysis method for nuclear forensics (2024), JRNC, DOI: 10.1007/s10967-023-09313-5.

# Ab initio study of point defect diffusion in $\delta$ -Pu.

Romuald Béjaud<sup>\*1,2</sup>, François Bottin<sup>1,2</sup>, Lucas Baguet<sup>1,2</sup>, Marc Torrent<sup>1,2</sup>

<sup>1</sup>CEA, DAM, DIF, F-91297 Arpajon, France.

<sup>2</sup>Université Paris-Saclay, CEA, LMCE, 91680 Bruyères-le-Châtel, France.

\*e-mail: [romuald.bejaud@cea.fr](mailto:romuald.bejaud@cea.fr)

Plutonium is arguably the most complex chemical element on the periodic table. At ambient pressure, it comprises 6 stable allotropes across different temperature ranges [1]. The thermophysical properties of Pu can vary considerably depending on the crystal phase considered. Under room temperature conditions, Pu exists in its  $\alpha$  phase (monoclinic, brittle), but it can dynamically stabilize into its  $\delta$  form (face-centered cubic, ductile) at elevated temperatures. Understanding and studying the structural/mechanical properties of Pu  $\delta$  has been a subject of study and controversy since 80 years. Additionally, significant natural self-irradiation of Pu can lead to significant variations in these properties over time. It is estimated that within 10 years, all atoms in a Pu sample have been displaced from their original positions, leading to possible aging problems.

Ab initio calculations have been conducted to understand how these diffusion mechanisms operate in Pu- $\delta$ . This study proposes a unified modeling of Pu- $\delta$  capable of addressing both explicit (anharmonic) [2] temperature effects and the specific structure of point defects at these temperatures. These calculations were made possible by incorporating machine learning tools within the MLACS (Machine Learning Assisted Canonical Sampling) framework [3,4], enabling a progressive substitution of costly ab initio calculations with a substitution MLIP (Machine Learning Interaction Potential) force field. This optimized MLIP can be reused to explore the specific domain of long timescales and rare events, without losing an ab initio accuracy level.

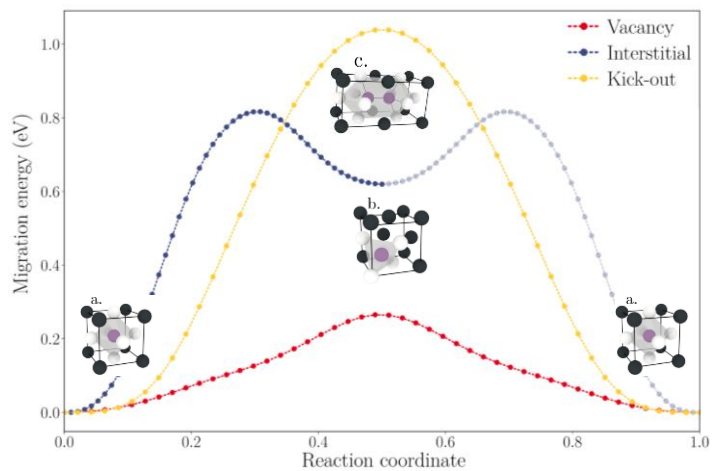


Figure 1: Migration energy profile following three different diffusion mechanisms.

## References

- [1] S. Hecker, *Los Alamos Science*, Number 26 (2000).
- [2] F. Bottin, R. Béjaud, B. Amadon, L. Baguet, M. Torrent, A. Castellano and J. Bouchet, *Phys. Rev. B* **109**, L060304 (2024).
- [3] A. Castellano, F. Bottin, J. Bouchet, A. Levitt, and G. Stoltz, *Phys. Rev. B* **106**, L161110 (2022).
- [4] A. Castellano, R. Béjaud, P. Richard, O. Nadeau, C. Duval, G. Geneste, G. Antonius, J. Bouchet, A. Levitt, G. Stoltz, F. Bottin, *Comput. Phys. Commun.* **submitted**.

# Machine learning assisted *ab initio* simulations for actinides

F. Bottin<sup>1,2\*</sup>, R. Béjaud<sup>1,2</sup>, A. Castellano<sup>3</sup>, and J. Bouchet<sup>4</sup>

<sup>1</sup>CEA, DAM, DIF, F-91297 Arpajon, France.

<sup>2</sup>Université Paris-Saclay, CEA, LMCE, 91680 Bruyères-le-Châtel, France

<sup>3</sup>NanoMat/Q-Mat/CESAM and ETSF, Université de Liège Belgium

<sup>4</sup>CEA, DES, IRESNE, DEC, Cadarache, F-13018 St Paul Les Durance, France.

\*e-mail: francois.bottin@cea.fr

The study of actinides by means of *ab initio* simulations requires heavy calculations, both in terms of computing time and number of processors to use. This drawback often prevents us from performing long *ab initio* molecular dynamic (AIMD) trajectories with large supercells while including in the calculation all the physics necessary for a good treatment of electronic and atomic structures: electronic correlations, spin-orbit coupling, non-collinear magnetism, anharmonic effects...

The emergence of Machine Learning Interatomic Potentials (MLIP) enables us to tackle this issue. We implemented [1] a new method named MLACS (Machine Learning Assisted Canonical Sampling) which accelerates by one to two orders of magnitude *ab initio* simulations (AIMD, geometry relaxation, free-energy calculation, transition path sampling...) by training a MLIP potential on the fly [2,3]. We applied this scheme to the  $\delta$  phase of plutonium and highlighted the importance of anharmonic effects [4]. More recently, we also evaluated the interplay between temperature effects and Ga/Al content on the stability of  $\delta$ -Pu.

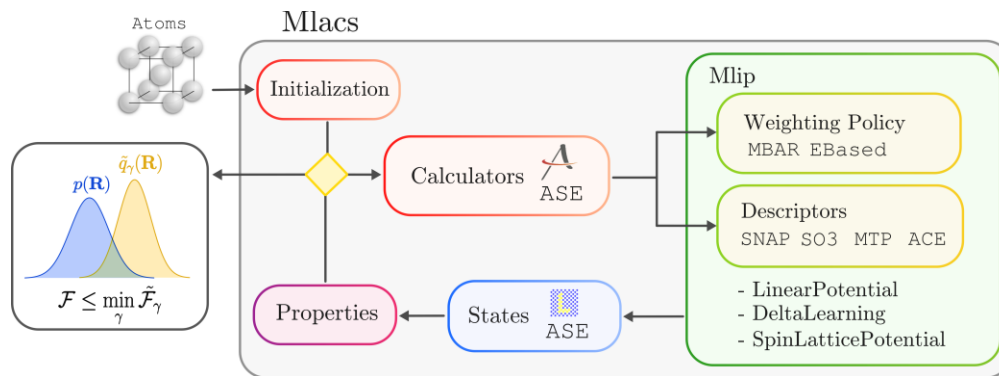


Figure 1: Workflow of MLACS.

## References

- [1] A. Castellano, F. Bottin, J. Bouchet, A. Levitt, and G. Stoltz, *Phys. Rev. B* **106**, L161110 (2022).
- [2] P. Richard, A. Castellano, R. Béjaud, L. Baguet, J. Bouchet, G. Geneste, and F. Bottin, *Phys. Rev. Lett.* **131**, 206101, (2023).
- [3] A. Castellano, R. Béjaud, P. Richard, O. Nadeau, C. Duval, G. Geneste, G. Antonius, J. Bouchet, A. Levitt, G. Stoltz, and F. Bottin, *Comput. Phys. Commun.* (submitted).
- [4] F. Bottin, R. Béjaud, B. Amadon, L. Baguet, M. Torrent, A. Castellano, and J. Bouchet, *Phys. Rev. B* **109**, L060304 (2024).

# Evaluating 5f Orbital Covalency in $UX_6^-$ (X = F, Cl) with U M-edge Resonant Inelastic X-ray Scattering

J. A. Branson,<sup>1</sup> B. Schacherl,<sup>1</sup> S. Schenk,<sup>1</sup> E. Reynolds,<sup>1</sup> H. Kaufmann-Heimeshoff,<sup>1</sup> T. Pruessman,<sup>1</sup> S. G. Minasian,<sup>2\*</sup> T. Vitova<sup>1\*</sup>

<sup>1</sup> Institute for Nuclear Waste Disposal (INE), Karlsruhe Institute of Technology, D-76021 Karlsruhe, Germany

<sup>2</sup> Lawrence Berkeley National Laboratory, Berkeley, California 94720, United States

\*e-mail: sgminasian@lbl.gov, tonya.vitova@kit.edu

The nature of covalent orbital mixing between the An 5f orbitals and ligand orbitals remains an outstanding question. Actinide electronic structure is often difficult to evaluate due to large spin-orbit coupling and the presence of multiple 5f electrons ( $l = 3$ ). However, this evaluation can be simplified by choosing high-symmetry systems with a low number of 5f electrons [1, 2]. Systems with a single 5f electron are particularly useful, as f-orbital energetic splitting can be modeled relatively simply using group theory [2]. In this study, the electronic structure of the  $f^1 UX_6^-$  (X = F, Cl) molecules is studied using U M-edge resonant inelastic X-ray scattering (RIXS). With the results of core-to-core and valence band RIXS, the energetic splitting of the 5f orbitals and the delocalization of 5f electron density is evaluated [3, 4]. These results are compared to similar studies on other U(V) systems, most of which exist as the linear  $UO_2^+$  moiety. This comparison helps quantify the stabilization of U(V) systems enabled by terminal oxo ligands relative to similarly electronegative halide ligands.

## References

- [1] Edelstein, N. M.; Lukens, W. W. *J. Phys. Chem. A* **2020**, *124* (21), 4253–4262.
- [2] Lukens, W. W.; Edelstein, N. M.; Magnani, N.; Hayton, T. W.; Fortier, S.; Seaman, L. A. *J. Am. Chem. Soc.* **2013**, *135* (29), 10742–10754.
- [3] Vitova, T.; Pidchenko, I.; Fellhauer, D.; Bagus, P. S.; Joly, Y.; Pruessmann, T.; Bahl, S.; Gonzalez-Robles, E.; Rothe, J.; Altmaier, M.; Denecke, M. A.; Geckeis, H. *Nat. Commun.* **2017**, *8* (1), 16053.
- [4] Schacherl, B.; Tagliavini, M.; Kaufmann-Heimeshoff, H.; Goettlicher, J.; Mazzanti, M.; Popa, K.; Walter, O.; Pruessman, T.; Vollmer, C.; Beck, A.; Ekanayake, R. S. K.; Branson, J. A.; Neill, T.; Fellhauer, D.; Reitz, C.; Schild, D.; Brager, D.; Cahill, C.; Windorff, C.; Sittel, T.; Ramanantoanina, H.; Haverkort, M. W.; Vitova, T. *Nat. Commun.* **2024**. <https://doi.org/10.1038/s41467-024-54574-7>

# Materials research for the development of Americium-based RTGs and RHUs used in space missions

D.J. Cette<sup>1,2\*</sup>, J. Vlieland<sup>1</sup>, S. Couweleers<sup>1</sup>, C. Guéneau<sup>3</sup>, R.J.M. Konings<sup>1</sup> and A.L. Smith<sup>1</sup>

<sup>1</sup>Delft University of Technology, Radiation Science & Technology Department, Nuclear Energy and Radiation Applications (NERA), Mekelweg 15, 2629 JB Delft, The Netherlands

<sup>2</sup>b European Commission, Joint Research Centre, P.O. Box 2340, D-76125 Karlsruhe, Germany

<sup>3</sup>Université Paris-Saclay, CEA, Service de recherche en Corrosion et Comportement des Matériaux, Gif-sur-Yvette, 91191 France

\*e-mail: D.J.Cette@tudelft.nl

Radioisotope Thermoelectric Generators (RTGs) and Radioisotope Heater Units (RHUs) play a crucial role in enabling the exploration of our solar system. These devices rely on the natural decay of radioisotopes, typically plutonium-238, to provide spacecrafts with reliable power and heat. However, recent geopolitical events have significantly constrained Pu-238's availability, highlighting the need for a new and more suitable radioisotope. The best candidate in Europe for this endeavor is americium-241, a byproduct of nuclear fuel reprocessing that can be produced at acceptable costs and suitable quantities [1].

The Rosalind Franklin rover, scheduled for launch to Mars in 2028, will carry the first Am-based RHU, marking a significant milestone in the adoption of this technology [1]. However, several challenges remain. First, americium's application in RTGs and RHUs requires stabilization through alloying with uranium. Second, the buildup of neptunium, a decay product of americium, introduces additional complexities by potentially altering the overall chemistry of the system. Lastly, possible chemical interactions between the fuel source and the platinum-rhodium cladding are understudied.

This research will combine both experimental and computational approaches to investigate the U-Am-Np-Pt-Rh-O system, with the aim to identify the optimal fuel source for americium-based RTGs and RHUs. The initial phase involves studying the surrogate U-Ce-O system and developing an Oxygen Solid Electrolyte Coulometry (OSEC) setup to gather critical oxygen potentials data [2]. These efforts aim to ensure the feasibility, reliability, and efficiency of americium-powered technologies, paving the way for European-led space exploration to the Moon, Mars, and beyond.

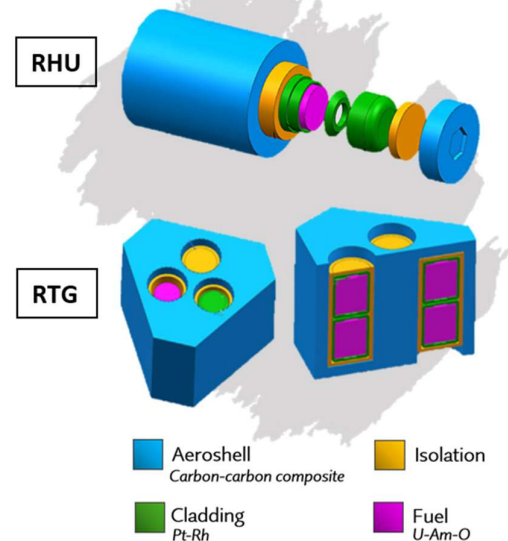


Figure 1: Schematic representation of an RHU and RTG. Retrieved from [1]

## References

- [1] R.M. Ambrosi, H. Williams, E.J. Watkinson, A. Barco, R. Mesalam, T. Crawford, C. Bicknell, P. Samara-Ratna, D. Vernon, N. Bannister, et al. *Space Science Reviews*, 215 1–41 (2019).
- [2] A. Herms, J. Yao, J. Zosel, V. Vashook, V. W. Oelßner and M. Mertig. *Journal of Sensors and Sensor Systems*, 7(2), 621-625 (2018).



# Gas-phase syntheses and structures of organothorium complexes

Xiuting Chen<sup>1</sup>, Zhixin Xiong<sup>1,2</sup>, Meixian Yang<sup>1,2</sup>, Yu Gong<sup>1,\*</sup>

<sup>1</sup>Key Laboratory of Thorium Energy, Shanghai Institute of Applied Physics, Chinese Academy of Sciences, Shanghai, 201800

<sup>2</sup>School of Nuclear Science and Technology, University of Chinese Academy of Sciences, Beijing, 100049

\*e-mail: gongyu@sinap.ac.cn

Transition metal complexes of benzyne (1,2-didehydrobenzene) and substituted benzyne are very important and highly reactive intermediates in organic synthetic chemistry. Since the first fascinating benzyne complex of transition metal ( $\eta^2\text{-C}_6\text{H}_4$ )Ta( $\eta^5\text{-C}_5\text{Me}_5$ )Me<sub>2</sub> was discovered, the syntheses, structures and reactivities of group 4, 5, 10 and other metal/metalloid benzyne complexes have been exhaustively investigated. In contrast to the rich chemistry of transition metals, it is surprising that actinide benzyne complexes have received far less attention. To the best of our knowledge, the isolable thorium benzyne complex has not been reported yet, and the corresponding structure and reactivity remain elusive.

Electrospray ionization mass spectrometry (ESI-MS) with the aid of density functional theory (DFT) calculations has proven a valuable tool to uncover the gas-phase chemistry of novel, reactive and even transient organometallic species including their structures, reactivities and reaction mechanisms. The first thorium benzyne complex ( $\eta^2\text{-C}_6\text{H}_4$ )ThCl<sub>3</sub><sup>-</sup> was synthesized in the gas phase through consecutive decarboxylation and dehydrochlorination from the (C<sub>6</sub>H<sub>5</sub>CO<sub>2</sub>)ThCl<sub>4</sub><sup>-</sup> precursor upon collision-induced dissociation [1]. Theoretical calculations suggest that ( $\eta^2\text{-C}_6\text{H}_4$ )ThCl<sub>3</sub><sup>-</sup> exhibits a metallacyclopropene structure with two polarized Th-C<sub>benzyne</sub>  $\sigma$  bonds. This procedure can be generally extended to the synthesis of a wide range of gas-phase thorium substituted benzyne complexes by employing substituted benzoic acids with hydrogen atoms but not electron-withdrawn groups at the ortho position as precursors.

During the synthesis process of thorium benzyne complex, a fast and reliable mass spectrometry-based method has been developed to discriminate the positional isomers of *o*-, *m*- and *p*-C<sub>6</sub>H<sub>4</sub>XCO<sub>2</sub>H (X = F, Cl and Br) [2]. This is based on the distinct fragmentation patterns of isomeric (C<sub>6</sub>H<sub>4</sub>XCO<sub>2</sub>)ThCl<sub>4</sub><sup>-</sup> ions generated by electrospray ionization of the solutions with C<sub>6</sub>H<sub>4</sub>XCO<sub>2</sub>H isomers and ThCl<sub>4</sub>. Moreover, the composition of these positional isomers can be conveniently quantified without any pre-treatment according to the proportion of gas-phase fragmentation products.

## References

[1] X. Chen, Z. Xiong, M. Yang, and Y. Gong\*, Chem. Commun., 58, 2658-2661 (2022).

[2] X. Chen, Z. Xiong, M. Yang, and Y. Gong\*, Chem. Commun., 58, 7018-7021 (2022).

# ActUsLab (Actinide User Laboratory)

E. Colineau\*, K. Boboridis, D. Serrano-Purroy, A. Seibert, P. Raison and R. Eloirdi

European Commission, Joint Research Centre (JRC), Karlsruhe, Germany

\*eric.colineau@ec.europa.eu

Large research infrastructures are expensive to build and operate and are often beyond the resources of a single institution or country. In particular, nuclear research infrastructures need an expensive licence and access to strategic materials.

Among its different sites in the European Union, JRC operates licensed laboratories in Karlsruhe (Figure 1), where actinide materials including transuranics can be handled within a safe and secure infrastructure and their chemical and physical properties explored. The "Actinide User Laboratory" (ActUsLab) provides access free of charge for external scientists from eligible countries to three laboratories : PAMEC (Properties of Actinide Materials under Extreme Conditions), FMR (Fuels and Materials Research) and HC-KA (Hot Cells) [1,2].

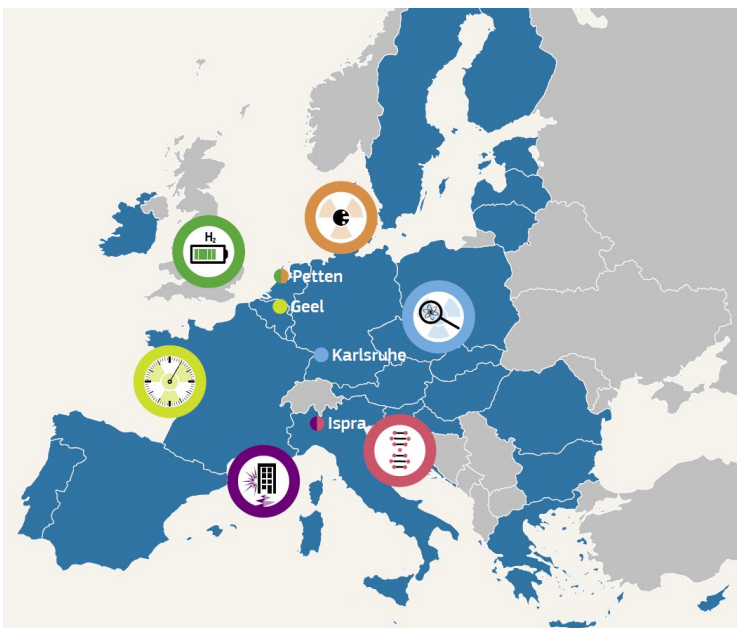


Figure 1: The different sites of JRC involved in Open Access to Research Infrastructures. The Karlsruhe site allows the handling of actinide materials for chemical and physical studies.

## Acknowledgements

We are grateful to Ms. Krisztina Varga for administrative support to the programme and to the scientific and technical staff of PAMEC , FMR and HC-KA laboratories for scientific and technical support to Users. We also thank the support Units of JRC-Karlsruhe for making the access possible.

## References

- [1] Web portal: [https://joint-research-centre.ec.europa.eu/tools-and-laboratories/open-access-jrc-research-infrastructures\\_en](https://joint-research-centre.ec.europa.eu/tools-and-laboratories/open-access-jrc-research-infrastructures_en)
- [2] A. Seibert et al., Nuclear Engineering and Design 420, 113000 (2024)

# An investigation of $(U_{(1-(x+y))}Th_xGd_y)O_{2-\delta}$ solid solutions as a function of synthesis method: Supporting disposal of the UK's plutonium

C. L. Corkhill<sup>1\*</sup>, M. R. Cole<sup>2</sup>, L. T. Haigh<sup>2</sup>, D. J. Bailey<sup>2</sup>, L. T. Townsend<sup>2</sup>, L. R. Blackburn<sup>2</sup>,  
K. Kvashnina<sup>3,4</sup> and G. Kerboul<sup>5</sup>

<sup>1</sup>*School of Earth Science, The University of Bristol, UK*

<sup>2</sup>*Department of Materials Science and Engineering, The University of Sheffield, UK*

<sup>3</sup>*Helmholtz-Zentrum Dresden-Rossendorf (HZDR), Institute of Resource Ecology, Germany*

<sup>4</sup>*The Rossendorf Beamline at ESRF – The European Synchrotron, France*

<sup>5</sup>*Technical Authority, Orano, France*

\*e-mail: [c.corkhill@bristol.ac.uk](mailto:c.corkhill@bristol.ac.uk)

The safe and secure management of civil separated plutonium is a UK government priority. One potential solution to address this considers the manufacture of a modified version of mixed oxide (MOX) fuel, comprising  $PuO_2$  dispersed within a  $UO_2$  matrix and doped with a suitable neutron absorbing element to maintain criticality control.

The feasibility of different synthesis routes for simulant “disposal-MOX”, using  $Th^{4+}$  as a  $Pu^{4+}$  surrogate and containing  $Gd^{3+}$  in a suitable quantity to ensure criticality control, was evaluated. Firstly, compositions of  $(U_{(1-(x+y))}Th_xGd_y)O_{2-\delta}$ , where  $x = 0.1, 0.2$  and  $x : y = 10: 1$  or  $100: 1$ , were synthesised by a solid state route mimicking the industrial MIMAS (Micronized MASTerblend) MOX fuel fabrication process and *via* an oxalic wet co-precipitation method. Both synthesis routes gave a single phase fluorite structure upon heat-treatment at  $1700\text{ }^\circ\text{C}$ , with a grain size similar to  $(Pu,U)O_2$  MOX fuel. The relative density of the sintered pellets was  $>90\%$  but was highest in co-precipitated materials, with  $Th^{4+}$  and  $Gd^{3+}$  additions more homogeneously distributed. Though no unincorporated  $ThO_2$  or  $Gd_2O_3$  was observed in any sample, Th and Gd-rich regions were more prevalent in materials produced through solid state synthesis, in accordance with MIMAS MOX fuel microstructures. The incorporation of  $Gd^{3+}$  within the fluorite lattice, which is favourable from a criticality control perspective in a Pu wasteform, was found to be charge balanced via the generation of oxygen vacancy defects, but not  $U^{5+}$ .

A series of Gd-doped  $UO_2$  pellets, prepared by Orano at the CDA workshop of the MELOX facility in France, were also investigated. The materials produced were highly reproducible and similar in density and morphology, irrespective of the variables investigated, and similar to unirradiated UOX and MOX fuel. Gd was distributed in a similar manner to the distribution of  $PuO_2$  in unirradiated MIMAS MOX fuel and evidence for the existence of a solid solution between  $Gd_2O_3$  and  $UO_2$  was ascertained, which could be viewed as favourable from a GDF post-closure criticality control perspective. The source of the powder had the greatest effect on the final characteristics of the Pu-disposition MOX pellets, due to sintering reactivity; however, these differences were minor.

These results demonstrate feasible synthesis routes for a disposal-MOX wasteform product via both solid state and wet co-precipitation fabrication route, as well as at full-scale.

# Stabilization of $\alpha$ -UH<sub>3</sub> in U-Hf Hydrides: Effects on Structure and Magnetism

Shanmukh Veera Venkata U. K. Devanaboina<sup>1\*</sup>, Oleksandra Koloskova<sup>2</sup>, Ladislav Havela<sup>1</sup>, and Silvie Mašková Černá<sup>1</sup>

<sup>1</sup>*Department of Condensed Matter Physics, Faculty of Mathematics and Physics, Charles University, Prague, Czech Republic,*

<sup>2</sup>*Institute of Physics (FZU), Czech Academy of Sciences, Prague, Czech Republic*

\**e-mail: shanmukh.devanaboina@matfyz.cuni.cz*

Uranium hydride (UH<sub>3</sub>) belongs to the first known *5f* materials with ferromagnetic ordering [1]. It exists in two different cubic modifications: a stable  $\beta$ -UH<sub>3</sub> phase (complex cubic with  $a = 664$  pm), and a metastable  $\alpha$ -UH<sub>3</sub> (*bcc* cubic with  $a = 414$ - $416$  pm). Our prime objective is to explore the role of Hafnium (Hf) in stabilizing the *bcc*  $\alpha$ -UH<sub>3</sub> phase and examine its impact on the crystal lattice as well as magnetic and transport properties.

In the present work, the alloys U<sub>1-x</sub>Hf<sub>x</sub> with  $x = 0.10, 0.15, 0.30,$  and  $0.40$  were synthesized by arc-melting of pure elements (natural U-2N8, Hf-3N) in an Ar atmosphere. Subsequently, the alloys were hydrogenated by exposure to high pressure of H<sub>2</sub> gas ( $p = 100$  bar) for 120 hours at ambient temperature. X-ray diffraction confirmed that 40 at.% of Hf alloying stabilizes the  $\alpha$ -UH<sub>3</sub> phase, suppressing  $\beta$ -UH<sub>3</sub> formation at room temperature, and the determined lattice parameters of the stabilized  $\alpha$ -UH<sub>3</sub> phase are in good agreement with the literature.

DC magnetization measurements reveal a ferromagnetic ground state with a Curie temperature ( $T_C$ ) of 178 K, while increasing Hf concentration reduces spontaneous magnetization due to lattice dilution. The deviation from Curie-Weiss behavior, along with the downturn in the temperature-dependent inverse DC magnetic susceptibility and the peak formation above  $T_C$  in AC susceptibility measurements, supports the presence of magnetic inhomogeneities, likely due to the formation of the ferromagnetic clusters in the paramagnetic background [2]. Further, the specific heat data reveals a magnetic entropy change ( $\Delta S$ ) of 2.5 J/mol·K near the Curie temperature, highlighting the complexity of magnetic interactions around  $T_C$ . These findings demonstrate the potential of Hf alloying to effectively tune both the structural stability and magnetic properties of uranium hydrides.

## References

- [1] Troc R., and Suski W., The discovery of the ferromagnetism in U(H,D)<sub>3</sub>: 40 years later, *J. Alloys Comp.*, 219, 1 (1995).
- [2] Robert B. Griffiths, Nonanalytic Behavior Above the Critical Point in a Random Ising Ferromagnet, *Phys. Rev. Lett.* 23, 17 (1969)

# Utilization of Deep Learning for Star Segmentation and Classification using Semi-Automated Adaptive Threshold methodology

N. Elgad<sup>1,2\*</sup>, R. Babayew<sup>1,2</sup>, M. Last<sup>3</sup>, Y. Yehuda-Zada<sup>1,2</sup>, J. Lorincik<sup>4</sup>, I. Orion<sup>2</sup>, E. Gilad<sup>2</sup>, A. Weiss<sup>5</sup>, G. Katarivas Levy<sup>6</sup>, and I. Halevy<sup>2</sup>

<sup>1</sup>Physics Department, Nuclear Research Center Negev, Beer-Sheva, Israel

<sup>2</sup>Unit of Nuclear Engineering, Faculty of Engineering Sciences, Ben Gurion University of the Negev, Israel

<sup>3</sup>Department of Software and Information Systems Engineering, Faculty of Engineering Sciences, Ben Gurion University of the Negev, Israel

<sup>4</sup>Nuclear Fuel Cycle Department, Research Centre Řež, Hlavní 130, Řež 250 68, Husinec, Czech Republic

<sup>5</sup>Faculty of Engineering, Bar Ilan University, Ramat Gan P.O.B. 90000 5290002 Israel

<sup>6</sup>Department of Biomedical Engineering, Faculty of Engineering Sciences Ben-Gurion University of the Negev, Beer-Sheva, Israel

\*e-mail: n.elgad@gmail.com

This study presents an innovative approach for detecting and classifying star-shaped patterns in microscopic images, leveraging advanced deep learning techniques of segmentation and classification [1] for fission track analysis mission in the domain of nuclear forensics. The U-Net model, a fully convolutional neural network, employed to segment various star-like patterns in both single-class and multi-class settings (figure 1 [1]). In order to train the model, artificial star shapes were used, among other data, generated through a specialized simulation tool which was developed by our research team [2].

The model which conducted with a 5-fold cross validation analysis was built for small sized stars, less than 60 $\mu$ m, and under 200 pixels with less than 10 leaves and without black center. This model achieved a total area of 0.84 under the ROC curve. In addition, a model for bigger and richer stars was built that achieved a total area of 0.90 under the ROC curve. Also, preliminary models were built which can differentiate between roses of different shapes and sizes at the same time.

Furthermore, this study also summarizes focused research conducted to determine thresholds for background noise filtering and to improve identification and established a new methodology for semi-automated adaptive threshold setting.

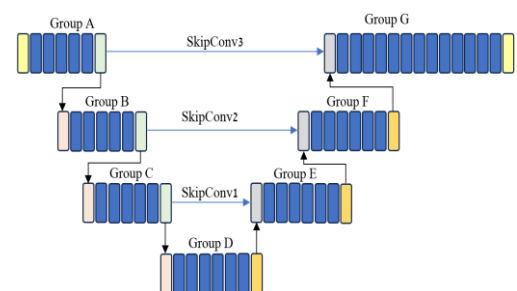


Figure 1: Design and implementation of a U-Net architecture for segmentation and classification.

## References

- [1] N. Elgad, R. Babayew, M. Last, E. Gilad, G. Katarivas Levy, and I. Halevy, Image segmentation and classification for fission track analysis for nuclear forensics using U-net model, JRNC, Akadémiai Kiadó, Budapest, Hungary, DOI: 10.1007/s10967-024-09461-2 (2024).
- [2] R. Babayew, Y. Yehuda-Zada, N. Elgad, J. Lorincik, I. Orion, A. Weiss, G. Katarivas Levy, and I. Halevy, Simulation tools for improvement of the fission track analysis method for nuclear forensics, JRNC, Akadémiai Kiadó, Budapest, Hungary, DOI: 10.1007/s10967-023-09313-5 (2024).

# Influence of Pu(IV) and Pu(VI) on the extraction properties of anion exchange resins

G. Verwaerde<sup>1\*</sup>, G. Bailly<sup>1</sup>, S. Faure<sup>2</sup>, and G. Bourguès<sup>1</sup>

<sup>1</sup>CEA, DAM, VALDUC, F- 21120 Is sur Tille

\* e-mail: [Guillaume.verwaerde@cea.fr](mailto:Guillaume.verwaerde@cea.fr)

Anion exchange in nitric acid is a process used to purify plutonium from metallic impurities. The process is based on the selective extraction of the anionic hexanitrate complex  $[\text{Pu}(\text{NO}_3)_6]^{2-}$  formed at high concentrations of nitric acid.

The principle of this anion exchange method is based on the fact that plutonium forms anionic species at high nitric acid concentrations, whereas the other elements, such as americium, do not form such anionic complexes. However, Pu(VI) can be present in the feed solution. This oxidation state may perturb the purification process, as Pu(VI) species cannot be fixed by the resin.

In the present study, lab scale investigations were carried out to qualify the purification of an aged Pu nitrate solution in the frame of facility dismantling preparation operations. Pu(VI) was observed by spectrophotometry in the solution before (a) and after (b) ion exchange for Am/Pu separation (figure 1).

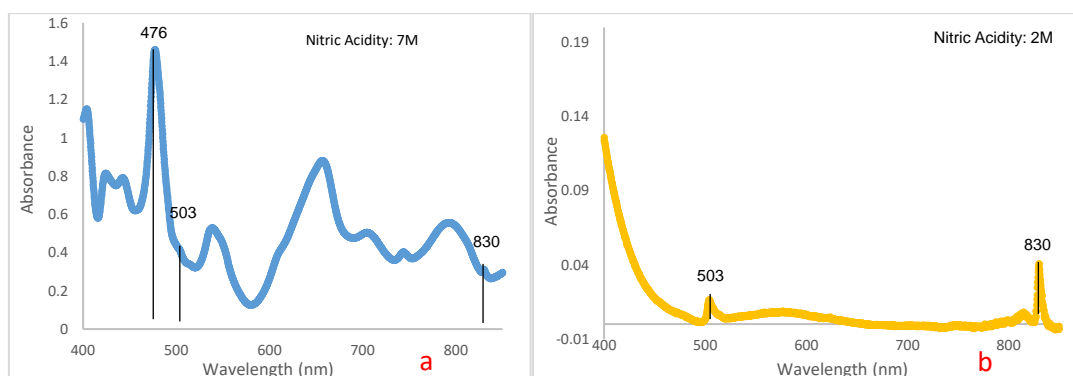


Figure 1 : Absorption spectra of a solution before Am/Pu separation (a) and effluent generated by separation process with anionic resins (b) (Wavelength: 476 nm: Pu(IV), 503 nm: Am, 830 nm: Pu(VI))

These results confirmed that presence of plutonium within the effluents was mainly due to Pu(VI). Consequently, hydrogen peroxide was added to the solution to reduce Pu(VI) to Pu(IV). Finally, this oxidation state adjustment restored the anion exchange separation selectivity leading to a considerable reduction of the plutonium concentration within the effluents.

# Underpinning National Nuclear Safety via the Safe Storage of Legacy Nuclear Waste

*Leo Gilliver, Lottie Harding, Ross Springell, Thomas Scott,*

*University of Bristol, United Kingdom*

*e-mail: uk24091@bristol.ac.uk*

Accurate prediction of uranium metal corrosion in aqueous environments is crucial for managing uranium-containing legacy wastes at Sellafield. As metallic uranium readily converts to uranium hydride—a pyrophoric powder—understanding the fundamental formation mechanisms of this compound is essential for accident mitigation [1]. Previous studies on metallic uranium often used pristinely prepared surfaces, which do not represent the conditions of legacy waste. Intermediate and high-level uranium wastes are subject to mechanical loads, leading to the formation of cracks that serve as preferential sites for hydride initiation [2]. The relationship between load and stress corrosion cracking is largely undefined and merits further research. This research will utilise polycrystalline and single-crystal thin films of uranium oxide (common on U metal surfaces) to explore dissolution behaviour in simulant storage environment waters. Measurement approaches will combine x-ray diffraction (lab and synchrotron) with high-speed atomic force microscopy to provide real-time and in-situ observations of surface processes [3].

## References

- [1] A.Banos, N.J. Harker, and T.B.Scott, Corrosion Science, Volume 136, 129-147 (2018).
- [2] C.A.Stitt, C.Paraskevoulakos, N.J.Harker, Corrosion Science, Volume 98, 63-71 (2015)
- [3] R. Springell, B. E.Lawrence Bright, D.A Chaney, Advances in Physics, Volume 71, 87-165 , (2022)

# Novel Uranium Hybrid Materials

Pedro de Almeida Silva<sup>1</sup>, Sandra Rabaça<sup>1</sup>, and António P. Gonçalves<sup>1\*</sup>

<sup>1</sup>C<sup>2</sup>TN, DECN, Instituto Superior Técnico, Universidade de Lisboa, Campus Tecnológico e Nuclear, 2695-066  
Bobadela, Portugal

\*e-mail: [apg@ctn.tecnico.ulisboa.pt](mailto:apg@ctn.tecnico.ulisboa.pt)

Van der Waals materials have a high scientific and practical interest due to their wide range of mechanical, thermal, electrical, and optical properties. These materials are characterized by strong in-plane covalent bonding and weak Van der Waals bonding between the layers. Their physical properties can be modified by creating hybrid materials through the intercalation of atoms, ions, and molecules into the Van der Waals gap.

UTe<sub>3</sub> is a binary uranium telluride that crystallizes into two Van der Waals polymorphs: the  $\alpha$  phase, which adopts the ZrSe<sub>3</sub>-type monoclinic structure, and the  $\beta$  phase that crystallizes in the orthorhombic NdTe<sub>3</sub>-type structure. Our previous studies on ZrSe<sub>3</sub>-type UTe<sub>3</sub> single crystals indicated a semiconducting behaviour and the inexistence of any magnetic transition down to 2 K [1]. However, its structural similarity to the unconventional superconductor UTe<sub>2</sub> motivated us to explore tuning its properties through intercalation.

Here, we present intercalation studies using Bi<sub>2</sub>Te<sub>3</sub> as a model system, along with preliminary results of similar attempts on UTe<sub>3</sub>. The intercalation was performed electrochemically, and the resulting materials were characterized by XRD, SEM, and EDS. Resistivity measurements were conducted using the four-points method.

Initial results of the intercalation of Cu and PF<sub>6</sub><sup>-</sup> into Bi<sub>2</sub>Te<sub>3</sub> demonstrated the formation of a hybrid inorganic/inorganic and inorganic/organic materials, respectively. These modifications led to significant improvements in electrical conductivity, increasing by over 20% and 120%, respectively.

## References

[1] A. P. Gonçalves, L. C. J. Pereira, E. B. Lopes, L. C. Alves, V. Corregidor, I. C. Santos, 51<sup>emes</sup> Journées des Actinides, April 10–14 2022, Santa Margherita Ligure, Italy (2022).



# New Uranium Carbides for ISOL targets

André Silva<sup>1</sup>, Beatriz A. Santos<sup>1</sup>, and António P. Gonçalves<sup>1\*</sup>

<sup>1</sup>C<sup>2</sup>TN, DECN, Instituto Superior Técnico, Universidade de Lisboa, Campus Tecnológico e Nuclear, 2695-066  
Bobadela, Portugal

\*e-mail: [apg@ctn.tecnico.ulisboa.pt](mailto:apg@ctn.tecnico.ulisboa.pt)

Radionuclides are widely used as both diagnostic and therapeutic tools for illnesses, mainly in oncological cases. Until recently, they were mainly produced in nuclear reactors, but due to both the closing of a large amount of those facilities and the increase of demand, other production options have been looked at. One alternative technique is the ISOL method.

The ISOL method comprises the irradiation of a target using a primary beam, usually a proton beam, inducing nuclear reactions in the target and the formation of radionuclides. The radionuclides are then sublimated at high temperatures (~2000°C), ionized and mass separated from the irradiated target. The most important family of ISOL targets are UC<sub>2</sub>+C composites.

This work consists on the development and study of new target materials to be used in the ISOL method, which would allow the increase of efficiency of the process. They are based on the U<sub>1-x</sub>M<sub>x</sub>C<sub>2</sub> solid solutions, where M represents a transition metal that form refractory carbides. It follows previous investigations on U<sub>1-x</sub>M<sub>x</sub>C composition samples, where a significant increase of the melting temperature was observed [1]. The transition metals, hafnium, niobium, tantalum and zirconium were added to uranium and carbon and arc melted to synthesize samples with the 1-xU:xM:2C (x = 0.025, 0.075 for Hf, Ta, and Nb; x = 0.05, 0.15 for Zr) nominal composition. Powder X-ray Diffraction (XRD) and Scanning Electron Microscopy combined with Energy Dispersive Spectroscopy (SEM/EDS), were employed to characterize the structure and microstructure of the samples. In all cases, the formation of a UC<sub>2</sub>-based phase was confirmed.

Nevertheless, for some of the compositions the solubility range was small in these samples and further thermal treatments at high temperatures are needed to homogenize the samples and check their stability at temperatures close to the working ones.

## References

[1] Beatriz A. Santos, David Robba, Luka Vlahovic, Antonio Bulgheroni, Konstantinos Boboridis, António P. Gonçalves, 53<sup>rd</sup> Journées des Actinides, April 15–18 2024, Lille, France, Page 22 (2024).

# Resonant inelastic X-ray scattering tools to count 5f electrons of actinides and probe bond covalency

H. Kaufmann-Heimeshoff<sup>1\*</sup>, B. Schacherl<sup>1,2</sup>, M. Tagliavini<sup>3</sup>, J. Göttlicher<sup>4</sup>, M. Mazzanti<sup>5</sup>, K. Popa<sup>6</sup>, O. Walter<sup>6</sup>, T. Prüssmann<sup>1</sup>, C. Vollmer<sup>1</sup>, A. Beck<sup>1</sup>, R. S. K. Ekanayake<sup>1</sup>, J. A. Branson<sup>2</sup>, T. Neill<sup>7</sup>, D. Fellhauer<sup>1</sup>, C. Reitz<sup>1</sup>, D. Schild<sup>1</sup>, D. Brager<sup>8</sup>, C. Cahill<sup>8</sup>, C. Windorff<sup>9</sup>, T. Sittel<sup>1</sup>, H. Ramanantonina<sup>1</sup>, M. Haverkort<sup>3</sup>, T. Vitova<sup>1</sup>

<sup>1</sup> Karlsruhe Institute of Technology (KIT), INE, P.O. Box 3640, 76021 Karlsruhe, Germany

<sup>2</sup> Lawrence Berkeley National Laboratory (LBNL), Chemical Sciences Division (CSD), Berkeley, CA, 97420, USA

<sup>3</sup> Heidelberg University, Institute for Theoretical Physics (ITP), Philosophenweg 19, 69120 Heidelberg, Germany

<sup>4</sup> Karlsruhe Institute of Technology (KIT), IPS, P.O. Box 3640, 76021 Karlsruhe, Germany

<sup>5</sup> Institut des Sciences et Ingénierie Chimiques, EPFL, CH-1015 Lausanne, Switzerland

<sup>6</sup> European Commission, Joint Research Centre Karlsruhe (JRC), Karlsruhe, Germany

<sup>7</sup> Research Centre for Radwaste Disposal and Williamson Research Centre, Department of Earth & Environmental Sciences, The University of Manchester, Oxford Road, Manchester M13 9PL, UK

<sup>8</sup> Department of Chemistry, George Washington University, 800 22nd Street, NW, Washington, DC, 20052, USA.

<sup>9</sup> Department of Chemistry and Biochemistry, NMSU, MSC 3C, P.O. Box 30001, Las Cruces, NM, USA 88003

\*e-mail: hanna.kaufmann-heimeshoff@kit.edu

The actinides possess a complex electronic structure, making their chemical and physical properties among the least understood in the periodic table. Advanced spectroscopic tools, able to obtain deep insights into the electronic structure and binding properties of the actinides, are highly desirable. Here, we introduce two sensitive spectroscopic tools: one determines the number of localized 5f electrons on an actinide atom, and another assesses the covalent character of actinide-ligand bonding. Both tools are based on the multiplet structure present in actinide M4 edge core-to-core resonant inelastic X-ray scattering (CC-RIXS) maps. The spectral intensity of different many-body final-state multiplets directly depends on the local many-electron ground-state symmetry including the local 5f spin configuration. By comparing U M4 edge CC-RIXS data for 21 U, Np, Pu and Am compounds, we demonstrate the ability to compare the number of localized 5f electrons and bond covalency across the actinide series.

## References

- [1] A. Zimina *et al.*, 'CAT-ACT—A new highly versatile x-ray spectroscopy beamline for catalysis and radionuclide science at the KIT synchrotron light facility ANKA', *Review of Scientific Instruments*, vol. 88, no. 11, p. Art.-Nr., Nov. 2017, doi: 10.1063/1.4999928.
- [2] Aran, E. KIT, IPS - SUL-X <https://www.ips.kit.edu/5931.php> (accessed Jul 28, 2018).
- [3] F. de Groot and A. Kotani, *Core Level Spectroscopy of Solids*. CRC Press, 2008. doi: 10.1201/9781420008425.
- [4] S. M. Butorin, '3d-4f Resonant Inelastic X-ray Scattering of Actinide Dioxides: Crystal-Field Multiplet Description', *Inorg Chem*, vol. 59, no. 22, pp. 16251–16264, Nov. 2020, doi: 10.1021/acs.inorgchem.0c02032.
- [5] T. Vitova *et al.*, 'The role of the 5f valence orbitals of early actinides in chemical bonding', *Nat Commun*, vol. 8, Jul. 2017, doi: 10.1038/ncomms16053.

# Accessing single-crystal $\text{U}_4\text{O}_9$ and $\text{U}_3\text{O}_7$ using topotactic oxidation

E. Lawrence Bright<sup>1,2</sup>, C. Giacobbe<sup>3</sup>, L. M. Harding<sup>4</sup>, R. Springell<sup>4</sup>, and G. H. Lander<sup>4</sup>

<sup>1</sup>*The Rossendorf Beamline at ESRF – The European Synchrotron, Grenoble, France*

<sup>2</sup>*Helmholtz-Zentrum Dresden-Rossendorf (HZDR), Institute of Resource Ecology, Dresden, Germany*

<sup>3</sup>*European Synchrotron Radiation Facility, Grenoble, France*

<sup>4</sup>*University of Bristol, Bristol, United Kingdom*

*e-mail: e.lawrencebright@esrf.fr*

The oxidation of uranium dioxide,  $\text{UO}_2$ , is of major interest to the nuclear industry. As  $\text{UO}_2$  is oxidised to  $\text{U}_4\text{O}_9$ ,  $\text{U}_3\text{O}_7$ , and  $\text{U}_3\text{O}_8$ , often during short- or long-term storage, the physical and chemical properties of the fuel are altered. The crystal structure of these higher oxide phases is somewhat uncertain. Crystallographic relations during an oxidation process can have significant effects on the rate, mechanism, and properties of the product, and recent lab-based work has shown that the  $\text{UO}_2$  (001) surfaces oxidise to form  $\text{U}_3\text{O}_8$  (130) in a topotactic transformation [1,2].

We present work from an experiment where x-ray diffraction data was obtained during in-situ oxidation of a (001)  $\text{UO}_2$  thin film as it topotactically transformed to (130)  $\text{U}_3\text{O}_8$ . With this data, we show new insight into the mechanisms of this topotactic transformation, revealing that the intermediate oxide phases ( $\text{UO}_{2+x}$ ,  $\beta\text{-U}_4\text{O}_9$ ,  $\text{U}_3\text{O}_7$ ) forming as multi-domain single crystals during this process. This provides a novel route for obtaining single crystal of these intermediate oxides, allowing single crystal x-ray diffraction analysis of their crystallographic structures, which we will compare with published structures.

## References

[1] G. C. Allen, N. R. Holmes, *J. Nucl. Mater.* **231-237**, 223 (1995)

[2] J. Wasik *et al.*, *npj Mater. Degrad.* **8**, 68 (2024)

# 8-Hydroxyquinoline as a potential Ligand for Actinide Decorporation

J. Ross<sup>1,\*</sup>, R. Gericke<sup>2</sup>, P. Kaden<sup>2</sup>, M. Schmidt<sup>2</sup>, T. Stumpf<sup>1,2</sup>, J. März<sup>2</sup>

<sup>1</sup> Technical University of Dresden, Germany, <sup>2</sup> Helmholtz-Zentrum Dresden-Rossendorf, Germany

\*email: j.ross@hzdr.de

Internal contamination with radioactive material is a serious and persistent health hazard, particularly for workers and individuals exposed to radioactive materials through nuclear industry operations, environmental contamination, and medical applications. Once internalized in the human body, these toxic effects cause severe organ damage, chronic health conditions, and often irreversible or fatal injuries due to prolonged exposure. Despite this, current therapeutic options for actinide decorporation remain extremely understudied, with the all agents approved for chelation therapy demonstrating limited efficacy for actinides. More specifically, most available treatments are effective only for a select subset of actinides and also favor transition metals leading to dangerous nutrient depletion within the human body [1]. This leaves a significant issue in radiological safety strategies underscoring the critical and urgent need to develop more versatile and efficient agents for actinide decorporation.

In the framework of a joint German- French Initiative supported by ANR-DFG, we investigate 8-hydroxyquinoline, a ligand known for its strong chelating properties, as a potential decorporation agent. 8-hydroxyquinoline forms stable complexes with a variety of metal ions, including actinides and is the subject of the presented work [2]. Also, halide-substituted derivatives of 8-hydroxyquinoline can be found providing synthetic handles for further functionalization, such as installing carbon chains to create linked chelators [3]. These properties position 8-hydroxyquinoline as a strong candidate for further development as a decorporation agent. To gain a deeper understanding of the coordination chemistry of 8-hydroxyquinoline with actinides (An), a series of An(IV) complexes (An(IV) = Th, U, Np, Pu) were synthesized and thoroughly characterized using advanced analytical techniques. Preliminary findings reveal an effective and reproducible method for forming the desired complexes. Precise layering and optimized reactions yielded high-quality crystals for structural analysis. The reproducibility of these results provide a framework for investigating the binding modes of 8-hydroxyquinoline with actinides. Crystallographic studies demonstrate the ligand's ability to form strong, selective bonds with actinides, stabilizing various coordination geometries. NMR analysis confirms electronic properties and bonding, supporting the ligand's targeted potential. Notably, this systematic approach offers novel insights into the behavior of 8-hydroxyquinoline in non-polar solvents, a previously unexplored area in actinide coordination chemistry. These findings are crucial for understanding how solvent environments influence ligand binding properties and complex stability. This newly acquired knowledge lays the groundwork for the rational design of pharmacologically relevant decorporation agents.

This work was funded by the Deutsche Forschungsgemeinschaft (DFG, German Research Foundation) – Project number 530101100 (ActiDecorp).

## References

- [1] Kazantzis, G. Chapter 15 - Diagnosis and Treatment of Metal Poisoning—General Aspects. In Handbook on the Toxicology of Metals (Third Edition), Nordberg, G. F., Fowler, B. A., Nordberg, M., Friberg, L. T. Eds.; Academic Press, 2007
- [2] Frazer, M. J.; Rimmer, B., J. Chem. Soc. A, 1968, 2273-2275
- [3] Moeller, T.; Ramaniah, M. V. J. Am. Chem. Soc. 1954, 76, 23, 6030–6032

# Dissolution of unirradiated MOX fuel in the presence of metallic iron

M. Saleh<sup>1, \*</sup>, M. Hedberg<sup>1</sup>, K. Spahiu<sup>1,2</sup>, C. Ekberg<sup>1</sup>

<sup>1</sup> Nuclear Chemistry / Industrial Materials Recycling, Chalmers University of Technology, SE-412 96 Gothenburg, Sweden, \*Corresponding author. gidam@chalmers.se

<sup>2</sup> Swedish Nuclear Fuel and Waste Management Co., SE-101 24 Stockholm, Sweden

## **Abstract**

Spent nuclear fuel, primarily composed of UO<sub>2</sub>, exhibits very low solubility in the anoxic and reducing conditions expected in deep geological repositories. However, the radiolytic dissolution of spent nuclear fuel, driven by ionizing radiation, generates oxidants (e.g., H<sub>2</sub>O<sub>2</sub>, O<sub>2</sub>) that can accelerate fuel corrosion [1–2]. In a breached repository canister, iron from the canister material will corrode in groundwater, producing repository reductants such as Fe(II) and H<sub>2</sub>. These species, alongside iron corrosion products (e.g., magnetite, green rust), have the potential to mitigate the oxidative dissolution of spent nuclear fuel [3].

This study investigates the dissolution behavior of unirradiated MOX fuel pellets (10% Pu content, simulating aged spent fuel with high alpha activity) in the presence of metallic iron. Experiments were conducted under reducing conditions using synthetic Forsmark groundwater in an autoclave system. The preliminary experiments determined the maximum Fe(II) concentrations (10<sup>-4</sup>–10<sup>-3</sup> M) and dissolved H<sub>2</sub> pressures achievable through anoxic iron corrosion, consistent with prior studies [4]. Subsequent leaching experiments assessed the interaction of Fe(II), dissolved H<sub>2</sub>, and iron corrosion products with MOX fuel. The results revealed significant suppression of oxidative dissolution, with uranium concentrations in solution (4 × 10<sup>-9</sup>–4 × 10<sup>-10</sup> M) aligning with the solubility of UO<sub>2</sub>·xH<sub>2</sub>O. The findings indicate that Fe(II) and H<sub>2</sub> produced during iron corrosion, interact with radiolytic oxidants to suppress the oxidative dissolution of MOX fuel. These observations align with earlier models predicting suppression of oxidative dissolution at low H<sub>2</sub> pressures (0.1 bar) [5]. The study highlights the pivotal role of iron corrosion products in reducing actinide solubility and mobility under repository conditions. By advancing the understanding of these interactions, this work contributes to improving the predictability of spent fuel stability, thereby supporting the development of safer and more effective nuclear waste disposal.

## **References**

- [1] K. Spahiu., D. Cui., M. Lundström, Radiochim. Acta 92, pp. 625– 629. (2004) .
- [2] S. Sunder., D.W. Shoemaker., N.H. Miller, J. Nucl. Mater. 244 pp. 66–74 (1997) .
- [3] A. Puranen., A.F. Barreiro., L.Z. Evins., K. Spahiu, J. Nucl. Mater. 542, pp. 152423, (2020) .
- [4] M. Odorowski., C. Jegou., C.L. de Windt., V. Broudic., G. Jouan., S. Peugeot., C. Martin, Geochim. Cosmochim. Acta 219, pp.1-21. (2017) .
- [5] M. Jonsson., F. Nielsen., O. Roth, E. Ekeröth., S. Nilsson., M. M. Hossain., Envir. Sci. Technol. 41, pp.7087-7093. (2007).

# Interstitial-Oxygen doping induced Insulator-Metal transition and structure phase transition in $UO_{2+x}$

Rui Song<sup>1</sup>

<sup>1</sup> Institute of Materials, China Academy of Engineering Physics, 621908, Jiayangou, China,  
e-mail: pkusongrui@pku.edu.cn

$UO_2$ , which is one of the most important nuclear fuel and the most common product of uranium oxidation, has attracted many attentions due to its application value. Meanwhile, the strong correlated interaction between U-5f electrons drives it into a Mott insulator, which shows a deep physical connection. The negative formation energy of impurity oxygen atom in its octahedral interstice makes it a naturally doped Mott insulator. Here, by the means of first-principles DFT+ $U$  calculations and virtual crystal approximation (VCA), we show that the disordered interstitial-O doping can drive an insulator-metal transition due to the hybridization between U-5f and O-2p orbitals (as shown in Fig. 1). Along with the increase of the density of states near the Fermi level, the phonons of  $UO_{2+x}$  begin to soften until a structure phase transition happens. In an extreme case, the new structure is  $U_3O_8$  type which has a large volume expansion, and that would be harmful for its functional properties.

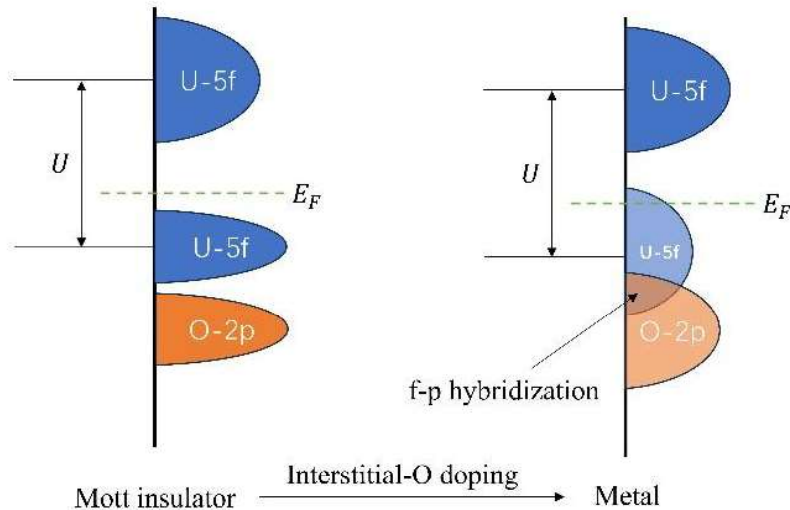


Fig. 1. Schematic of interstitial-O doping induced insulator-metal transition

## References

- [1] S.-W. Yu, *et al.*, *Phys Rev B*. **83**, 165102 (2011).
- [2] L. Desgranges, *et al.*, *Inorg. Chem.* **48**, 7585 (2009).

# **Under pressure to uncover a record $T_c$ in uranium - Synthesis and electrical transport of new uranium hydride phases**

William Thomas\*

*School of Physics, University of Bristol, Bristol BS8 1TL, United Kingdom*

*\*e-mail: [william128.thomas@bristol.ac.uk](mailto:william128.thomas@bristol.ac.uk)*

High pressure super-hydride compounds provide a promising avenue to finding room-temperature superconductivity. At present, the LaH10 phase exhibits the highest measured superconducting transition temperature,  $T_c = 250\text{K}$  observed experimentally at a pressure of 200 GPa. The next step is to find new high  $T_c$  superconductors at lower pressures. The higher order uranium poly-hydride phase, UH7 has been experimentally observed to be dynamically stable at moderate pressures (hcp-UH7 at 36 GPa) and predicted to become superconducting at temperatures  $\approx 55\text{K}$  but needs to be confirmed experimentally. I present the synthesis route, characterisation and in-situ transport measurements achieved within our unique diamond anvil cell (DAC) design.